The origin and anisotropy of high energy cosmic rays

Nicholas R. Stapley

The Origin and Anisotropy of High Energy Cosmic Rays

by

Nicholas R. Stapley, B.Sc.

A thesis submitted to the
University of Durham
for the Degree of Doctor of Philosophy
1981

ABSTRACT

The evidence for the anisotropy of cosmic rays from 10^{11}eV to 10^{20}eV is considered in detail from both a Galactic and extragalactic viewpoint and placed in astrophysical context. The importance of recent measurements of the local interstellar wind (consistent with a direction from $(\alpha,\delta) = (252^{o}, -16^{o})$ and velocity 21 - 23 kms^{-1}) is noted. Cosmic ray streaming along the lines of the local Galactic magnetic field appears to account for the constant observed anisotropy of 0.05% at (1 - 2)hrs R.A. below 10^{14}eV. However, the distribution of cosmic rays does not appear to conform to the expectations of axial symmetry.

Observational and statistical aspects of anisotropy are considered with particular reference to harmonic analysis. The results are used for analysis of the collection of data by Linsley and Watson which are shown to be inconclusive for anisotropy measurements in the range 10^{14}eV to 10^{17}eV. The power of using only phase or only amplitude information from collections of measurements is noted.

Anisotropy measurements from 10^{17}eV to 10^{20}eV are considered and seen to favour a mixed origin model in which particles above $\sim 10^{17}$eV are of extragalactic origin. The cosmic ray spectrum above 10^{18}eV can then be interpreted purely in terms of an effect of extragalactic particles.

Three models to account for the upturn in the cosmic ray spectrum at high energies are considered. A simple model in which neutrons escape from clusters of galaxies before decaying into protons is found to account for the observed spectrum if a source spectrum of the form $j(E) \propto E^{-2.25}$ is adopted.

A model based on diffusion of particles from the Virgo Supercluster is seen to give a satisfactory fit to the data if a diffusion coefficient of $D(E) = 5 \times 10^{33} E_{19}^{\frac{1}{2}}$ $cm^2 s^{-1}$ is taken. The model also accounts for the observed amplitude of the anisotropy above 10^{17}eV.

A model assuming production of high energy particles in radio galaxies is shown to be less satisfactory than the neutron or diffusion models.

PREFACE

The work presented in this thesis was carried out during the period 1976-1979 while the author was a research student under the supervision of Professor A.W. Wolfendale in the Physics Department of the University of Durham.

Parts of the work were carried out in collaboration with Professor Wolfendale, Professor J. Wdowczyk and Mr. P. Kiraly of the Hungarian Academy of Science and has been published as follows:

Stapley, N.R., Wolfendale, A.W., and Wdowczyk, J., 1977, Proc. 15th Cosmic Ray Conf., 2, 316.

Kiraly, P., Kota, J., Osborne, J.L., Stapley, N.R., and Wolfendale, A.W., 1979, Riv. del Nuovo Cim., 2, No. 7

Kiraly, P., Kota, J., Osborne, J.L., Stapley, N.R., and Wolfendale, A.W., 1979, Lett. al Nuovo Cim., 24, No. 8

Kiraly, P., Kota, J., Osborne, J.L., Stapley, N.R., and Wolfendale, A.W., 1979, Proc. 16th Int. Cosmic Ray Conf., MG7, 221.

LIST OF CONTENTS

CHAPTER 1

GENERAL INTRODUCTION

The first extensive air-shower anisotropy experiment was performed by Hodson (1951) and since then many measurements at different energies have been made to elucidate the problems of the origin and propagation of cosmic rays, problems which have remained unsolved since the discovery of cosmic rays by Hess in 1912. The establishment of the existence of a large scale Galactic magnetic field of about 2-3 μGauss strength has added to the complexities since particles will be deflected by the field and their arrival directions will hence bear little relationship to the direction of their sources, at least up to energies of 10^{18} eV or so. Thus, indirect measurements have to be made to solve the origin problem.

The origin problem is so severe that it is still uncertain if the bulk of locally observed particles are of Galactic or extragalactic origin although the evidence and theoretical considerations indicate that Galactic sources provide most of the local flux, at the lowest energies, below 10^{10} eV. At these energies, observations of the distribution of gamma rays (which are presumably produced by interactions of cosmic rays with the interstellar medium) have been used to show that there is a gradient of cosmic rays in the Galaxy, which provides corroborative support for the Galactic origin hypothesis (Dodds et al. 1975, Strong et al. 1978). At higher energies, and particularly above 10^{12} eV, where solar modulation effects are minimal, it is measurements of the anisotropy of arrival directions which provide information about propagation effects and thus, hopefully, about the

origin and sources of cosmic rays. If the particles revealed only a small anisotropy consistent with the cosmic rays being "at rest" in the frame of the Galaxy, then we would not expect the particles to be of Galactic origin. Any extra-galactic anisotropy would have been smeared out and reduced by long Galactic residence times. On the other hand a significant anisotropy, changing in phase and increasing in amplitude with increasing energy, would strongly indicate that the particles originated from within the Galaxy.

Prior to 1951, relatively few anisotropy measurements had been made and these few were for primary energies of below 10^{14} eV and were based on either sea level ionisation (Hogg, 1950) or muon (then "meson") intensity at various depths (e.g. Duperier, 1946). The results showed little or no sidereal variation which could not be accounted for as statistical fluctuations. After 1951, however, small extensive air-shower (EAS) arrays began to detect significant anisotropies which showed a good agreement in phase. Hodson, for a mean primary energy of 5×10^{14} eV, measured a first harmonic amplitude of $1.15 \pm 0.61\%$ with a phase of 23.5 hrs., R.A. Daudin and Daudin (1952) found an amplitude of $0.39 \pm 0.13\%$ with phase 22.0 hrs while Farley and Storey (1954) obtained the most significant result yet measured of $1.1 \pm 0.26\%$ and phase 19.8 hrs for $\bar{E}_p = 10^{15}$eV. Unfortunately, later measurements of greater precision failed to confirm the original results, showing little or no sign of the hoped for anisotropy. Nevertheless, the measurements were useful in setting upper limits to restrict some types of propagation and origin models.

The first really strong evidence for anisotropy, free from effects of the solar field, did not appear until 1975 when improved experimental techniques were used by the Budapest-Sofia collaboration at Peak Musala to show the existence of a definite anisotropy at around 6 x 10^{13} eV (Gombosi et al. 1975). In 1977 the measurements of Nagashima et al. (1977) at 2 x 10^{13} eV were found in good phase and amplitude agreement with those of Peak Musala. Detailed tests to reveal spurious effects were performed by both these groups (Gombosi et al. 1977, Nagashima et al. 1977) which served to strengthen the evidence for anisotropy and at the same time made it difficult to think of explanations in terms other than genuine effects.

A recent paper by Linsley and Watson (1977) based on the collation of data published between 1951 and 1965, for the range 10^{14} to 3 x 10^{17} eV, has given not inconsiderable support to the existence of anisotropies in this region. This paper is considered in more detail later. At still higher energies a recent review (Edge et al. 1978) of the Haverah Park data has summarised the results on anisotropy above 6 x 10^{16} eV and drawn support from measurements of other groups. The claim is again for strong evidence of a genuine anisotropy, particularly at 10^{17} eV.

Below 10^{13} eV, the existence of Sidereal variations is well established, but problems arise in disentangling the effects of the solar interplanetary field from genuine Galactic (or extragalactic) effects. Below 10^{11} eV the results must be treated with caution since the Larmor radii of such particles in the interplanetary field are so small

that modulation effects are overwhelming. Just above 10^{11} eV, where underground muon telescopes are most effective in supplying data, the effects are still hard to disentangle: protons at this energy have a Larmor radius of less than 10 AU in a 3 μG field and the solar field has about this value at a heliocentric distance of ∿ 11 AU and rises to about 30 μG at the earth (Sakurai 1974). The firmest claim so far for anisotropy in this energy range has come from the Holborn Imperial College group using a model of the Solar field to obtain 'true' viewing directions (Marsden et al. 1976, Davies et al. 1978). In the Southern hemisphere, and somewhat higher in energy, at 10^{12} eV, the Poatina results, though less statistically significant, are compatible with those obtained between 10^{13} and 10^{14} eV. However, Fenton et al. (1977) have shown that the interplanetary field may have some effect even at this energy which, if true, would invalidate all measurements below 10^{12} eV and cast some doubt on the origin of the anisotropy observed at Poatina.

It is worth noting here that the amplitude of the claimed anisotropies increase with energy as about $E^{\frac{1}{2}}$ while the number of events detected decreases at about E^{-1}. Therefore, assuming that the anisotropies are genuine, the statistical errors would increase in direct proportion to the genuine signal so that establishing a genuine anisotropy would be equally difficult at every decade in energy.

The possibility of 'narrow angle anisotropies' has been suggested in recent years. Wolfendale (1977) has investigated this topic but found no conclusive evidence for such a phenomenon. They will not be considered here.

Summarising briefly, claims for a genuine anisotropy have been made for each energy region from 10^{11} eV to 10^{20} eV though there have been many negative results in each decade also. Only those measurements at 10^{13} - 10^{14} eV using small EAS arrays are really convincing and can be taken as established. In the following chapters the anisotropy question will be considered in detail and the experimental results in each decade examined. Astrophysical observations and expectations will be used to link anisotropy measurements to the characteristics and properties of the Galaxy, and to the propagation of cosmic rays. Consideration to both Galactic and Extragalactic origin will be given.

CHAPTER 2

INTRODUCTORY CONCEPTS

2.1 Mathematical Notation

Anisotropy measurements hope to reveal the local (extra solar cavity) behaviour of cosmic rays with regard to their distribution in phase space. The distribution of cosmic rays may be considered to be represented as a smooth function $f(\underline{x},\underline{p},t)$ except in the vicinity of some "exceptional" regions such as stars which occupy only a minute fraction of the volume of the Galaxy. It is usually assumed that the dimension for spatial variation of $f(\underline{x},\underline{p},t)$ is considerably greater than the dimensions of the zone of influence of the sun and it is hoped that the time scale for change is considerably longer than the 30 years or so in which measurements have been made (it is known that the intensity of cosmic rays has not changed significantly in the last 10^5-10^6 years, and probably not over the last 10^8-10^9 years) so that the time dependence of $f(\underline{x},\underline{p},t)$ may be neglected.

With these assumptions we may regard $f(\underline{x},\underline{p},t)$ as dependent only on momentum $\underline{p}$ so that $f(\underline{x},\underline{p},t) = f(\underline{p})$. Introducing spherical polar co-ordinates p,α,δ (where $p = |\underline{p}|$ and α and δ are right ascension and declination) and the unit vector $\underline{e} = \frac{\underline{p}}{p}$, we may express the change of $f(\underline{p})$ with direction by expanding into a series of multipole type terms such that

$$f(\underline{p}) = f(\underline{e},p) = f^{(0)}(p) + f_i^{(1)}(p)e_i + f_{ij}^{(2)}(p)e_ie_j + f_{i,j\ldots n}^{(k)}(p)\, e_ie_j\ldots e_n + \ldots \qquad 2.1.1$$

where $\{i,j,\ldots n\} = \{1,2,3\}$ and the usual summation convention applies. We have for $\underline{e}$:

$$e_1 = \mathrm{Cos}\alpha\mathrm{Cos}\delta,\ e_2 = \mathrm{Sin}\alpha\mathrm{Cos}\delta,\ e_3 = \mathrm{Sin}\delta \qquad 2.1.2$$

$f^{(o)}, f^{(1)}, f^{k\geq 2}$ are the scalar, vector and tensor components respectively. To uniquely define the tensors in the above equation we require firstly that they are symmetric in each pair of indices since the antisymmetric parts would give no contribution (for $f^{(2)}_{ij}$, $f^{(2)}_{ij} = f^{(2)}_{ji}$). Secondly, we require that higher order terms should not contribute to any variation that can be written in terms of lower order terms. Obviously $f^{(o)}$ and $f^{(1)}$ are not affected by these conditions and are unrestricted; $f^{(2)}$ is required to be traceless and symmetric. A requirement that tensors of any order be symmetric in any pair of indices for all combinations of the rest is equivalent to the second condition. Consequently $f^{(2)}$ has five independent components which correspond to the five independent second spherical harmonics and in general $f^{(k)}$ depends on $2k + 1$ scalars.

If we consider an idealised cosmic ray detector of good angular and momentum resolution, then the differential cosmic ray intensity pointing towards $\underline{e}$ is proportional to the density in phase space in the opposite direction so that

$$I(\underline{e},p) = vp^2 f(-\underline{e},p) \qquad 2.1.3$$

At the energies we are concerned with, $v \simeq c$, so we may write $I^{(k)}(p) = (-1)^k cp^2 f^{(k)}$ and express $I(\underline{e},p)$ as:

$$I(\underline{e},p) = I^{(o)}(p) + I^{(1)}_i(p)e_i + I^{(2)}_{ij}(p)e_ie_j + \ldots \qquad 2.1.4$$

The anisotropy function for a given momentum or energy can be defined as

$$\lambda(\underline{e}) = (I(\underline{e}) - I^{(o)})/I^{(o)} = (f(-\underline{e}) - f^{(o)})/f^{(o)} \qquad 2.1.5$$

The multipole expansion for $\lambda(\underline{e})$ is then

$$\lambda(\underline{e}) = \lambda^{(1)}_i e_i + \lambda^{(2)}_{ij} e_i e_j + \ldots + \lambda^{(k)}_{ij} \ldots {}^n e_i e_j \ldots e_n \qquad 2.1.6$$

where

$\lambda^{(k)}(\underline{e}) = I^{(k)}(\underline{e}) / I^{(o)}$. The anisotropy function of order k will then be the k^{th} term in the expansion of $\lambda(\underline{e})$, describing more and more complex angular distributions as k increases.

2.2 The Simple Vector-type Anisotropy

In the simplest case we may consider only a vector-type anisotropy and neglect all higher terms so that the anisotropy is

$$\lambda(\underline{e}) = \lambda_i^{(1)} e_i = \underline{\lambda} \cdot \underline{e} \qquad 2.1.7$$

In this case the measure of anisotropy will be defined as $|\underline{\lambda}|$ or alternatively as

$$\alpha = \frac{Imax - Imin}{Imax + Imin} \qquad 2.1.8$$

which is the normally accepted definition of a vector-type anisotropy. This could also be applied to the general case for the anisotropy of order k, but this encounters difficulties since detectors have a finite angular resolution so that weak but sharp intensity peaks would be smoothed out. A more useful definition is the absolute maximum value of the anisotropy function (equation 2.1.6) of order k, which for the simple vector case is the same as equation 2.1.8.

However complicated the angular distribution and anisotropy of cosmic rays is, it is unfortunate that experimental techniques are not yet adequate to reveal any 3rd or higher harmonics - experiments have not caught up with theory - and this provides the justification for using expansions of the above type. Since the angular resolution of detectors is poor and the direction of measurements depends largely on the rotation of the earth and the atmosphere, only the first two terms normally contribute to the anisotropy function, and are measured. At the highest energies, where point sources

may be detected, there is, of course, no point in using expansions of this type. However, the expansion is useful in multiple scattering models of propagation where higher order anisotropies are expected to decay faster.

There are two other points worth noting. Firstly, each component of the cosmic ray flux may have a different angular distribution with a different anisotropy function to describe it. Since at present it is relatively complicated to ascertain the nature of the primaries incident on the atmosphere, the measured anisotropy may only be considered as a kind of average. Secondly, for nearly isotropic distributions the vector anisotropy $\underline{\lambda}$ is related to the cosmic ray streaming $\underline{s}$ by

$$\underline{\lambda} = \frac{3\underline{s}}{uc} \qquad 2.1.9$$

where u is the cosmic ray density. Anisotropies of higher order do not contribute to $\underline{s}$.

CHAPTER 3

ASTROPHYSICAL ASPECTS : THE MAGNETIC FIELD AND INTERSTELLAR MEDIUM

3.1 Introduction

Magnetic fields are of obvious importance for cosmic ray propagation and anisotropy measurements since the particles are not only deflected by fields but may, in certain energy regimes, be expected to follow field lines closely. A knowledge of the magnetic field is,therefore, useful in attempting to predict anisotropies. If particles are mainly of Galactic origin then it is the Galactic field only that need be considered. If extragalactic particles make a significant contribution then the effect of extragalactic fields must also be taken into account. In this section our knowledge of magnetic field is summarised, and in view of the relevance to cosmic ray propagation, the data have been examined in some detail.

3.2 The Galactic Magnetic Field

3.2.1 Methods of Analysis Various methods have been devised to examine the Galactic Magnetic Field and it is now well established that a large scale field exists, though the details are still uncertain. The following methods have been most used, of which the first four are radio based and the fifth optically based.

1. Faraday rotation of extragalactic polarised radiation.
2. Faraday rotation of radiation from pulsars.
3. Polarisation of Synchrotron radiation from the Galactic background and radio synchrotron surveys.
4. Zeeman Splitting.
5. Polarisation of Starlight.

3.2.2 Faraday Rotation The first method relies on the rotation of polarised radiation from extragalactic radio sources in a magnetic field, and was first used by Gardner and Whiteoak (1963). The Faraday rotation in a line of sight field of strength B_{LS} is proportional to the product of B_{LS} with the thermal electron density n_e integrated along the line of sight:

$$\theta = .81(\frac{\lambda}{m})^2 \int \frac{n_e}{cm^{-3}} \frac{B_{LS}}{\mu G} \, d\ell/pc \qquad 3.2.1$$

Measurements are usually carried out at three wavelengths (if possible) to avoid possible ambiguities caused by rotations of more than 360°. Several problems are inherent in this method. There exists the possibility that sources have their own intrinsic rotation and in addition each observation involves a line of sight throughout the whole of our own Galaxy so that non-local fields can affect the measurements. Using Galactic pulsars, on the other hand, reduces these problems. The distance of a pulsar can be derived from the dispersion of its pulses and therefore the "local" field may be studied relatively free from distant field effects. Moreover, by combining the dispersion measure (D.M.) with the rotation measure (R.M.) the mean value of the field B_{LS} can be derived directly

$$\langle B_{LS} \rangle = \frac{\int n_e B_{LS} d\ell}{\int n_e d\ell} \qquad 3.2.2.$$

There is no evidence of any intrinsic pulsar rotation (Manchester 1972) and in general this method may well be the best.

The Zeeman Splitting of spectral lines also provides information on the line of sight component of the field, but

the results have not come up to their initial expectations since the errors of measurements obtained by this technique have been comparable to the measurements themselves, long integration times being needed.

3.2.3 Optical Polarisation The optical polarisation of starlight, first observed by Hiltner (1949) and Hall (1949) gives information on the direction of the magnetic field but not its magnitude. The technique relies on the accepted method of Davies and Greenstein (1951) in which dust grains align perpendicular to a magnetic field. The grains scatter light leaving a transmitted component polarised parallel to the field. Fields of a few μG are required to align the ice/graphite grains. The measurements are useful in determining the large-scale directional properties of the Galactic field.

Synchrotron data are of use to obtain a global picture of the spatial variation of the energy density of magnetic fields in the disc. The emissivity depends both on the field strength and on the relativistic electron density. Synchrotron background polarisation data provides similar information to optical polarisation data, except that the field is perpendicular to the polarisation vectors normally plotted. Synchrotron polarisation has been most used in examining the structure of the various Galactic loops, and has been used to investigate magnetic field irregularities (Wilkinson and Smith, 1974).

3.2.4 Possible Field Reversal above and below the Galactic Plane The initial surveys of extragalactic rotation measures indicated a decreasing field with increasing latitude (as expected) and also indicated changes in field direction

above and below the Galactic plane (Gardner and Whiteoak 1963). However, as more rotation measures were added (e.g. Mitton, 1972) it became apparent that there were many anomalies which no simple field configuration could explain. Recent measurements (Simard-Normandin and Kronberg, 1979) still indicate a longitudinal field from $\ell = 270^{o}$ to $\ell = 90^{o}$ South of the Galactic plane, while suggesting that the confusing northern hemisphere measurements may be accounted for by a looped field north of the plane which may well be associated with Loop I, the north polar spur.

3.2.5 Valée and Krongburg Model Valée and Krongburg (1975) have found reasonable consistency of their measurements with a model in which the sun is located on the edge of an egg-shaped anomaly centred on $(\ell^{II}, b^{II}) = (330^{o}, 40^{o})$ which perturbs the more extensive longitudinal field*. In the Southern Galactic hemisphere the average field direction is $(\ell^{II}, b^{II}) = (90^{o} \pm 10^{o}, 5^{o} \pm 10^{o})$, while for $b^{II} > 0^{o}$, $40^{o} < \ell^{II} < 270^{o}$ the field was found to be towards $(\ell^{II}, b^{II}) = (90^{o} \pm 20^{o}, 10^{o} \pm 20^{o})$. The distortion was hypothesised to perturb the local direction of field towards $\ell^{II} = 55^{o}$ (see figure 3.1). The most likely explanation of the anomaly is that it is the result of a supernova explosion and connected with the NPS. Fields of about 2μG have been derived for typical electron densities of 0.05 cm^{-3}.

* This is the general direction of the North Polar Spur, which is centred on $(\ell^{II}, b^{II}) = (329^{o}, 17.5^{o})$.

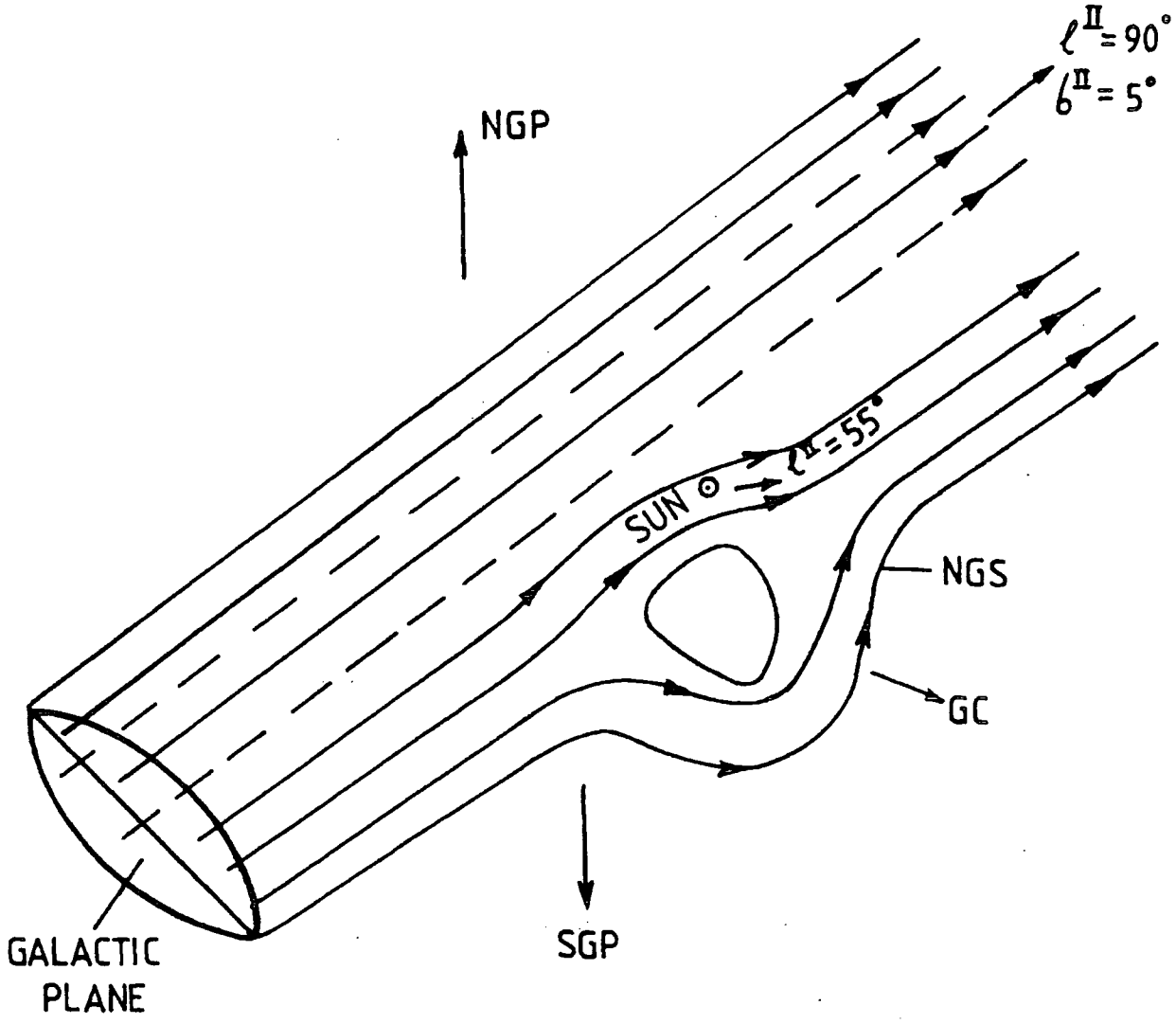

Fig 3·1

Idealised model of the smooth component of the spiral arm magnetic field (from Vallée and Kronburg , 1975)

NGS — North Galactic spur

NGP — North Galactic pole

SGP — South Galactic pole

GC — Galactic centre

Centre of bulge $l^{II}= 330°$ $b^{II}= 40°$

3.2.6 Large scale field Starlight polarisation and pulsar rotation measures give information on the regular component of the field in the local few hundred to few thousand parsecs, primarily in the region of the galactic plane. Both of these techniques give somewhat different directions for the magnetic field so that uncertainty remains about the exact geometry of the field. Gardner et al. (1969) concluded that from the optical data $\ell^{II} = 50^{o}$, from the radio data $\ell^{II} = 85^{o}$.

Axon and Ellis (1976) and Ellis and Axon (1978) have compiled and examined a catalogue of stellar polarisation measurements and concluded that overall the field points towards $\ell^{II} = 60^{o} \pm 15^{o}$ while within 500 pc its direction is nearer $\ell^{II} = 45^{o}$. Some evidence for an inclination to the plane was also found. Mathewson (1968) was in favour of interpreting the optical data in terms of a local helical field with an axis along $\ell^{II} = 270^{o} - 90^{o}$, an idea that was supported by the radio data at that time showing a field reversal above and below the Galactic plane. In a review of these observations Vershuur (1972) concluded that the results were consistent with a longitudinal field towards $\ell^{II} = 50$. Examining the Axon and Ellis data at different distance ranges from the sun an estimate of the field direction can be obtained by comparing with a longitudinal field model and performing a least squares type of analysis. A preliminary version of this analysis has been given by Wolfendale (1977). Points $B_1 - B_3$ on figure 3.2 show the change in direction of field for distances from < 250 pc to < 1 Kpc,

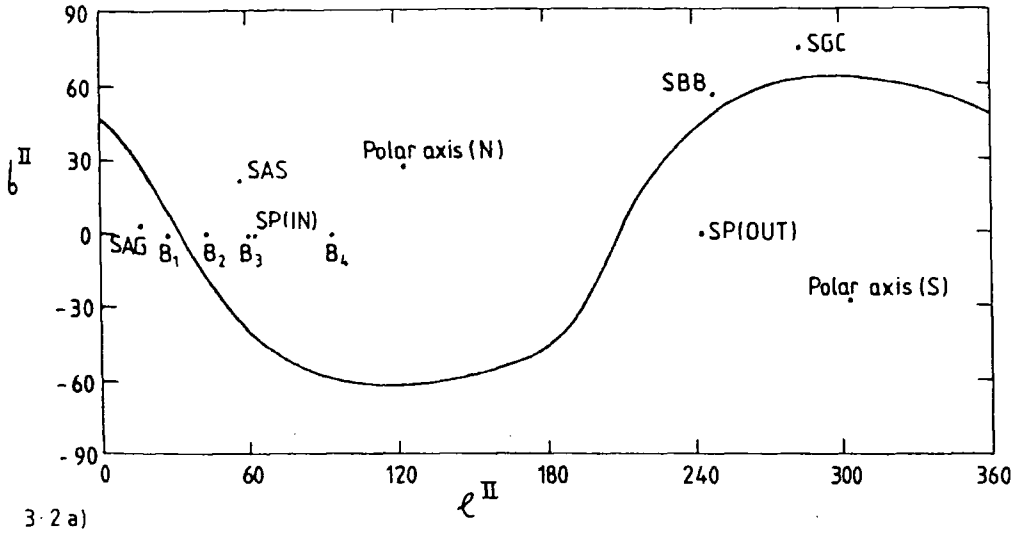

Fig 3·2 a)

Directions of importance in the Galaxy given in 3·2a - Galactic coordinates and 3·2 b - Equatorial coordinates. SP(IN) : Inwards local spiral arm direction. SP(OUT) : Outwards local spiral arm direction. SBB : Direction of solar motion relative to the black body radiation. SAS : Direction of solar apex relative to the stars . SAG : Direction of solar apex with respect to the local interstellar medium. SGC : Supergalactic centre :— centre of Virgo supercluster. B1 – B4 : Directions of the local magnetic field at

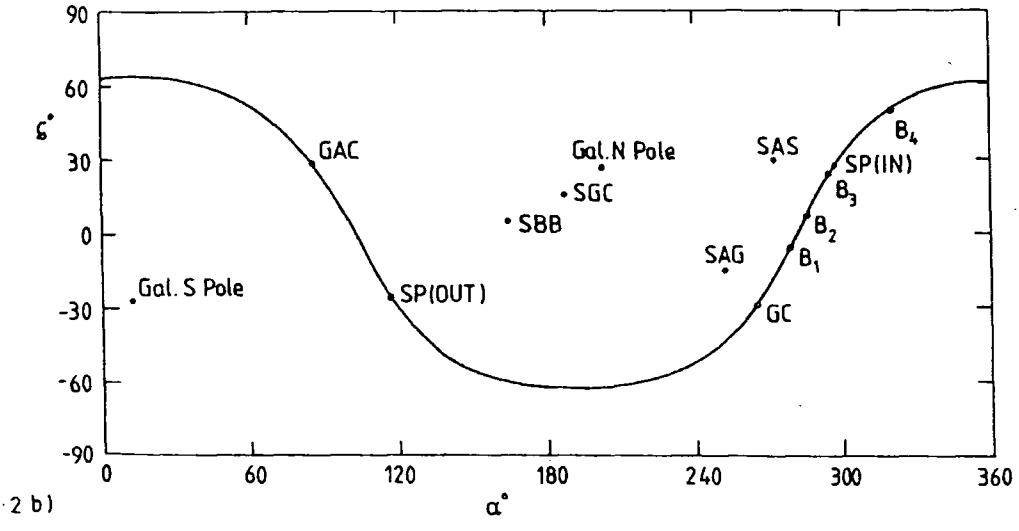

Fig 3·2 b)

varying distances from the sun, being 200, 500, 1000, and 2000 pc respectively. The last measurement is that of Heiles ,1976, derived from pulsar rotation measurements. B1, B2, B3 are from the stellar polarisation measurements of Ellis and Axon ,1978, as interpreted by Kiraly et al. , 1979. GC : The Galactic centre . GAC : The Galactic anticentre .

Pulsar measurements have been reviewed by Heiles (1976) who gives the field direction as $\ell^{II} = 94^{o}$ and a field strength of 2.5 μG. The most recent measurements by Manchester and Taylor (1977) give (for a least squares fit) $\ell^{II} = 90^{o} \pm 14^{o}$ and B = 1.7 ±0.3 μG. The region out to 2 Kpc where both pulsar and polarisation data are available therefore shows some considerable disagreement between the two methods. As pointed out by Heiles this anomaly is presumably due to the two techniques sampling different regions occupied by dust and non-thermal electrons, where the distribution is not the same for both components. The pulsar measurements are not always in agreement with the Valée and Kronburg model either.

3.2.7 Information from Synchrotron radiation The polarisation of the Synchrotron background results have found most use in investigating the fine structure of the magnetic field (e.g. Spoelstra 1972). Other results have been consistent with a longitudinal field in the region $\ell^{II} = 50^{o} - 70^{o}$. Note that the distribution of non-thermal electrons responsible for Faraday rotation need not be the same as that for the relativistic electrons producing synchrotron radiation (Whiteoak 1974).

3.2.8 Mean field as a function of distance from the sun In general, then, there does appear to be a trend of field direction with increasing distance from $\ell^{II} = 45^{o}$ to $\ell^{II} = 90^{o}$. It appears likely that the North Polar Spur has had a perturbing influence on the local field and that it is this that has caused the observed change in field direction. Certainly the structures of the fields in Loops I and II are complex and appear to be consistent with the effect of super-

nova explosions (Spoelstra 1972). The regular local field is certainly of 1.5 - 3.5 μG strength and most probably in the range 2-3 μG. Irregularities of comparable strength to the regular field are also present, and probably have dimensions 10-50 pc (Wilkinsonand Smith 1974).

Synchrotron radio emission is useful in that not only does it give information about the large scale structure of the Galaxy but the polarisation from the Galactic background can be used to trace the local magnetic field. The radiation is substantially polarised between 400-1400 MHz and is believed to have an origin limited by Faraday depolarisation to distances of a few hundred pc. Spoelstra (1972) has performed the most detailed analysis of polarisation, with reference to the North Polar Spur. His results are consistent with a field running along the ridges of enhanced radio emission. If loop I is about 75 pc away he finds consistency with an electron density of .06 cm^{-3} and with the low rotation measures he derives a field of 1-2 μG.

Berkhuijson (1971) and Mathewson et al. (1966) have both interpreted the polarisation directions and Faraday rotations in terms of a field running parallel to the plane. They find the best direction towards $\ell^{II} = 60^{o}$ and 70^{o} respectively. The discrepancy with the pulsar results may arise from a differing field direction within the local few 100 pcs or alternatively from differing distributions of the relativistic electrons (Synchrotron rad^{n}) compared with the thermal electrons (Faraday rotation).

3.2.9 Spiral Arm Enhancement The Galactic magnetic field is expected to be enhanced in spiral arms as a result

of compression of the interstellar gas when it overtakes a density wave. Osborne et al. (1977) have found a good fit to the observations assuming that the sun is in an interarm position and the spiral arms have fields of about 10 μG (stronger than those observed locally). Wilkinson and Smith (1974) found that the energy density of irregular fields is similar to that of the regular field; in other words, the fluctuating component required by synchrotron observations is comparable to the reasonably smooth component found by other methods.

3.2.10 Halo Field Ginzburg and Ptuskin (1976) present good evidence using synchrotron surveys for the existence of extensive halo fields. These fields are still the cause of some dispute, but it is evident that the halo field falls off much slower with Z (the height above the Galactic plane) than the gas density. Parker (1976) suggests that dense gas clouds hold the field to the disc. In between these clouds the disc field can escape, bulging out so that the field in an extended halo is probably small. White (1977) has performed calculations on a number of Galactic dynamo models and these too tend to favour weak halo fields.

3.2.11 Field Fluctuations Instabilities in the interstellar gas, the decay of large-scale turbulence, and propagating shock waves are all expected to give rise to small scale field fluctuations. Skilling (1975) notes that turbulence can lead to a fast separation of magnetic field lines and can also cause scattering of cosmic rays with gyroradii of the same order as their wavelength. Damping may not be sufficiently strong to reduce the intensity of waves below 1pc except for cosmic ray self-excited waves.

However, if this barrier can be passed the wave spectrum may extend down to 10^{-3} pc (McIvor, 1975). The only observational evidence comes indirectly from pulsar scintillation measurements which suggest that turbulence exists on scales as small as 10^{-8} pc. Assuming a Kolmogorov spectrum (equation 4.5.3) between 10^{-8} - 3 pc, even the lowest energy cosmic rays would be subject to Fermi acceleration, and as a result far-reaching changes in our picture of astrophysical processes would be needed. Alternatively, the damping of turbulence below 10^{-3} pc restricts Fermi acceleration to energies of 10^{12} eV and above. Clearly pulsar scintillations should be examined with a view to finding alternative explanations before the drastic assumption of a continuous wave spectrum is accepted.

3.3 The Extragalactic Magnetic Field

Piddington (1969) has argued the case for an intergalactic magnetic field of primordial origin of about 10^{-10} gauss, demonstrating its importance for the magnetic theory of galactic forms, spiral arms, and its dynamical effects in determining the orientation of galactic discs. Brecher and Blumenthal (1970) consider that primordial fields, if they exist, cannot be much more than 10^{-9} G if the gas density is $\simeq 10^{-5}$ cm^{-3}. In this picture, Galactic fields are derived from compressed and distorted intergalactic fields and might have a fairly open configuration. However, this view has very little theoretical or observational support and it appears more likely that Galactic fields are generated by a dynamo mechanism (Parker 1955) on various scales. In this

case any extragalactic field results from fields 'escaping' from galaxies along with gas and cosmic rays, possibly being amplified by turbulence rather than being of primordial origin. Parker (1976) has theorised that cosmic rays cause "bubbles" in the Galactic field which "burst" and carry their field outside the Galaxy. These fields may not be strong enough to influence the bulk motion of most cosmic rays so that extragalactic cosmic rays should be at rest with respect to the frame defined by the Universal black body radiation. With cluster models, though, the proposed intracluster magnetic field plays an important part in the anisotropy and propagation of cosmic rays (Chapter 8).

3.4 Anisotropy and the Interstellar Medium

The motion and nature of the local interstellar medium (LISM), surrounding the cavity dominated by the solar wind, is of importance for anisotropy studies. It is likely that the magnetic field of the Galaxy is frozen into the partially ionised gas which constitutes the LISM so that an axially symmetric distribution of cosmic rays (with respect to the magnetic field) would preserve its symmetry in the frame comoving with the gas. Changes in the magnetic field then affect the gas and hence the cosmic ray distribution and vice versa. Transformed to the solar frame, the first (vector) harmonic of the distribution will change considerably because of the Compton-Getting effect (section 4.5) but higher harmonics will remain almost unaltered, so that any test for axial symmetry must allow for relative motion. Note that the Compton-Getting correction should be applied

relative to the frame of the gas, and not the local standard of rest, since it is in the gas frame in which cosmic rays are expected to be at rest.

The LISM is also important in that the constancy of its various parameters (such as velocity, density, temperature) in the local few pc indicate that the magnetic field is also constant in this region. Linked to anisotropy measurements, the wind velocity and direction gives us a probable direction for the very local magnetic field. Until recently, the paucity of data precluded any conclusions but new data are proving to be of great interest (see later).

3.5 Measurements of the LISM

3.5.1 Techniques of study Measurements of the interstellar wind and its properties have come primarily from Satellite observations of backscattered UV light from neutral Helium and Hydrogen atoms; a summary of such results is given in table 3.1. Fahr (1974) has given an excellent review of the observations and theories relevant to the problem, and a summary of the measurements prior to 1974.

As hydrogen atoms approach the solar cavity they experience both a gravitational attraction and a repulsion from Solar H Lyα radiation. With moderate solar activity the radiation pressure is sufficient to push away the incoming hydrogen. Atoms are lost by charge-exchange and photo-ionisation, the net result of these processes being a "Snowplough" effect with a much larger concentration in the "upwind" direction.

In the case of helium, the greater mass of the helium

Measurement	Upstream Direction α^o	δ^o	Velocity km s^{-1}	Technique	
Fahr 1974	263	-23	5-20	H and He	Review of early measurements. Favours higher velocity range
Weller-Meier 1974	252±3	-15±3	$\sim$ 10	He STP 72-1	
Freeman et al. 1976	not given		10-15	Rocket Measurement	Lower limit 95% confidence claimed
Bertaux et al. 1977	not given		15-20	Lyα, Mars probe	
Adams and Frisch 1977	not given		21.6 ± 2.8 HeI or 22.1 ± 2.8 Lyα	Lyα Copernicus	Eliminated background Lyα to measure velocity directly
Arjello 1978	252±5	-17±5	Uses 22 km s^{-1}	584Å and 1216Å Mariner 10	Solar minimum. Direction is for Lyα only
Weller-Meier 1979	not given		21 km s^{-1} (Best fit)	584Å OSO-8 Measurement	

Table 3.1 Measurements of the interstellar wind giving direction and velocity information.

atom and the much lower Solar He 584 Å flux (compared to Lyα) means that radiation pressure in this case is insignificant. Helium, therefore, penetrates deeper into the solar cavity - photoionisation is the only loss process. The helium atoms are therefore gravitationally focussed, resulting in a maximum buildup in the downwind direction. For both H and He the densest region backscatters more solar radiation, and it is this maximum which is looked for. The helium results are expected to be somewhat more accurate since there is some uncertainty about the possible contribution from the background Lyα (see, however, Arjello, 1978). The interstellar extinction of the 584 Å radiation is thought sufficient to prevent Galactic interference.

3.5.2 Results from the measurements on the local wind

The early H measurements were found to be consistent with a reasonably well defined upwind direction of $(\alpha, \delta) = (263^{\circ} \pm 5^{\circ}, -22^{\circ} \pm 5^{\circ})$ (Fahr 1974) but the model dependence in interpreting the results left the velocity of approach rather uncertain, from 5 - 20 km s^{-1}. Initial helium measurements (Weller and Meier, 1974) were slightly in disagreement with the H direction, giving $\alpha = 250^{\circ} \pm 3^{\circ}$, $\delta = -15^{\circ} \pm 3^{\circ}$, but recent improved Lyα results have confirmed the direction (Arjello, 1978). Adams and Frisch (1977) have measured the velocity of the wind directly (using the high resolution U1 spectrometer from the Copernicus satellite) by scanning the Lyα line profile close to the upwind direction. They also eliminated most of the background from the geocoronal Lyα line by making use of the spectral shift caused by the

orbital motion of the earth. The wind speed derived was $v = 22.1 \pm 2.8$ km s^{-1}. Overall, examination of the results give a consistent set of parameters as $(\alpha, \delta) = (252^{o}, -16^{o})$ with a wind speed of 21 - 23 km s^{-1}.

Data on the density and temperature of the LISM are also derived indirectly in backscatter measurements and are consistent with $T \simeq 10^{4} K^{o}$ and $0.05 < n_{H} < 0.1$ cm^{-3} (Weller and Meier, 1979) with a velocity dispersion of 13 km s^{-1} for H. For He the values are $.002 < n_{He} < 0.03$ and $T \simeq 10^{4}$ K^{o}.

These local measurements actually only probe a distance of about 2×10^{-5} pc but the consistency of the results over a number of years indicate constancy over 10^{-3} pc because of the velocity of the wind.

3.5.3. Wind direction out to several parsecs. Further information about the interstellar wind has come from the detailed examination of spectral lines coming from nearby cool stars (McClintock et al., 1978, Moos et al., 1974, Dupree et al., 1977). The I/S gas along the line of sight absorbs some of the UV light, the absorption being strongest nearer the line centers. By measuring the Doppler shift the motion of the gas can be detected. The line shape also depends on the velocity dispersion (which may be partly thermal, partly of turbulent origin) and the average line-of-sight density, but separating these effects can be difficult. McClintock et al. have examined the Copernicus observations of the I/S hydrogen and deuterium Lyα lines towards four nearby cool stars and tabled measurements for another eight.

The results are compatible with gas densities of n_H = 0.02 - 0.2 cm^{-3}, in agreement with local values. When suitable allowance has been made for the direction of observation, the line-of-sight velocities are also compatible with the local backscatter velocities, even for stars as far away as 20 pc. From measurements of ε - eri (ℓ^{II}, b^{II}) = (195^{o}, - 48^{o}) a heliocentric line-of-sight velocity of 15.4 ± 7.8 km s^{-1} was obtained, equivalent to a velocity of 18 km s^{-1} along (α,δ) = (252^{o}, - 16^{o}). Derived temperatures by this method have given T ≃ 5 x 10^{3}K. These values are suggestively close to the locally derived values, so that the local values probably extend over a few pc from the sun. The local magnetic field is, therefore, also constant over this region, or at most slowly varying. This view is supported since the energy density associated with the bulk motion of the LISM is of the order of 0.2 eV cm^{-3} (for n_H =0.1 cm^{-3}) which is comparable to that of a 3μG field. Any strong variation in the field would affect the direction of flow.

Other evidence, for distances beyond a few parsecs, is rather scarce, but there is a suggestion of a drastic reduction in gas density beyond 3.5 pc (McClintock et al. 1978, Anderson and Weller, 1978) in some particular directions. Even further away fluctuations on the scale of tens of parsecs are expected because of field irregularities (Section 4.5).

3.5.4 Relevance to propagation of low energy cosmic rays

As far as propagation is concerned, the LISM data lead us to expect that the local propagation of cosmic rays will be

relatively smooth, at least over a few pc. Small scale irregularities in the magnetic field are, of course, expected and will cause some pitch angle scattering, but the energy density associated with such irregularities is expected to be a small fraction of the regular field. The local field direction is also expected to fix the direction of anisotropy. The Larmor radius of protons with energy E in a 3 μG field is $r(pc) = \frac{E(eV)}{2.7 \times 10^{15}}$, so that cosmic rays with energies up to about 3×10^{15} eV (r = 1 pc) should follow the field lines closely up to about this energy. The simplest and most easily measurable anisotropy (simple first harmonic vector) should be either parallel or antiparallel to the magnetic field if the field is slowly varying and the particle density is constant, in the frame comoving with the gas. Table 3.2 shows a list of the first sidereal harmonics for the most reliable data with 5.10^{11} eV < E < 10^{14} eV (see sections 6.1 & 6.2 for a detailed discussion). To allow a valid comparison to be made these values have been corrected by dividing by cos δ, allow for the declination of viewing. The results are shown transformed to the LISM frame. The data show a striking agreement in phase and similar amplitudes - only the Holborn result has a somewhat lower amplitude but this is at an energy where interplanetary deflections are expected to cause a reduction. Hence the upstream direction of the local cosmic ray streaming is close to 3 hours in the LISM frame, which value should be either parallel or anti-parallel to the local magnetic field. However, the discrepancies between the first and second harmonics must be resolved

Station	Viewing Declination	Median Energy (eV)	10^4 Anisotropy x amplitude	Phase (hrs)
Holborn	0^o	5×10^{11}	9.0 ± 1.7 7.7 ± 1.4	3.6 ± 0.7 (1) 3.7 ± 0.7 (2)
Poatina	42^oS	10^{12}	9.0 ± 2.7	3.2 ± 1.2
Norikura	36^oN	2×10^{13}	8.5 ± 0.8	2.2 ± 0.3
Musala	42^oN	6×10^{13}	12.2 ± 3.1	2.4 ± 1.0

Table 3.2 Equatorial (COS δ corrected) first harmonic phase and amplitude sidereal anisotropies in the frame of the local interstellar medium. The two Holborn measurements are (1) with and (2) without corrections for deflections in the interplanetary magnetic field.

before the result is considered final. Attempts to determine the declination of anisotropy have led to conflicting conclusions.

The uniformity of phase and amplitude up to 10^{14} eV not only support the idea of a smooth local field configuration, but also lead us to infer that there is not much difference in propagation between 10^{11} eV and 10^{14} eV. Consequently the age of cosmic rays should not be dissimilar at the two energies.

It should be noted that only in the gas frame are the cosmic rays expected to follow the field lines. In other frames there will be a small electric field present due to the motion of the magnetised gas, of order $\frac{v}{c}$ B, which also changes the motion of the particles. The magnetic field will be reduced by a similar amount ($\frac{v}{c}$B) but its direction will not change significantly. At higher energies, of course, the direction of anisotropy will correspond to the average field direction over bigger distances than referred to here and changes are expected.

CHAPTER 4

ORIGIN OF COSMIC RAYS

4.1 Sources and Propagation

When considering the origin of cosmic rays, a distinction must be made between the various components. Referring to the major nucleon and electron components, although a case can be made for at least part of the nucleon component being of extragalactic origin, the electron component is certainly of Galactic origin. In order to see this, the energetics of production and propagation must be considered.

Dealing with the electron component first, and considering the inverse compton effect (ICE) of electrons on the Universal 2.7 K radiation field, the maximum distance an electron can travel (assuming rectilinear motion) in the photon field is

$$R(\text{cm}) = \frac{4.7 \times 10^{23}}{(W_{ph} + H^2/_{8\pi})E(\text{eV})} \qquad \text{(Ginzburg \& Syrovatskii 1964)} \quad 4.1.1$$

where W_{ph} is the energy density of the black-body radiation and starlight. Taking the lower term to be 4×10^{-13} ergs cm^{-3} and assuming an energy of 30 GeV, then $R \simeq 4$ Mpc - the distance of Cen A. Electrons of energy below 30 GeV could just reach us from nearby active galaxies. That the electron spectrum shows no break at this energy leads us to suppose that few, if any, electrons are of extragalactic origin.

The total Galactic radio emission is of the order of 10^{38} ergs s^{-1} so, assuming a power input of 10^{39} ergs s^{-1} and a lifetime of $10^7 - 10^8$ years, the total energy in electrons is $\sim 10^{54}$ ergs.

The Synchrotron data also strongly favour a Galactic origin.

Turning to the main nucleonic component, it is still possible to argue in terms of either a Galactic or an extragalactic origin, and each has different implications for anisotropy. If it is first assumed that at least some particles of every energy are extragalactic, then some indication of the relative contributions (the ratio extragalactic/Galactic) may be expected from estimates of the relative importance of Galactic and extragalactic components of the electromagnetic spectrum in general. Table 4.1 shows the ratio for different frequencies, though in most cases the two components are hard to separate and the values must be regarded as approximate. On this basis, with the exception of starlight, it appears as though extragalactic sources should contribute a not inconsiderable amount of the local cosmic radiation. This is also true if galaxies contribute according to their mass. However, the effect of the Galactic magnetic field (unimportant for photons) has been neglected. Galactic particles will, to some extent, be trapped by the field so that their contribution will be correspondingly enhanced. Assuming a lifetime of 2×10^7 years (at $< 10^9$ eV - Section 4.7) and a Galactic lifetime of free escape of 10^4 years (the light travel time for a reasonable Galactic halo) then we expect an enhancement of Galactic particles by a factor of about 2,000 and Galactic sources should predominate. At higher energies, however, the trapping factor presumably falls so that the extragalactic component could become more important. Having said this, it is still possible that extragalactic particles predominate at all energies if Galactic sources are unusually inefficient at production.

Component	Ratio Extragalactic to Galactic
Synchrotron Radiation (at 150 MHz)	0.1
Starlight	0.02
X-ray (at (2-10(KeV)	2.5
γ-ray (for > 100 MeV)	0.5
Mass (yield α M/r^2)	0.1

Table 4.1 Approximate ratio of energy densities for extragalactic and Galactic Components. The values are of necessity approximate.

4.2 The Energetics of Origin

To sustain the locally observed energy density of cosmic rays (about 1 eV $cm^{-3} \simeq 10^{-12}$ ergs cm^{-3}) the power Q required is

$$Q = \frac{Wc\ M_g}{X} \qquad 4.2.1$$

where M_g is the mass of the interstellar gas and X is the 'grammage', about equal to 5 g cm^{-2}. Taking $M_g \simeq 3 \times 10^{42}$ - 10^{43} grams we have $2.8 \times 10^{40} < Q$ ergs $s^{-1} < 9 \times 10^{40}$. The Galactic origin hypothesis favours supernova explosions as the most likely sources, particularly of higher energy particles. Determining the rate of Galactic supernova explosions is therefore important and 'best estimates' of this factor range from 1 per $11^{+\ 14}_{-\ 4}$ years (Tamman 1977) to 1 per 150 years (Clark and Caswell, 1976), while data on external galaxies suggests 1 per $20^{+\ 20}_{-\ 10}$ years. To maintain W, the energy released in cosmic rays must, therefore, be about 7×10^{48} - 6×10^{49} ergs per Supernova. The total energy in a Supernova blast is of the order of 10^{50} - 10^{51} ergs so an efficient conversion of energy is needed. Consideration of the composition of cosmic rays favours type II Supernova as the more important source. Galactic Supernovae are just able, then, to supply the necessary energy to maintain the locally observed energy density.

Other likely Galactic sources include supernova remnants, pulsars, flare stars and white dwarfs, all of which have a spatial distribution that correlates with the Galactic

disc - the number of sources increases towards the Galactic center and falls further away from the plane. In this respect observations of gamma rays (from cosmic ray protons and nuclei of a few GeV energy) are very much in favour of a Galactic origin (Strong et al., 1977). One may also argue on aesthetic grounds that the sources of cosmic ray electrons should be the same as those for nucleons. Note that it is unlikely that second order Fermi acceleration in the interstellar medium (as opposed to operating in supernova remnants) will make a significant contribution to the energetics.

The main problem with an extragalactic Universal origin model lies in maintaining the local energy density throughout the Universe. The visible mass of galaxies corresponds to some 3×10^{-31} g cm^{-3} when spread over the entire Universe, so that to sustain 1 eV cm^{-3} a very efficient mechanism of production (0.5%) would be required. Likely sources in this scheme are radio galaxies, Seyfert galaxies, Quasars and rich clusters of galaxies (such as Coma or Virgo).

One possibility to counter the energy argument and yet include extragalactic origin is to demand that Galactic sources provide particles up to a given energy but are absent above this energy. If we demand that Galactic sources do not contribute above 10^{10} eV, then the energy density to be maintained can be reduced to $\sim$ 0.1 eV cm^{-3} throughout the Universe (see later). However, this energy density is still 20 to 100 times the average energy density of Starlight and would still need quite an efficient energy conversion mechanism. If extragalactic sources generated only particles

above $\simeq 10^{12}$ eV then only $\sim 10^{-2}$ eV cm^{-3} need be maintained, which may not be beyond the realms of the possible on a Universal scale.

It appears from the above arguments that, on balance, it is not easy to construct models in which the bulk of the observed radiation is extragalactic. However, purely Galactic origin models also encounter difficulties in explaining all the features of the observed data and the origin problem is still not fully resolved, even at low energies.

4.3 High Energy Galactic Origin

At the highest energies a Galactic origin would be indicated by a marked anisotropy with a peak in the direction of the Galactic plane, whereas the evidence suggests that particles at these energies arrive at high Galactic latitudes (Edge et al., 1978). Certainly, if the primaries are protons and halo fields are weak then a Galactic origin must be ruled out. A Galactic origin may still be possible if the particles are of high mass but Watson and Wilson (1974) have provided evidence that many of the primaries are indeed protons, though this is by no means absolutely certain. The radio synchrotron data are suggestive of a significant magnetic field, but it seems unlikely to be of sufficient strength to prevent high energy particles from escaping. Parker (1976) has suggested that the Galactic field is effectively fixed to the disc by gas clouds. If this is true then not only should halo fields be small but, in addition, one may expect field cancellation over scales large enough to ensure that particles above 10^{18}eV are not deflected back

into the Galaxy.

A stronger argument against Galactic origin comes with the flattening of the primary energy spectrum near 10^{19} eV, which forms the topic of a later chapter. This is hard to explain on a Galactic basis since containment should, if anything, decrease with increasing energy, as appears to be the case with the steepening of the energy spectrum at $\sim 10^{15}$ eV (see Figure 4.1).

There are also problems with producing the highest energy particles in Galactic sources: theoretical models of Supernova explosions, the most favoured source of Galactic particles, have difficulty in explaining how particles may be accelerated to energies above 10^{17} (Chevalier 1977).

On the whole, though not entirely ruled out, Galactic origin models at high energies ($E \gtrsim 10^{17}$ eV) are considered unsatisfactory: the evidence is firmly in favour of extra-galactic origin.

4.4 High Energy Extragalactic Origin

The energy density problem presents no difficulties if only the highest energy particles are regarded as extra-galactic. Above 10^{17} eV it is possible that cosmic rays are produced in extremely rare, energetic explosions and that in our Galaxy there has been no such event in the lifetime of the particles. In this case the observed high energy particles will be exclusively of extragalactic origin.

Alternatively, particles may be confined in Galactic systems such as the local Supercluster (centred on the VIRGO cluster). Models of this type will be considered later.

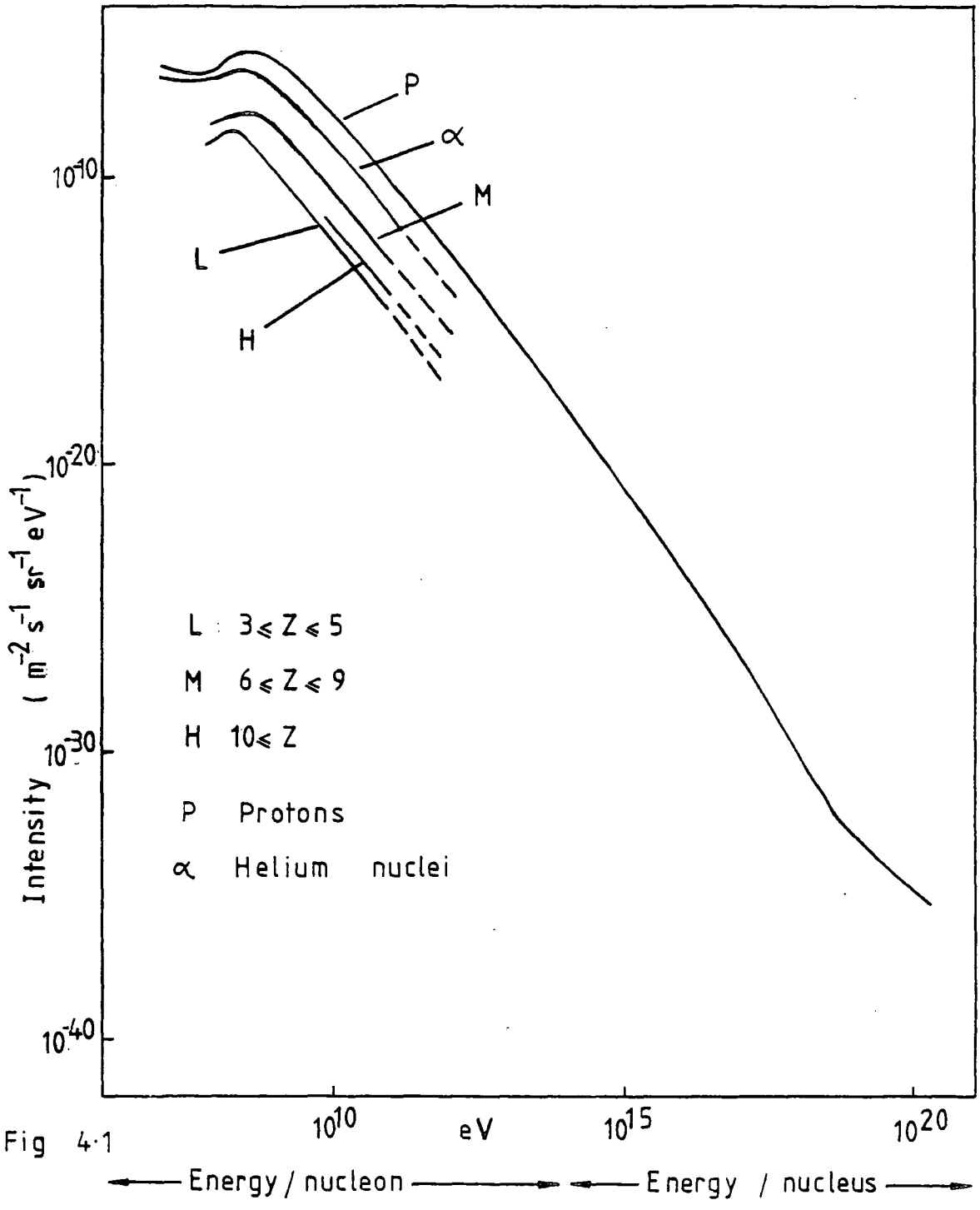

Fig 4·1

The primary differential energy spectrum of cosmic rays (from Wolfendale, 1975) as measured by a variety of techniques and corrected for geomagnetic effects.

Closer examination of the region near 10^{15} eV shows a change in the value of the spectral index of about 0·6 .

Note that by itself, confinement to clusters does not necessarily allow all the local particles to be extragalactic. If the local supercluster (co-ordinates of centre: $\ell^{II}, b^{II} = 284^{o}, 74^{o}$, d = 19 Mpc) is considered to be the source of cosmic rays, then 1 eV cm^{-3} must be maintained over some $\sim 10^{77}$ cm^{3}. The number of (visible) galaxies in Virgo has been estimated at 2,500 (Allen 1973) so each galaxy should have to provide $\sim 4 \times 10^{61}$ ergs : i.e. be of radiogalaxy strength.

An acceptable picture, then, is one in which the majority of particles are Galactic in origin while the high energy particles ($E \gtrsim 10^{17}$eV) are contributed by external sources.

In the rest of what follows we examine the observational evidence favouring this hypothesis.

4.5 Propagational Aspects and Anisotropy

The interstellar magnetic field ensures that cosmic rays (whether of Galactic or extragalactic origin) reach us only after considerable deflections from their original paths, and in both instances internal Galactic propagation effects are important. The gyroradius of a relativistic particle with charge Z, energy E in a field of strength B (μG) is given by

$$r_L \text{ (pc)} = \frac{E(eV)}{Z \times 9 \times 10^{14} \times B} \qquad 4.5.1$$

Over the range we are concerned with (10^{11} - 10^{20}eV) this means that r_L varies from about 3×10^{-5} pc - 30 Kpc in a typical 3 μG field. More significant, particles with $E \gtrsim 5 \times 10^{17}$eV have a Larmor radius which exceeds that of the thickness of the Galactic disc ($\sim$ 100 - 400 pc) while particles

with $E \lesssim 10^{14}$ eV should be closely bound to field lines, at least over several rotations. The disc appears to be at least 10^6 gyroradii for 10^{11} - 10^{12} eV particles, so that virtually all the information about the individual sources is lost at these energies. Hence, particularly for $E < 10^{14}$eV, we are more likely to detect an "anisotropy of propagation", and it is only at the higher energies or if neutral particles are involved that we may expect to see an "anisotropy of sources". For most of the energy range, then, we expect propagation conditions to determine the directional distribution, together with only some general features of the source distribution.

Large and small scale variations of the magnetic field are important in propagation. Low energy particles will not 'see' the field change significantly over a few rotations, but for particles in the upper energy range the paths traversed will hardly be helical, and may not complete even a single revolution in the regular field. A gradual changeover should take place somewhere between 10^{14} - 10^{17} eV. With field irregularities on the scale of 10 - 50 pc (Wilkinson and Smith 1974) we might expect a change at around 10^{16} eV.

Below 10^{14} eV, where particles are tracing field lines, pitch angle scattering will result from interactions of particles with the fluctuating component of the field as will small displacements of the center of gyration. At these energies the distribution should be axially symmetric about the field, in other words depending only on the pitch angle. Axial symmetry will strictly only be valid in the

frame of reference comoving with the gas (into which the field lines will be frozen). For an observer moving with velocity $\underline{v}$ with respect to this frame, the second and higher harmonics will appear almost unaltered, but the first (vector) harmonic $\underline{\lambda}_{rest}$ will be modified by a Compton-Getting vector

$$\underline{\lambda}_{CG} = (2 + \gamma)\frac{\underline{v}}{c} \qquad 4.5.2.$$

where γ ($\simeq 2.6$) is the index of the differential energy spectrum. $\underline{\lambda} = \underline{\lambda}_{rest} + \underline{\lambda}_{CG}$ will not in general be parallel to the magnetic field. Consequently axial symmetry will not be preserved if 2nd or higher harmonics are present. However, by correcting for $\underline{\lambda}_{CG}$ (our motion with respect to the gas is known) we can restore the symmetry.

The spectrum of small scale magnetic field fluctuations is critical for the energy dependence of propagation below 10^{14}eV. If there were no such fluctuations then particles would probably follow the field lines adiabatically such that $\mathrm{Sin}^2\phi/B$ = const where ϕ is the pitch angle (Pacholczyk, 1970), and either be reflected ($\mathrm{Sin}^2\phi = 1$) or escape. Even here the separation of the field lines will be fast enough to exercise a smoothing effect since local particles would have travelled widely different paths in the past. In this case particles which are closely following field lines should have a greater chance of escape since they are less easily scattered at boundaries. Hence viewing along the field line, the direction of easy escape, fewer particles would be detected. This "loss cone" effect (Nagashima et al., 1977) would produce both first and second harmonics. If the scale

of the mean free path were very much less than the"scale of divergence" (say the scale for the field to halve) then only first and second harmonics should contribute greatly. If, however, the scales are approximately the same, higher harmonics will be significant.

It is, however, unlikely that fluctuations are missing to the extent above where the pitch angle determines the escape probability. Rather, it is probable that Alfven waves (electromagnetic plasma waves) play a part in scattering particles even though their energy density may be small compared to the main component. For low energy particles, scattering results in the cosmic rays resembling a high energy gas. The spectrum of wavenumbers $k = {}^{2\pi}/_{\lambda}$ (neglecting sources and dissipation of turbulence) is expected to be given by a power law

$$F(k)\ dk \propto k^{-\gamma}\ dk \qquad 4.5.3$$

where γ may equal $\frac{5}{3}$ (Kolmogorov spectrum) or $\frac{3}{2}$ (Kraichen spectrum). Resonant scattering occurs when waves of wavelength comparable to $2\pi r_L$ are present- the mean free path between scatterings is then proportional to $E^{2-\gamma}$. This leads to a decreasing lifetime and hence to a proportionally increasing anisotropy, but at present the uncertainties in the amplitude of the wave spectrum, and the exact wavenumber when dissipation of turbulence becomes important prevent any real conclusions being drawn. At the moment, then, anisotropy measurements above 10^{11} eV and data on the interstellar medium provide much better information on propagation effects than theoretical predictions.

4.6 Propagation Models

Propagation parameters derived from anisotropy studies may be compared with other parameters if appropriate models for propagation are available. Daniel (1977) has classified these models into three main types, the Disc Halo model, the Leaky Box and the Closed Galaxy model.

In the Disc Halo model (see e.g. Ginzburg and Ptuskin, 1976), the cosmic ray sources are assumed to be distributed uniformly throughout the Galactic disc. Particles diffuse out of the disc and into a halo of diameter 10-20 Kpc and essentially random walk by scattering off field fluctuations in the (weak) halo field. On reaching the halo boundary the particles are assumed lost. If the halo gas density is assumed to be $\sim$ 100 times lower than the disc density then the age of cosmic rays should be about 10^8 years. Low anisotropies ($< 0.1\%$) are predicted on this model, and the grammage can be explained in the GeV region.

The Leaky Box model leads to cosmic ray lifetimes of 10^6 years and 5 gm cm^{-2} of matter traversed. It gives higher anisotropies ($>0.7\%$) than the Disc halo model which are not consistent with the low anisotropies observed below 10^{14} eV. However, as will be seen later, such large anisotropies may not be totally unexpected (Marsden et al. 1976).

Finally, in the closed Galaxy model (Rasmussen and Peters, 1975), it is assumed that sources are distributed in the Spiral arms but particles may drift readily along the arms. In addition, particles escape into the halo where they may not escape but lose energy by interaction with the ISM.

This leads to an "old" isotropic component throughout the Galaxy and a "young" component, which dominates at lower energies and is confined to the arms. The anisotropy of the young component rises with energy, as is observed.

These models will be distinguishable as more accurate measurements are made. In particular, the age of cosmic rays as deduced by different methods must be reconciled. The Be^{10} measurements favour the Disc-Halo model while the composition age favours the Leaky Box model.

4.7 Cosmic Rays Below 10^{11} eV

Below 10^{11} eV, examination of the chemical composition of cosmic rays can give information on two important characteristics - the lifetime and the energy dependence of grammage (x) or path length traversed by the particles. Examination of the fraction of light elements (Li^3,Be^4,B^5) in the flux reveals the amount of interstellar matter traversed while the proportion of radioactive nuclei in the flux (Be^{10},Mn^{53},Np^{237}) enables the lifetime of the particles to be derived.

Cosmic rays are known to be extremely overabundant in the light elements, Li, Be and B, compared with the measured solar and meteoric abundances (Rasmussen, 1975). These nuclei are unlikely to be produced directly in sources since they would be "burnt up" in nuclear reactions. However, carbon, nitrogen and oxygen, by interactions with the interstellar medium, can produce these light elements, the proportions of which give the amount of spallation of the parent nuclei. The measurements are consistent with a mean grammage of

5 - 10 g cm^{-2} at 1 GeV/nucleon, decreasing to about 1.5 g cm^{-2} at 100 GeV/nucleon (Juliusson, 1974, Caldwell and Meyer, 1977, Lezniak et al., 1977). The grammage may be represented by a power law $< x > \propto E^{-\beta}$, $0.3 < \beta < 0.6$, in this range but this remains in some doubt (Fontes et al., 1977). The path length distribution at a few GeV is apparantly exponential although there appear to be deficits of particles with short path lengths $x < 1$ g cm^{-2} (Garcia-Munoz et al., 1977, Shapiro and Silverberg, 1971). This implies that 'young' particles derived from local sources may be relatively scarce, a consequence which is examined later. Recent calculations (Fontes et al., 1977) suggest there may be two distinct propagation regions, one below 5 GeV/n (with leakage mean free path $\simeq$ 5.5 g cm^{-2}) and one between 20 - 100 GeV/n (1mfp $\simeq$ 1.7 g cm^{-2}), again indication of a lack of local sources. Composition measurements would be difficult, but useful, at higher energies.

The composition measurements give an estimate of the lifetime since $x = \rho c T_{CR}$. Using a typical disc density of $\rho \simeq 1$ cm^{-3} we obtain a lifetime of $T_{CR} \simeq (1\text{-}4) \times 10^6$ years. With a substantial halo, however, and assuming that the particles spend most of their life in the halo, then a better estimate for ρ is $\sim 10^{-2}$ cm^{-3} so that $T_{CR} \simeq (1\text{-}3) \times 10^8$ years.

The lifetime may be checked directly by using radioactive nuclei as a 'clock'. Data based on Be^{10} survival at about 100 MeV/n give $T_{CR} \simeq 1.6^{+2}_{-.8} \times 10^7$ years (Garcia-Munoz et al., 1977). At higher energies, the Be/B ratio gives a lower limit of 10^7 years (Webber et al., 1977) while more recent measurements (Webber & Kish, 1979) give $2.7^{+2.2}_{-.8} \times 10^7$ years.

Combined, the most probable lifetime is about 2.1×10^7 years. It should be noted that these ages may well be underestimates since they are derived using particular models of propagation - what is of real importance is the surviving fraction of Be^{10} which can then be used to predict the age for a given model. This is of the order of 0.15 between 200 and 300 MeV/nucleon.

It appears, then, that the low energy cosmic rays spend a considerable time in regions of lower gas density than the disc, but not as great a time as a spherical halo/grammage model would suggest. This hypothesis is supported by evidence from the relatively high Synchrotron radiation intensities observed at high Galactic latitudes which suggests that cosmic ray electrons are present at large distances from the plane. These electrons are certainly of Galactic origin (section 4.1).

Gamma ray observations provide data on the large scale distribution of 1 - 10 GeV cosmic rays. Combined with data on the gas density, the observations suggest a fall off in the cosmic ray density in the direction of the Galactic anti-center (Strong et al., 1977, Strong et al., 1978). The Supernova remnant distribution closely follows that of the implied cosmic ray density (as do the distributions of other possible sources) so that it is assumed that low energy cosmic rays propagate only a small distance (< 2 Kpc) in the Galactic plane. An asymmetry is also shown in the observations; the integrated cosmic ray density along the line of sight towards $\ell^{II} = 270^o$ (Vela direction) is 2.3 times higher than towards $\ell^{II} = 90^o$.

These data, although concerned with energies < 10^{11} eV have some relevance for propagation at higher energies. The constancy of the LISM wind direction and velocity (section 3.5.2) and the constant spectral slope of the differential energy spectrum (from 10^9 - 10^{14} eV)imply a smooth change of propagation parameters with energy. It is by no means certain, however, that the path length (and hence age) decreases at the same rate above 10^{11} eV or changes more slowly while source intensities decrease. A decreasing lifetime, as a result of resonant scattering, does not occur below $\sim 10^{11}$ eV since damping becomes progressively stronger as k increases. Any turbulence should be the result of excitations induced by the streaming of the cosmic rays themselves - such self-excited waves might restrict escape far from the plane while scattering nearer the plane might be less important.

4.8 Anisotropy for a Galactic Origin

An estimate of the first harmonic amplitude of a Galactic anisotropy is given by

$$\lambda = T_{de}/T_{conf.} \qquad 4.8.1$$

where T_{de} is the direct exit time (for a relativistic neutral particle such as a photon) for a particle to leave the Galaxy and T_{conf} is the confinement time. This equation is based on the assumption that there is not much more streaming than necessary for transporting cosmic rays from the inner (source) regions to the boundary where they escape.

For a halo of 5 - 10 Kpc, T_{de} will be of the order of a few x 10^4 years. T_{conf} will decrease with energy if

$\langle x \rangle \propto E^{-\beta}$. Between 10^{11} and 10^{14} eV the lifetime is likely to vary as $E^{o} - E^{-0.5}$. The anisotropy will then be proportional to $E^{o} - E^{0.5}$. At 10^{9} eV the lifetime is 2×10^{7} years and thus it may fall to 10^{6} years at 10^{14} eV. The anisotropy expected is then of the order of 10^{-4} to 10^{-3} though this will vary considerably with position in the Galaxy, depending on the source distribution and field structure. In or near the Galactic plane smaller anisotropies are expected due to the symmetry of the streaming. This will in part be compensated by the effects of any nearby sources or field irregularities, which act to increase the anistropy.

There is also an effect specific to the magnetic field and unrelated to escape : there will be an anisotropy (streaming) in the direction $\underline{B} \times \underline{\nabla} U$ where U is the cosmic ray density. The equivalent component of $\underline{\lambda}$ will be in the direction $\underline{\nabla} U \times \underline{B}$ and of approximate magnitude $r_L \frac{|\underline{\nabla} U|}{U}$ where r_L is the Larmor radius.

At higher energies, between 10^{14} - 10^{17} eV, higher anisotropies are expected as field effects become less dominant. Bell et al. (1974) have predicted anisotropies by examining the energy dependence of the scattering on magnetised interstellar clouds. From this, the energy dependence of the lifetime was predicted and with it the corresponding anisotropy. These predictions were only slightly in excess of the experimental observations.

Above 10^{17} eV individual Galactic sources could possibly be detected and might even give a large contribution to the

observed flux. However, above this energy events become increasingly scarce (and point sources harder to detect). There are no reliable predictions for the expected anisotropy in this regime and it is here where, as remarked earlier, an extragalactic origin seems more likely.

4.9 Extragalactic Anisotropy

With an extragalactic origin smaller anisotropies are expected even in the 'local cluster models' in which nearby clusters or groups of Galaxies are expected to be the dominant contributor to the local flux. There may be a significant streaming of particles between Galaxies but scattering by Galactic fields will reduce the Galactic anisotropy considerably, except at the highest energies where scattering may be neglected. The reduction expected is given by $K \frac{T_{dt}}{T_{res}}$ 4.9.1 where T_{dt} is the direct transit time (c.f. T_{de} in section 4.8) and T_{res} is the Galactic residence time (c.f. T_{conf}). K depends on the field geometry but is of order unity.

As mentioned previously, a true universal flux may be expected to be isotropic with respect to the frame of the universal microwave background radiation. Smoot et al. (1977) have measured the velocity of the Galaxy relative to this frame directly, and found a velocity of 603 km s^{-1} towards $(\ell^{II}, b^{II}) = (261^{o}, 33^{o})$. This would give, from the Compton-Getting effect, an anisotropy of 0.9% external to the Galaxy. This value will be reduced by a factor of about 10^{3} at 10^{11}eV and by 30 - 10^{3} at 10^{14}eV using the equation above. A

further reduction is expected since allowing for Galactic rotation the solar velocity is only 390 ± 60 km s^{-1} (towards $(\ell^{II}, b^{II}) = (248^{o}, 56^{o})$) relative to the universal frame. For the highest energy particles, assuming they are not deflected significantly by the Galactic field, the anisotropy will therefore be of the order of 5×10^{-3}, but local anisotropies will probably not exceed 10^{-4} at 10^{14}eV and 10^{-5} at 10^{11}eV, a result of the long measured residence times. The observed anisotropy values in the range $5 \times 10^{11} - 10^{14}$eV are, as will be seen later, approximately 5×10^{-4} over the range : this constancy gives a strong argument against an extragalactic origin. Even if an extragalactic component were important for $E_p > 10^{14}$eV it would be unlikely to cause an observable anisotropy up to 10^{18}eV where the Galactic field is in effect transparent to protons.

One final note here; the Galactic motion as measured by Smoot et al. is not in agreement with the measurements of Rubin et al., (1976) concerning Galactic motion with respect to the local group of galaxies. The obvious interpretation is that the local group is not stationary with respect to the black-body field.

4.10 General Direction for Anisotropy

Figure 3.2 shows the important directions relevant to anisotropy work for both a Galactic and Metagalactic origin. Assuming a Galactic origin, lower energy particles are expected to follow field lines and stream from more to less dense regions. This would make the inward spiral arm direction SPIN) the best general direction for the maximum

and presumably the local field direction associated with this sense would give the actual direction. The apparent trend of field direction with distance suggests that there should also be a change of streaming direction with energy. In addition, the streaming could be at 180^{o} from the SP(IN) direction (towards SP(OUT)) if a local reverse gradient were established as a result of the strongest source being in that direction. Alternatively, if there were a radial inward density gradient then a $\underline{B} \times \underline{\nabla} U$ type of anisotropy would be expected with a maximum towards $b^{II} = 90^{o}$ (for a field pointing towards $\ell^{II} = 90^{o}$). This component may be important from 10^{14} to 10^{17}eV where particles are not so confined to the spiral arm fields. For particles > 10^{17}eV the Galactic center (GC) would be a good direction to expect a maximum, and in addition there would be an enhancement towards the Galactic plane.

With a mixed or purely extragalactic origin, if the high energy particles are produced in Galaxies associated with the local supercluster, then a maximum in that direction (SGC) would be evident. With a purely Universal origin and at lower energies, the direction of motion of the Sun (SBB) relative to the black body radiation would give the direction of maximum, though Galactic fields would alter the anisotropy considerably.

The deflection of extragalactic particles in the Galactic field can be estimated for the most important case of incidence at high Galactic latitudes. For a particle of charge Z, and energy E(eV) the deflection is

$$\theta = (0.5 - 5)\ Z\ 10^{20}/E(eV) \text{ degrees.} \qquad 4.10.1$$

In the best instance, for protons of energy > 10^{19}eV, it therefore appears possible to identify specific extragalactic sources - assuming that extragalactic fields are negligible. With an extragalactic field of B_E(nG) and for a source r(Mpc) distant, then the deflection of a particle of charge Z and energy E(eV) will be

$$\theta_D \simeq 3 \times 10^{19} \; Z \; B_E(nG) \; r/E \qquad 4.10.2$$

assuming motion perpendicular to the field. If the field has n equal "cells" over r with a random orientation in each, however, then θ_D is reduced by a factor $\sqrt{n}$ (Kiraly et al., 1975).

The theoretical evidence suggests $B_E \lesssim 1$ nG, while Kronberg, (1977), using data from the rotation measures of Quasars, found that $B_E \; r^{\frac{1}{2}} < 9$ nGMpc$^{\frac{1}{2}}$ (with $H_o = 50$, $\Omega = 1$ and a completely ionised intergalactic medium). If this were to hold to a likely nearby source, M87 (r ≃ 20 Mpc), and there were no field irregularities then the deflection would not be greater than 15^o for protons of 10^{20}eV. This is of course an overestimate since the field would contain some irregularities and is unlikely to run perpendicular to the line of sight. It appears, then, as though extragalactic sources should also be detectable.

However, the magnetic field in clusters of Galaxies is almost certainly much larger than that suggested by the Kronberg relation. X-ray data imply intergalactic gas densities of 10^{-4} atoms cm^{-3}, and in some clusters densities as high as 10^{-2} atoms/cm^3. If equipartition of energy held, then fields of 0.1 μG would be expected. If fields as high as this were present throughout the Local Supercluster then identification of individual sources would be

impossible.

4.11 Implications of Higher Harmonics

It is usual with propagation models, particularly at low energies, to consider only the first vector harmonic, however both the Musala and Norikura experiments (10^{13}-10^{14} eV) observed significant second harmonics (supported by tests) which should be incorporated into anisotropy theory. The detailed angular structure of the anisotropy potentially carries information on the scattering processes in the interstellar field. Kota and Somogyi (1977) have considered several mechanisms which may be responsible for generating higher harmonics. Note that the local characteristics of the interstellar field may have maximum influence in determining the higher harmonics.

The second order anisotropy may be calculated using a simple diffusion model extended to include the second order moments of the usual transport equation. If λ is the scattering mean free path and r the characteristic length over which the cosmic ray density varies then the amplitude of the n^{th} harmonic will be of the order $(\lambda/r)^n$. Higher harmonics consequently rapidly become negligable.

Earl (1975) has, however, shown that higher harmonics with amplitudes of the same order as first harmonics arise if an anisotropic pitch angle diffusion model is adopted. Here, the amplitude of higher harmonics depends on scattering deviations from the isotropic norm and on the field changes over the distance λ. Isotropic scattering generates harmonics in a similar manner to diffusion models (for a constant background field) while anisotropic scattering (with a uniform magnetic field) generates large amplitude odd

harmonics, which contribute to lower (special) harmonics. Lastly, if the scale of variation of background field is considerably smaller than the scale for scattering, large even harmonics may be generated by adiabatic focussing. As a result, the measurements of second harmonics, though difficult, are useful in limiting the propagation modes and may reveal aspects of the detailed structure of the very local magnetic field.

CHAPTER 5

OBSERVATIONAL AND STATISTICAL ASPECTS

5.1 Observational Aspects

5.1.1 The various types of measurement Ideally the angular distribution of cosmic rays should be measured outside the sphere of solar influence - but at present this is clearly impossible and suitable detectors are too small to gain sufficient statistics to detect anisotropies above 10^{11}eV. The background of lower energy particles is difficult to remove and the counting rates too low to give any meaningful results.

Ground based detectors collect many more events but deducing the nature of the primary or its energy is difficult since only the secondary decay products, produced in the atmosphere, can be measured. In particular these products consist of three main components, the nucleon, meson and electromagnetic secondary radiation. To derive the energy of the primary, models of shower development must be employed and atmospheric/instrumental effects allowed for. It is this that leads to uncertainty in the measurements.

Underground muon detectors are used below $\sim 10^{12}$eV and provide valuable information. The background from lower energy primaries is eliminated by absorbtion of the equivalent low energy muons in the rock above the apparatus. Typical depths are 10 to 100 hg cm^{-2}. Unfortunately, above a few 10^{12}eV the muon intensity is not sufficiently high for adequate statistics since the higher energy secondary pions produced interact in the higher atmosphere instead of decaying to muons.

Small air shower arrays at mountain altitudes are used to observe particles of primary energy 10^{12} - 10^{15}eV. High counting rates are possible which makes this a useful range in which to accurately determine anisotropies. However, not much information can be gained about individual events except at slightly higher energies where the count rate is lower. The arrays rely on simple coincidence techniques and are normally run for several years. Beyond 10^{17}eV, complex giant air shower arrays are required. They yield good directional and primary energy information for individual showers. At such high energies, if atmospheric effects are corrected for, the detection of anisotropies is only limited by the statistics of arrival times.

Since the cosmic radiation is nearly isotropic, stable equipment is needed in anisotropy work. Therefore, detectors are stationary with respect to the earth, relying on the earth's rotation to scan in R.A. at constant declination. Intercalibration of detectors at different declinations is near impossible at the accuracy necessary. In essence, then, only the equatorial components of the anisotropy can be measured from the sidereal intensity variation. The polar component cannot, of course, be measured (but see Section 6.1).

5.1.2 Harmonic analysis of anisotropies Nagashima et al. (1972) have noted the importance of spherical harmonics $P_{km}(\delta,\alpha)$ in anisotropy work, and their relation to multipole expansions similar to equation 2.1.6. Multipole terms of order k

give spherical harmonics $P_{km}(\delta,\alpha)$ with $|m|<k$, P_{km} contributing to the m^{th} sidereal harmonic.

For m = o there is hence no variation (these terms contributing to the unobservable polar component). Note that if there is only a simple vector anisotropy then a measurement at just one declination is all that is required to measure the equatorial component, while if second order terms are also present, then two measurements at differing declinations are required to separate the contribution to the vector harmonic from the tensor term, called the first special harmonic. The second harmonics at equal but opposite declinations should then be the same.

A complete spatial description of the anisotropy is not possible even with measurements at all declinations - the polar component at the least remains unknown. If we may assume axial symmetry, for which we have a firm theoretical basis below 10^{14}eV, then there is some improvement in the situation. The symmetry axis of the distribution should then be along the direction of the local magnetic field. We then have, from equation 2.1.6 the anisotropy function reduced to

$$\lambda(\underline{e}) = \lambda^{(1)} \text{ Cos } \theta + \frac{3}{2}\lambda^{(2)} (\text{Cos}^2\theta - \frac{1}{3}) + \frac{5}{2}\lambda^{(3)}(\text{Cos}^3\theta - \frac{3}{5}\text{Cos}\theta) + \cdots \quad 5.1.1$$

where $\text{Cos } \theta = (\underline{e} \cdot \frac{\underline{B}}{B})$. The function is completely specified by a knowledge of the field direction and the $\lambda^{(\nu)}$ values. The constants are chosen so that with Cos θ = 1 (maximum value), the $\lambda^{(\nu)}$ values give the 'amplitude' or maximum

deviation from zero. Ignoring terms of order $\nu \geq 3$ and writing (in equatorial co-ordinates) $\underline{e}$ in terms of α, δ and $\hat{\underline{B}}$ in terms of α_o, δ_o (as in equation 2.1.2) we have

$$\lambda(\underline{e}) = \{\lambda^{(1)} \cos\alpha (\cos\delta \cos\alpha_o \cos\delta_o) + \frac{3}{2}\lambda^{(2)} \cos\alpha (2 \cos\delta \cos\alpha_o \cos\delta_o \sin\delta \sin\delta_o) + \lambda^{(1)} \sin\alpha (\cos\delta \sin\alpha_o \cos\delta_o) + \frac{3}{2}\lambda^{(2)} \sin\alpha (2 \cos\delta \sin\alpha_o \cos\delta_o \sin\delta \sin\delta_o)\}$$
$$+ \{\frac{3}{2}\cos^2\alpha\, \lambda^{(2)} (\cos^2\delta \cos^2\alpha_o \cos^2\delta_o) + \frac{3}{2}\lambda^{(2)} \sin^2\alpha (\cos^2\delta \sin^2\alpha_o \cos^2\delta_o) + \frac{3}{2}\lambda^{(2)} \cos\alpha \sin\alpha (2 \cos^2\delta \cos\alpha_o \cos^2\delta_o \sin\alpha_o)\}$$
$$+ (\lambda^{(1)} \sin\delta \sin\delta_o + \tfrac{1}{2}\lambda^{(2)}) \qquad 5.1.2$$

Considering first order terms in α with $A = \cos\delta \cos\delta_o$ $B = 3 \sin\delta \sin\delta_o \frac{\lambda^{(2)}}{\lambda^{(1)}}$ and differentiating with respect to α we have

$$-\sin\alpha\, \lambda^{(1)} A \cos\alpha_o (1+B) + \cos\alpha\, \lambda^{(1)} A \sin\alpha_o (1+B) \qquad 5.1.3$$

which has a maximum (or minimum) when $\tan\alpha = \tan\alpha_o$ or when $\alpha = \alpha_o + \pi n$.

Similarly, by considering second order terms in α the second harmonic can be shown to have a maximum when $\alpha = \alpha_o + \pi n$ or $\alpha = \alpha_o + n\pi - \frac{\pi}{2}$. Indeed, all harmonics of an axially symmetric distribution have maxima at $\alpha = \alpha_o$ so that in principle a single measurement at a given declination would reveal if the distribution were axially symmetric. This phase relation applies only to the "rest frame" for cosmic rays (the frame of the local interstellar medium) so the observed first harmonic should be corrected for solar motion relative to that frame. Note that the second harmonic

(tensor) term in equation 5.1.2 contributes two terms to the first harmonic and these we call the special first harmonic. If we consider a declination $-\delta$ then these terms change sign since $\mathrm{Sin}(-\delta) = -\mathrm{Sin}(\delta)$. If, therefore, we measure a first harmonic A + B in the Northern hemisphere and in the South A - B, the first special harmonic, B, is easily found by subtraction. Some typical angular distributions are shown in Figure 5.1.

Higher order spatial anisotropies are harder to establish experimentally for a variety of reasons and even if the $\lambda^{(\nu)}$ values are comparable to $\lambda^{(1)}$. First, for axially symmetric distributions, the ν^{th} Sidereal harmonic will be reduced by a factor $\mathrm{Cos}^{\nu}\delta\ \mathrm{Cos}^{\nu}\delta_o$ for purely geometrical reasons, as seen in equation 5.1.2 If either declination is well above the Galactic plane the reduction in amplitude will be substantial and will affect higher harmonics to a greater extent. Second, some reduction will result from the finite time and energy resolution of the equipment if the anisotropy is dependent on either time or energy. It is of course, improbable that the anisotropy is strongly time dependent over time scales of 10-20 years, but one remote possibility is that fluctuations could be caused by the arrival of large numbers of neutral particles (perhaps neutrinos) produced in a supernova explosion. These would arrive in a short burst possibly over a few months. A large number of high energy neutrinos would be needed. However, it is known that the cross-section for interaction of neutrinos increases with energy up to about 100 GeV. If this were to continue,

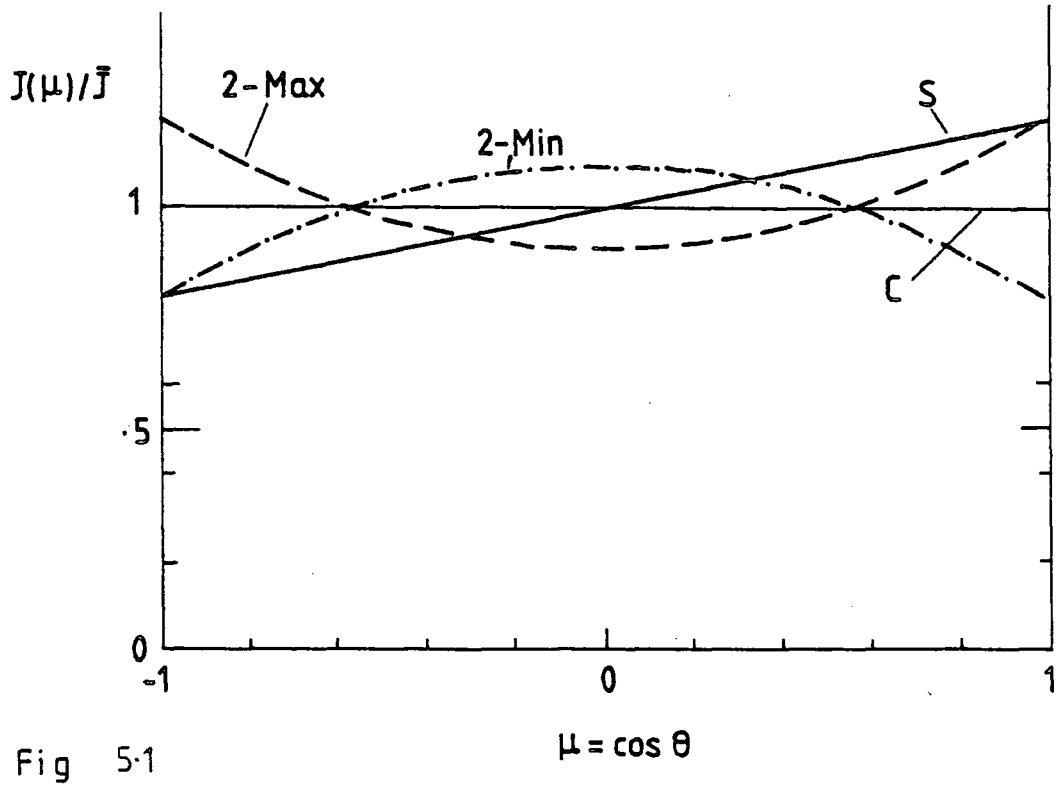

Fig 5·1

Simple directional distributions assuming axial symmetry, with the intensity plotted as a function of the cosine of the pitch angle θ.

C Complete isotropy

S Simple vector first harmonic anisotropy with 20 % amplitude

2-Max Second harmonic anisotropy with 20% amplitude of the two way maximum type

2-Min As for 2-Max but with two way minimum type anisotropy

extrapolation gives a cross-section that crosses that for nucleons at about 5 x 10^{17}eV. With regard to energy, most detectors have a fairly broad response so that primaries outside the decade centered on the median value contribute to the counting rate. About 20% of the total for muon detectors and 40% for small air shower arrays is gained in this way, and may well act to reduce the measured anisotropy.

Most arrays will accept particles from a large angular range resulting in a smoothing out of the angular distribution. particularly for higher harmonics. This effect can be considerable in reducing the amplitude of measured harmonics. If the angular acceptance is proportional to $\mathrm{Cos}^{\mu}\psi$, where ψ is the angle from the detector axis, then the amplitude reduction is $(\mu + 1)/(\mu + 2)$ for ordinary first harmonics, $\mu/(\mu + 3)$ for first special and second harmonics, and $(\mu - 1)(\mu + 1)/(\mu + 2)(\mu + 4)$ for first and second special, and third harmonics. μ is generally about 6 for small EAS detectors and about 2 for underground muon telescopes. For higher harmonics this reduction is considerable.

5.2 Statistical Aspects of Anisotropy

The initial aim of anisotropy measurements is to reconstruct the local angular distribution of cosmic rays. In most experiments, and particularly at higher energies, the data gathered are not of sufficient statistical accuracy to permit this. Consequently a more modest aim is to examine the data for the presence of a genuine Sidereal variation in a given energy range. Any positive indication of anisotropy can then be considered against the expectations derived from

astrophysical considerations such as the structure of the local Galactic field. Kiraly and White (1975) have drawn attention to three possible methods of analysis; harmonic, χ^2 test deviations from averages and comparison with theoretical expectation. Only the first method is considered here, since not only is it the most commonly used but in addition appears best suited for anisotropy analysis, except at ultra-high energies where data are scarce. The statistical aspects connected with anisotropy have recently been analysed in detail by Linsley (1975a). Here, a brief review of the main results is given for the analysis of a single data measurement. This is followed by an analysis of the effect of combining several measurements at comparable energies in order to find the best energy dependence of amplitude from a series of marginally or non-significant data. In this case the conclusions drawn will be somewhat different from those of Linsley.

5.3 Single Measurement Analysis

In an experiment at a given energy performed with a detector pointing towards declination δ, the raw data collected are the n individual arrival directions (phases) of the detected events. It is here initially assumed that the number of events detected in a given interval of sidereal time obeys Poissonian statistics. It is also assumed that the exposure of each time interval to events is equal and that spurious sidereal variations caused by atmospheric effects or instrumental instabilities have been removed or are insignificant. Further, it is assumed that the data set of n

phases $\psi_1, \psi_2, \ldots \psi_n$ ($o \leq \psi < 2\pi$) have negligible error and equal weight.

The problem, then, is to determine a best estimate from the phases of the two dimensional vector $\underline{s}$ (composed of amplitude s and phase α) which represents the genuine first sidereal harmonic. (Note that in general all the harmonics can be handled independently provided all are small compared with the constant term). At the least it should be determined if $\underline{s}$ is significantly different from zero. In general we estimate the perpendicular components of the first harmonic $\underline{s}$ to be

$$a = \frac{2}{n} \sum_{\nu=1}^{n} \mathrm{Cos}\psi_\nu \qquad b = \frac{2}{n} \sum_{\nu=1}^{n} \mathrm{Sin}\psi_\nu \qquad 5.3.1$$

which combine to define a first sidereal amplitude r and phase ψ of a vector $\underline{r}$ such that

$$r = \sqrt{(a^2 + b^2)},\ R = nr \text{ and } \psi = \begin{cases} \psi' & \text{if } b>o,\ a>o \\ \psi' + \pi & \text{if } a<o \\ \psi' + 2\pi & \text{if } b<o,\ a>o \end{cases} \qquad 5.3.2$$

where R is the total amplitude, and $\psi' = \arctan\left(\frac{b}{a}\right)$, $\frac{-\pi}{2} \leq \psi' \leq \frac{\pi}{2}$. The estimates a and b are unbiased (a statistic t, used to estimate a parameter s, is <u>biased</u> if the mean value of t over all possible samples is <u>not</u> equal to s) and hence $\underline{r}$ forms an unbiased estimate of $\underline{s}$. Linsley has pointed out that an exact analogy exists to the problem of a random walk in two dimensions (with equal step length) if the data set are drawn from a population in which the phases are uniformly distributed over o - 2π, in other words when $\underline{s}$ is zero. Exact solutions to this problem exist

(e.g. Kluyver 1906) but all that need concern us here is the Rayleigh formula (Rayleigh, 1880) giving the probability of obtaining, in the limit for large n, an amplitude greater than r

$$w(>r) = \exp \frac{-nr^2}{4} = \exp - k_o \quad \text{or alternatively}$$

$$P_R = \frac{R}{2n} \exp \left(-\frac{R^2}{2n}\right) \qquad 5.3.4$$

This formula has been shown to be accurate for values of n as small as 5 (Linsley, 1975(b)).

For large n, the estimates of a and b in equation 5.3.1. are independent though they are of course linked for individual ψ_i. The central limit theorem ensures that a and b have normal distributions so that the distribution of $\underline{r}$ is given by the two-dimensional Gaussian

$$f(\underline{r}) = \frac{1}{2\pi\sigma^2} \exp - \frac{(\underline{r} - \underline{s})^2}{2\sigma^2} \qquad 5.3.5$$

with $\sigma^2 = \frac{2}{n}$.

This corresponds to the situation in which data were drawn at random from a population characterised by phase α and amplitude $\underline{s}$, relaxing the first assumption mentioned above.

The factor $(\underline{r} - \underline{s})^2/\sigma^2 = t$ may be identified with the χ^2 distribution with two degrees of freedom so that

$$\theta(t) = \tfrac{1}{2} \exp - \frac{t}{2} \quad \text{and}$$

$$p(t' > t) = \exp - \frac{t}{2} \qquad 5.3.6$$

We may then construct a confidence circle around the endpoint of $\underline{r}$ so that if the origin lies outside of the circle we can reject the hypothesis that the genuine anisotropy vector $\underline{s}$ is equal to zero to the given level of confidence. Normally, though, we test the zero hypothesis

by application of equation (5.3.4) to determine the chance probability of obtaining r. If $\exp - k_o < 0.05, (k_o \gtrsim 3)$, we have less than a 5% chance that the distribution was initially random.

From equation (5.3.5) we may derive the probability of r in dr and ψ in $d\psi$ as

$$P_{r,\psi}\, dr\, d\psi = \frac{\Omega}{4\pi} \exp - \left[\frac{\Omega}{4}\,(r^2 + s^2 - 2rs\cos\psi)\right] r\, dr\, d\psi \qquad 5.3.7$$

By integrating with respect to r or ψ the differential probability distribution of amplitude or phase may be obtained. Putting $r^2 + s^2 - 2rs\,\mathrm{Cos}\,\psi = (r - s\,\mathrm{Cos}\,\psi)^2 - s^2\,\mathrm{Cos}^2\,\psi + s^2$ and $k = s^2\Omega/4$ we have

$$2\pi\, P_\psi = \frac{\Omega}{2} \exp(-k)\, \exp\,(k\,\mathrm{Cos}^2\psi) \int_o^\infty r \exp(-\tfrac{\Omega}{4})(r - s\,\mathrm{Cos}\,\psi)^2 dr$$

$$\text{or } 2\pi\, P_\psi = A \int_o^\infty r \exp - \frac{\Omega}{4}\,(r - s\,\mathrm{Cos}\,\psi)^2 dr \qquad 5.3.8$$

with $x = r - s\,\mathrm{Cos}\psi$ we have

$$2\pi\, P_\psi = A \int_{-s\,\mathrm{Cos}\psi}^\infty x \exp - \frac{\Omega x^2}{4}\, dx + A \int_{-s\,\mathrm{Cos}\psi}^\infty s\,\mathrm{Cos}\,\psi \exp - \frac{\Omega x^2}{4}\, dx \qquad 5.3.9$$

Substituting $y^2 = \frac{\Omega x^2}{4}$ we get

$$2\pi\, P_\psi = A\left(\frac{2}{\Omega} \exp\,(-k\,\mathrm{Cos}^2\,\psi) + \frac{2}{\Omega^{\frac{1}{2}}} \int_{-k^{\frac{1}{2}}\mathrm{Cos}\psi}^\infty \exp\,(-y^2)\, s\,\mathrm{Cos}\psi\, dy\right)$$

$$= \exp -k\,\{1 + s\Omega^{\frac{1}{2}}\,\mathrm{Cos}\,\psi \exp\,(k\,\mathrm{Cos}^2\,\psi) \int_{-k^{\frac{1}{2}}\mathrm{Cos}\psi}^\infty \exp - y^2\, dy\} \qquad 5.3.10$$

Now

$$\int_{-k^{\frac{1}{2}}\mathrm{Cos}\psi}^\infty \exp - y^2 dy = \int_o^\infty \exp - y^2 dy \begin{cases} + \int_o^{k^{\frac{1}{2}}\mathrm{Cos}\,\psi} \exp - y^2 dy, & \text{if } \mathrm{Cos}\psi \text{ is positive} \\ - \int_o^{-k^{\frac{1}{2}}\mathrm{Cos}\,\psi} \exp - y^2 dy, & \text{if } \mathrm{Cos}\psi \text{ is negative} \end{cases} \qquad 5.3.11$$

and $\operatorname{erf}(x) = \frac{2}{\sqrt{\pi}} \int_0^{\infty} \exp - u^2 du$, $\int_0^{\infty} \exp - y^2 dy = \frac{\sqrt{\pi}}{2}$ 5.3.12

so

$$2\pi P_{\psi} = \exp - k\{1 + \sqrt{(\pi k)}\cos\psi \exp (k \cos^2\psi)[1 + L \operatorname{erf}(Lk^{\frac{1}{2}}\cos\psi)]$$

5.3.13

The sign of L depends on the sign of $\cos(\psi - \alpha)$.

Integrating equation (5.3.13) with respect to r we have

$$P_r = \frac{\Lambda r}{4\pi} \exp - \frac{\Lambda}{4}(r^2 + s^2) \int_0^{2\pi} \exp \frac{\Lambda r s \cos\psi}{2} d\psi$$

$$= \frac{\Lambda r}{2} \exp - \frac{\Lambda}{4}(r^2 + s^2) \frac{1}{2\pi} \int_0^{2\pi} \exp \frac{rs\Lambda \cos\psi}{2} d\psi$$

$$= \frac{r\Lambda}{2} \exp - \frac{\Lambda}{4}(r^2 + s^2) I_o (\tfrac{rs\Lambda}{2})$$

or $P_{k_o} dk_o = e^{-(k + k_o)} I_o (2\sqrt{kk_o})\, dk$ 5.3.14

where I_o is the zero order modified Bessel function.

By using equation (5.3.14) and expanding using

$$I_o(Z) = \sum_{n=o}^{\infty} \frac{(\frac{1}{2}Z)^{2n}}{n!}$$ 5.3.15

to integrate term by term, the expectation value of k_o can easily be shown to be (appendix 1)

$$< k_o > = k + 1$$ 5.3.16

Alternatively equation (5.3.5) may be directly used to show

$$< r^2 > = s^2 + 2\sigma^2$$ 5.3.17

when $s >> \Lambda^{\frac{1}{2}}$, P_{ψ} and P_r approximate normal distributions with standard deviation equal to $\sigma_{\psi} = (2k_o)^{-\frac{1}{2}}$ and $\sigma_r = \sqrt{\frac{2}{n}}$ 5.3.18 respectively. It should be stressed that $\sqrt{\frac{2}{n}}$ corresponds to the standard deviation of just one component of the vector amplitude and is correspondingly smaller than the deviation of the scalar amplitude unless the amplitude is very much greater than the error, and further that it is only a valid

measure of the standard deviation under the condition stated.

It is apparant that from a single measurement the best estimate we can make for α is ψ, but for s or s^2 there is no such obvious choice. Linsley, by taking the simplest possible case of assuming a priori a uniform distribution for s and α in which all possible values of $\underline{s}$ are equally represented, derived the probability of s in ds, α in $d\alpha$ to be

$$P_{s,\alpha} = [(k_o/\pi)^{\frac{1}{2}} \pi \; r \; I_o(k_o/2)][\exp - \Lambda(s^2 + \tfrac{1}{2}r^2 - 2rs \cos\theta)/4] \qquad 5.3.19$$

from which the α and s distributions can be derived in a similar manner to the r and ψ distributions:

$$2\pi P_\alpha = [I_o(k_o/2)]^{-1} \exp[k_o(\cos^2\theta - \tfrac{1}{2})][1 + L \operatorname{erf}(L\, k_o^{\frac{1}{2}} \cos\theta)] \qquad 5.3.20$$

and $P_{\underline{s}} = [2(k_o/\pi)^{\frac{1}{2}}/I_o(k_o/2)] \exp[-k_o(\xi^2+\tfrac{1}{2})]\, I_o(2k_o\xi)$

where $\xi = \frac{s}{r}$

However, it is not altogether reasonable to assume, for example, that the probability that .2<s<.21 is the same as e.g. the probability that 1.5<s<1.51. Moreover, the estimate of s formed in this way is biased - s can only be positive and will tend to increase as energy increases because σ^2 will increase. From equation (5.3.17) an unbiased estimate of s^2 is seen to be $r^2 - 2\sigma^2$ but care must be taken not to reject negative values as 'non physical' or this too will become biased.

5.4 Multiple Measurements

When several measurements have been made at comparable energies and declinations the problem arises of how best to

combine the data. We assume that there are N measurements of n_i events (equivalent to one experiment repeated N times) yielding amplitudes $\underline{r}_1, \underline{r}_2, \ldots \underline{r}_N$. Clearly more weight should be given to the measurements with the greatest number of events so the total amplitudes should be used:

$$\underline{r}' = \frac{1}{\Sigma n_i} \Sigma n_i \, \underline{r}_{ij} : \begin{pmatrix} a \\ b \end{pmatrix} = \frac{1}{\Sigma n_j} \Sigma n_i \, r_i \begin{pmatrix} \text{Cos } \theta_i \\ \text{Sin } \theta_i \end{pmatrix} \qquad 5.4.1$$

It can be shown that $\underline{r}'$ has the smallest standard deviation of all unbiased estimates of s and in this sense is the best combination of the N measurements. $\underline{r}'$ is also a sufficient statistic - the joint distribution of the $\underline{r}_i$ values can be expressed as a product of two factors, one independent of $\underline{s}$ and the other giving the distribution of $\underline{r}'$ for a given $\underline{s}$.

However, if extra fluctuations are present such as arise from failure to correct properly for atmospheric fluctuations, instrumental instabilities, or we combine measurements at different energies, the simple vectorial combination may not be safe to use. In such cases it may be better to combine only the phases of the experiments.

Alternatively, and especially at higher energies, we may suspect the phases to vary rapidly with both energy and the declination of viewing, in which case a combination of the scalar amplitude data (such as the sum of the squares of the amplitudes) would be appropriate. The amplitude fluctuations at high energies are unlikely to be substantial.

Of course, by using either of these alternatives we are rejecting half of the available information so it is of interest to test the relative efficiency of using only

amplitude or phase data.

To this end the following four methods of combination were compared by computing the 'power' of each test:

1. Using the vectorial (amplitude and phase) amplitudes (This is simply for use as a reference).
2. Using the sum of the squared scalar amplitudes.
3. Using only phase information.
4. Using only the maximum amplitude of each measurement.

The effect of combining, for example, just two or five or N experimental results was also considered.

The second method completely rejects the phase of each measurement and deals only with the sum of the squares of amplitudes, while the third test adds N unit vectors with the phases as observed. Method 4 is expected to be the "weakest" overall, since only 1/2N of the information is being used, although it must be remembered that it is the most significant amplitudes that are being considered.

To compute the loss of information, N random (i.e. with $X = s/\sigma = 0$) sets of amplitude and phase were numerically generated many times and combined according to methods 2-4 above. This was done in order to establish the absolute value for each test at which it would be assumed, to 95% confidence, that there was a genuine signal. For the vectorial combination this value is simply $\sqrt{6N}$. We then compute the probability that a genuine signal x is shown to be genuine at the 95% confidence level, when the combination relates to 1-4 above, by simulating data drawn from a population characterised by $\bar{x}$ and rejecting the $\bar{x} = 0$ case whenever

the value of the combined amplitudes (or sum of the squares) exceeds the absolute value. x is allowed to vary from zero to infinity. The cases where N = 2,5 and 10 are shown on figures (5.2 - 5.4). The y axis represents the probability of arriving at the conclusion that s is genuine to 95% confidence.

Having found the power of the tests for N measurements each with the same underlying s/σ, the case for N values with different values of X was evaluated assuming a "spectrum" of the form $s_\nu = a^{-\nu} s_o$ where a is a constant and $o<s_o<\infty$. This corresponds to the combination of results of different energy. Two values of a were chosen, a = 1.15 to correspond to the value implied by the Linsley and Watson (1977) data (see section 6.7) and a somewhat larger value, a = 1.5, to test the effect of a steep spectrum. The results are shown for N = 10 on figures 5.5 and 5.6.

Note that for N<5 using amplitude information is as good as or better than using only the phase information. However, for N>5 the phase information proves progressively better than amplitudes alone. In all cases the vector combination is the most powerful method of combining series of data, as one would expect, while use of just the maximum amplitude proves progressively worse as N increases.

With the spectral assumption only the $\overset{\text{largest}}{\wedge}$ (small ν) values have a great effect on the final result. The sharper the spectrum becomes, the less efficient each test becomes.

5.5 Maximum likelihood

The technique of maximum likelihood is of use in obtaining best fits to anisotropy data. If we have reason to suspect from a series of anisotropy results at differing energies that $s^2 = aE_L^b$, where a and b are constants, then a and b may be estimated as follows:

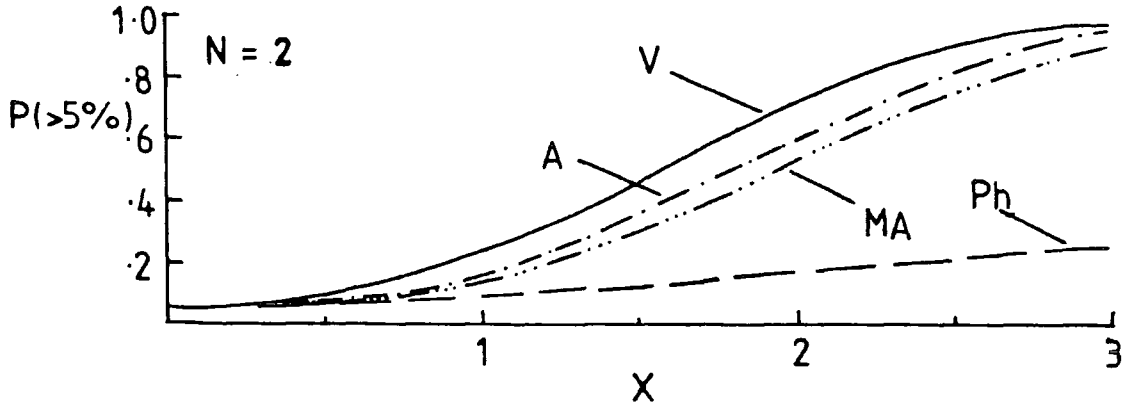

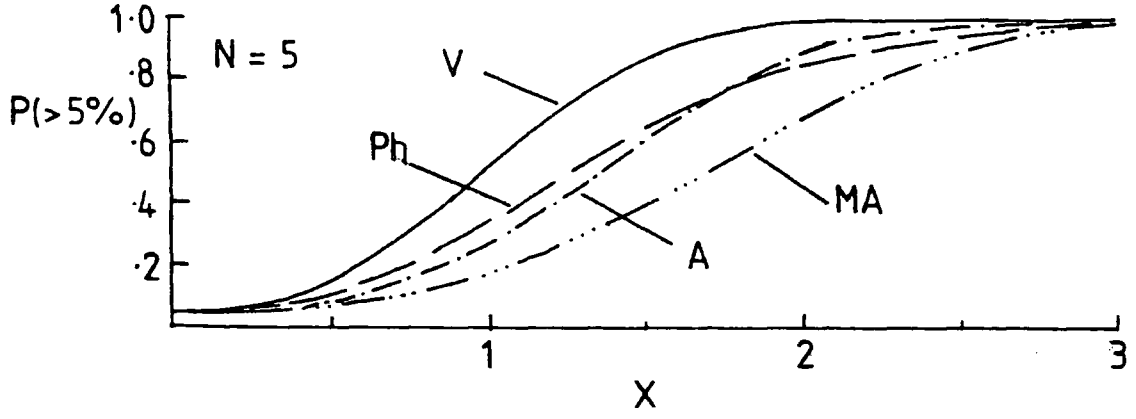

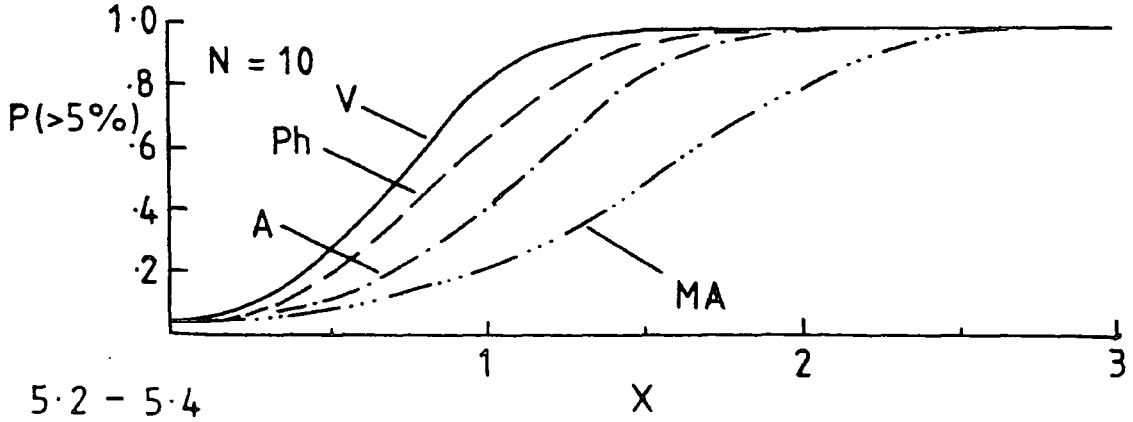

Figs 5·2 – 5·4

The effect of combining anisotropy measurements. P is the probability of arriving at the conclusion that s is genuine to 95 % confidence. X is the ratio of the genuine sidereal amplitude (s) to the standard error $\sqrt{(2/n)}$. N is the number

of experiments , which each detected n particles , to be combined .

The various types of combination are :

V : Vector combination

Ph : Phase information only , assuming unit amplitude

A : The sum of the squared scalar amplitudes

MA : Using only the maximum amplitude

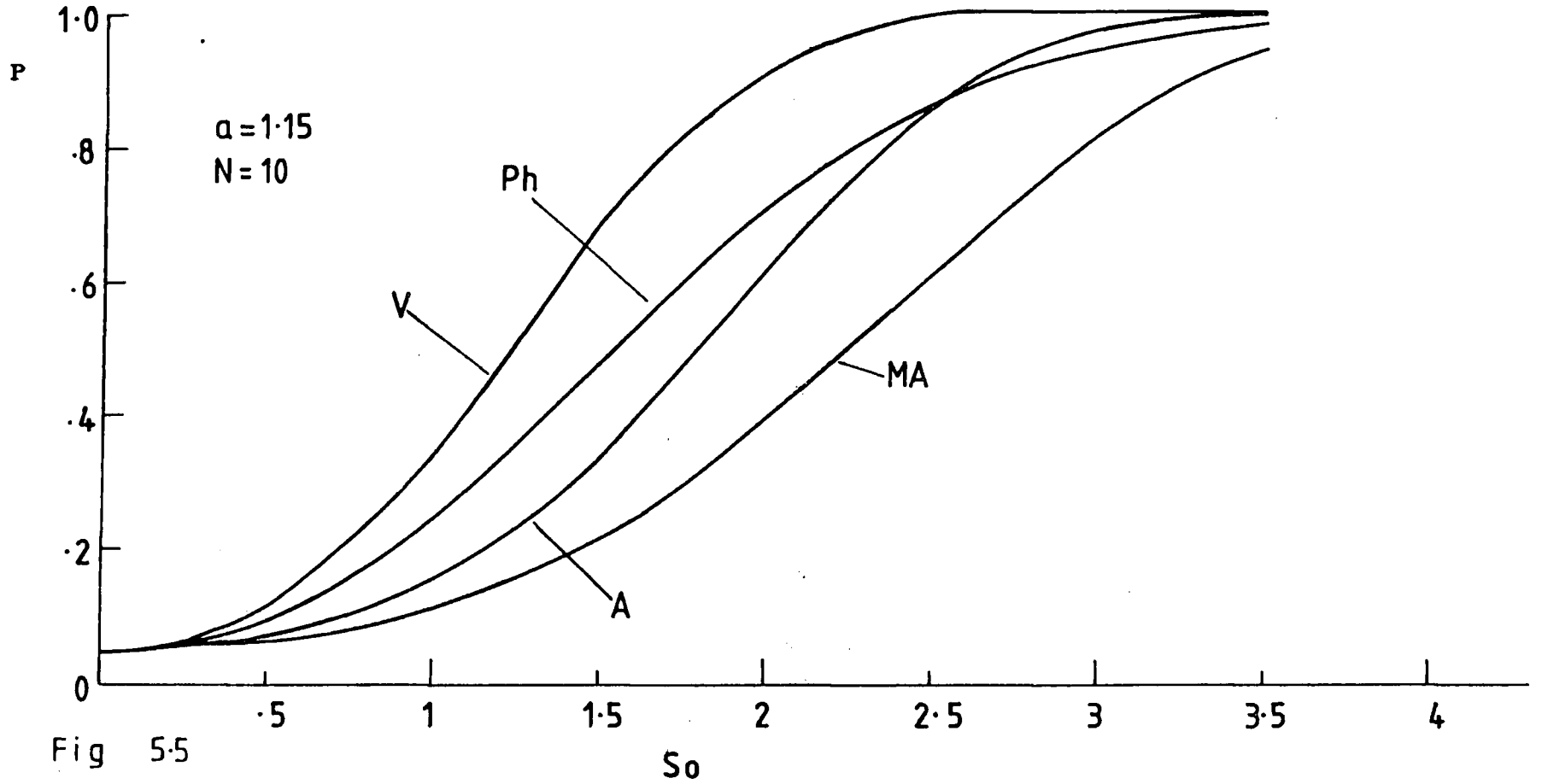

Fig 5·5

Power of combining N measurements assuming a spectrum of the form $s_\nu = a^{-\nu} s_o$ where $a = 1{\cdot}15$, $0 < s_o < \infty$ and $N = 10$. V - Vector, Ph - Phases only, A - Amplitudes only, MA - Maximum amplitude.

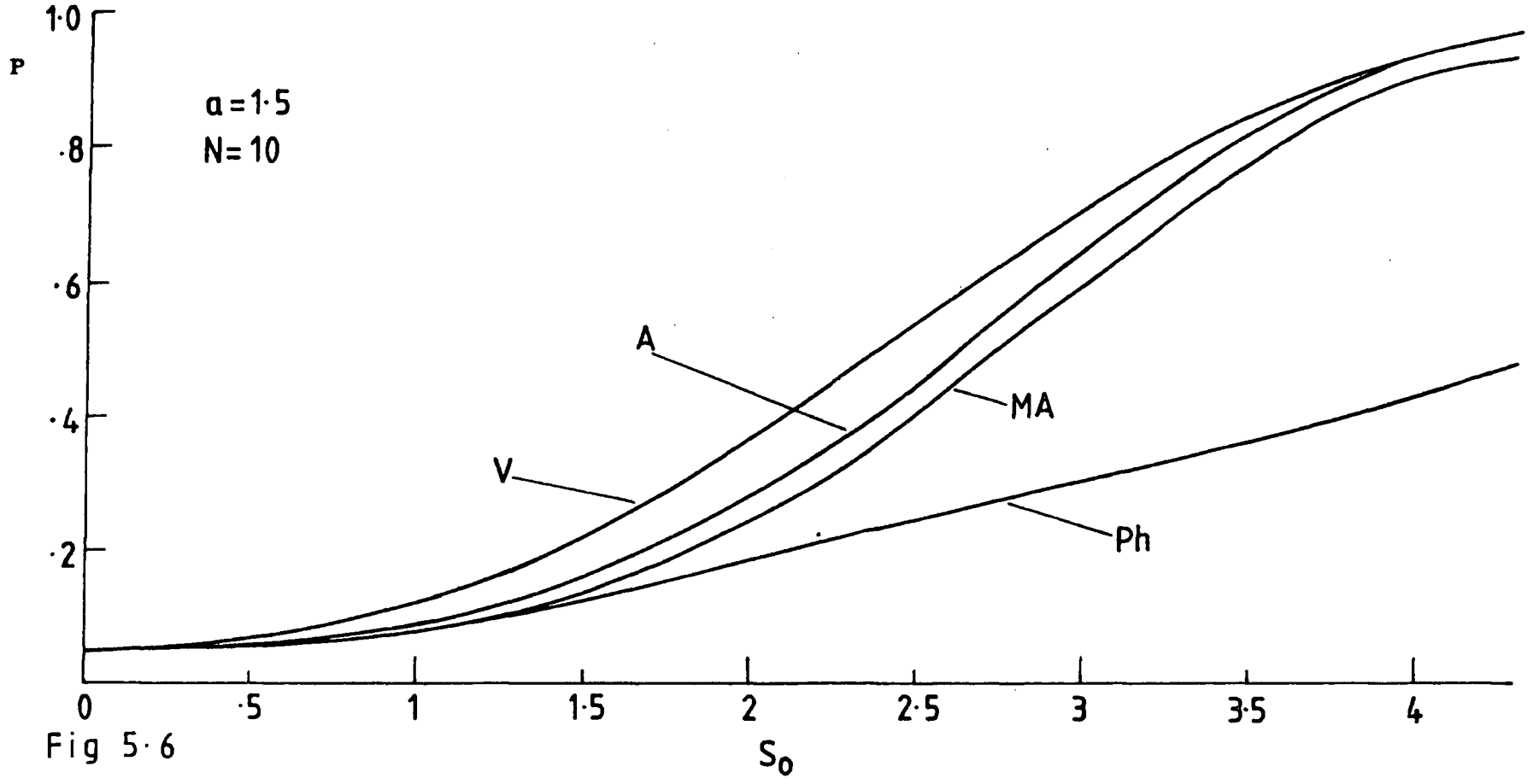

Fig 5·6

Power of combining N measurements assuming a spectrum of the form $s_y = a^{-2y} s_o$ where $a = 1{\cdot}5$, $0 < s_o < \infty$, and $N = 10$. V - Vector, Ph - Phases only, A - Amplitudes only, MA – Maximum amplitude.

From equation 5.3.14 the probability density for k_o is

$$p(k_o)dk_o = I_o(2\sqrt{kk_o})e^{-(k + k_o)}\, dk_o \qquad 5.5.1$$

For n equally spaced measurements (in energy) with the lowest energy equal to E_L we may write

$$s_\nu^2 = a\, 2^{\nu b} \quad (\nu = o,1...n) \text{ or}$$

$$k_\nu = a\, 2^{\nu b}/2\sigma_{r\nu}^2 \qquad 5.5.2$$

The probability density of the observed amplitudes is then simply

$$p(k_{oo}, k_{o1},...k_{on}) = \prod_{\nu=o}^{n} [I_o(2\sqrt{k_\nu k_{o\nu}})\, e^{-(k_{o\nu}+k_\nu)}] \qquad 5.5.3$$

The k_ν values can be written in terms of a and b and the known $\sigma_{r\nu}$ values. This gives a likelihood function

$$L(a,b|k_{oo},k_{o1}...k_{on}) = \prod_{\nu=o}^{n}[I_o(2\sqrt{k_{o\nu}k_\nu(a,b)})e^{-(k_\nu(a,b)+k_{o\nu})}] \qquad 5.5.4$$

The factors $\prod_{\nu=o}^{n} e^{-k_{o\nu}}$ are independent of a and b so that there is a product $L_o(a,b)$ that is normalised (unity) for a = o:

$$L_o(a,b) = \prod_{\nu=o}^{n}[I_o(2\sqrt{k_{o\nu}k_\nu(a,b)})\exp^{-k_\nu(a,b)}] \qquad 5.5.5$$

By varying the parameters a,b to find the maximum value of L_o the maximum likelihood estimates of a,b are found and hence the estimate of s^2. This technique is used in section 7.2.

5.6 Spurious sidereal variations

Any anisotropy data, but particularly that gained at lower energies, may be subject to a number of effects that introduce spurious sidereal or solar variations. Specifically these may arise from atmospheric, instrumental or extra-terrestrial effects.

Since the period of the sidereal day differs only by 4 minutes from the solar day data are needed for at least one complete year to separate the effects. The problem arises

because an effect of periodicity one solar day may be modulated by a yearly variation to produce two sidebands with periods of 23 hrs 56 mins (sidereal day) and 24 hrs 04 mins (anti sidereal-day). Consequently atmospheric pressure and temperature variations must be carefully monitored to allow appropriate corrections to be made. Temperature induced harmonics are less easily separated from the data.

Instrumental effects are hopefully small in modern experiments. Systematic errors can probably be reduced to about 0.01%.

Extraterrestrial effects can generate harmonics in both sidereal and solar time. Since the earth spins in the same sense as it orbits the sun a Compton-Getting type anisotropy results of about .5% at 6 hrs solar time. The eccentricity of the orbit results in an annual modulation of some 1% which fortunately causes negligible sidereal anisotropy. Below 3×10^{11}eV a so-called 'corotation anisotropy' is expected to become significant with a phase of 18 hrs solar time, arising from the balance of outward convection and inward diffusion of cosmic rays in the Heliosphere. In addition, if cosmic rays are isotropic with respect to the Galaxy (which is questionable) then a straightforward Compton-Getting anisotropy results at 18 hrs sidereal time with amplitude 3×10^{-2}%.

5.7 Aspects of Solar Modulation

Solar modulation is a direct result of solar magnetic fields being carried out with the highly ionised inter-

stellar wind. At some point equilibrium will be reached with the interstellar plasma and the magnetic field beyond the earth orbit. A complication arises however, since the UV emission from the sun can ionise the interstellar gas. Consequently both solar wind and ionising UV are important in determining the boundary of the solar influence (heliosphere). The size of the HII region thus generated is > 100 AU (Obayashi 1970). The solar wind, with velocity of about 300-500 km s^{-1}, establishes an interplanetary field of the form (in heliocentric co-ordinates)

$$B_r = B_o \left(\frac{r_o}{r}\right)^2, \quad B_\phi = B_o \left(\frac{r_o}{r}\right)^2 \left(\frac{\nu_\phi - r\Omega}{\nu_r}\right) \text{Sin } \theta \qquad 5.7.1$$

where r_o = Solar radius, Ω is the angular velocity of the sun, ν is the solar wind velocity, and B_o is the field at $r = r_o$ (Sakurai, 1974). The total field is approximately

$$B \simeq B_o \left(\frac{r_o}{r}\right)^2 \sqrt{1 + (r\Omega/\nu_r)^2} \qquad 5.7.2$$

Theoretically the equations may be used to calculate cosmic ray trajectories at the low energies and this has indeed been done (Marsden et al. 1976). The difficulty with this approach is that the boundary is suspected to be unstable and in addition the heliosphere may not be spherical.

It is interesting to examine the equilibrium point for solar cosmic rays and radiation with the interstellar norm. The radiation from the whole sun is some 3.8×10^{33} erg s^{-1}. The energy density at the earth is then about 3.6×10^{8} eV cm^{-3}. Taking the CR energy density throughout the Galaxy as 1 eV cm^{-3} equilibrium is reached at about 1.8×10^{4} AU. The solar wind has an energy density of about

5.3×10^3 eV cm^{-3} at the earth. This balances with the average Galactic magnetic energy density at a distance of about 130 AU. These should be compared with the equilibrium of interplanetary magnetic field/interstellar field at $\sim$ 11 AU.

CHAPTER 6

EXPERIMENTAL OBSERVATIONS

6.1 Experimental Data 10^{11} - 10^{12} eV

Measurements here are made primarily with underground muon telescopes at shallow depths, but while large numbers of events are detected (enabling variations as small as 0.01% to be measured - the limit to which systematic instrumental errors can be reduced) this region remains the most confusing and controversial. The problems arise from deflections introduced by the interplanetary field which must be allowed for in interpreting the data. There are two aspects of importance:

1. The interplanetary field can change the direction and reduce the amplitude which would be observed if there were no distorting field. In principle by knowing the detailed structure of the field and calculating the trajectories of particles through the field this can be allowed for.
2. Incoming particles may gain or lose energy as a result of the electric field associated with the Solar wind. This produces an anisotropy of the form

$$\Delta I(t) = I(\gamma + 2)\, \Delta E(t)/E \qquad 6.1.1$$

where E is the primary energy, $\Delta E(t)$ the energy loss (or gain) of a particle along its path and arriving at time t, and γ is the exponent of the differential energy spectrum. ΔE will be the same along any trajectory in a potential field (and hence $\Delta I/I = o$), but it is apparent that the sector structure of the interplanetary field will introduce distortions since a changing magnetic field results in a non-potential electric field.

We have noted already that an anisotropy arising from Solar induced sidereal variation is expected with phase at 6 hrs, so that any experiment that reveals a phase near this may be the result of Solar influence. However, a different phase can be expected if we admit the possibility of a non-spherical solar cavity. There is as yet no evidence on the shape of the solar modulation region. It appears from the Socorro measurements (Swinson 1976) that increasing solar activity increases the field dependent component, suggesting a solar origin.

Prior to 1970 measurements in the Northern hemisphere at London (60 m.w.e. $\simeq 6 \times 10^3$ g cm^{-2}), Budapest (40 m.w.e.), Socorro (80 m.w.e.) and Torino (80 m.w.e.) were all consistent with an amplitude of $\sim$ 0.03% at 18 hrs R.A. as expected by a Compton-Getting Solar motion with respect to the local standard of rest. A recent Budapest result (Kecskemeti, 1978) using Hobart and Budapest data from 1958 - 63 similarly gives an amplitude and phase of 0.02% at 5 hrs R.A. for the first harmonic. Yet in the Southern hemisphere a long standing result at Hobart (Fenton, 1976), though showing a dependence on the polarity of the interplanetary field (Humble and Fenton 1977), measured an anisotropy of 0.031% $\pm$0.001 at 5.73 hrs. Note, though, that corrections for I/P deflections would probably change the phase and result in larger amplitudes for extra-solar cavity anisotropies.

This North-South disparity was interpreted in terms of a two-way anisotropy (Sekido 1971). However, after 1970 the Northern Hemisphere stations reported a remarkable change in phase from $\sim$ 18 hrs to 6 hrs while the Southern Stations

observed no such change (Fenton 1975, Cini-Castagnoli et al. 1975). This change has been attributed to the change of polarity of the large scale solar photospheric field (Howard 1974) and appears to have occurred gradually over several years. As a result of these changes, presumably connected with a change in the interplanetary field which is related to the photospheric field, the London group have attempted to derive the local interstellar anisotropy from the observed sidereal variation on the basis of calculating trajectories from a plausible model of the magnetic field (Marsden et al., 1976, Davies et al., 1977, Davies et al., 1978). In the first of these papers data from the Holborn verticle telescopes was combined with the results at Hobart to produce an intensity distribution across the whole sky (Figure 6.1). In the second paper the analysis was repeated, this time combining results obtained at greater depth from the Holborn inclined telescopes (92 m.w.e.) and Poatina (365 m.w.e. Figure 6.2). Both combinations were corrected for solar motion.

Although these measurements were made at different energies, both are in remarkable agreement showing an (I max - I min) assymmetry of about 0.34%. Together they give an anisotropy of $\sim$ 0.17% from the general direction $(\ell^{II}, b^{II}) = (285^{o}, -35^{o})$ $(\alpha, \delta) = (71^{o}, -73^{o})$. It should be noted that this anisotropy is nearly an order of magnitude greater than the individually observed sidereal variations (e.g. 0.02% and 0.04% for Holborn and Hobart). This is a direct result of the near alignment of the anisotropy

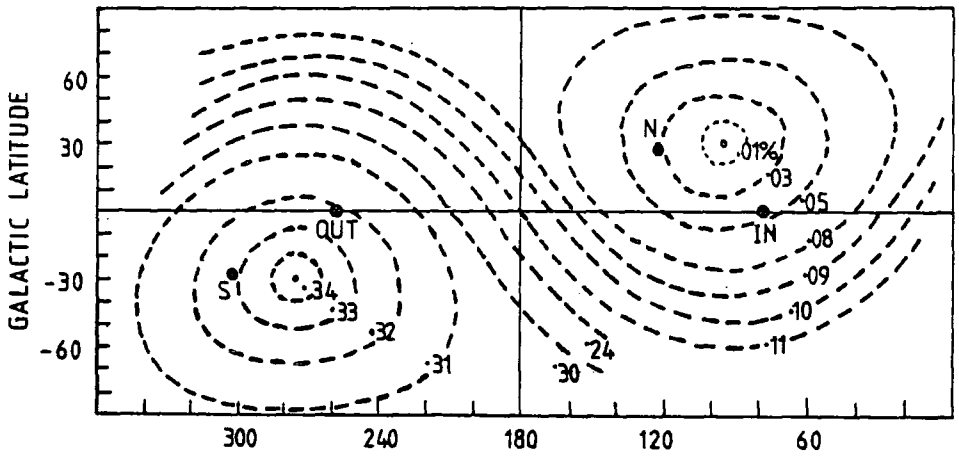

Fig 6·1

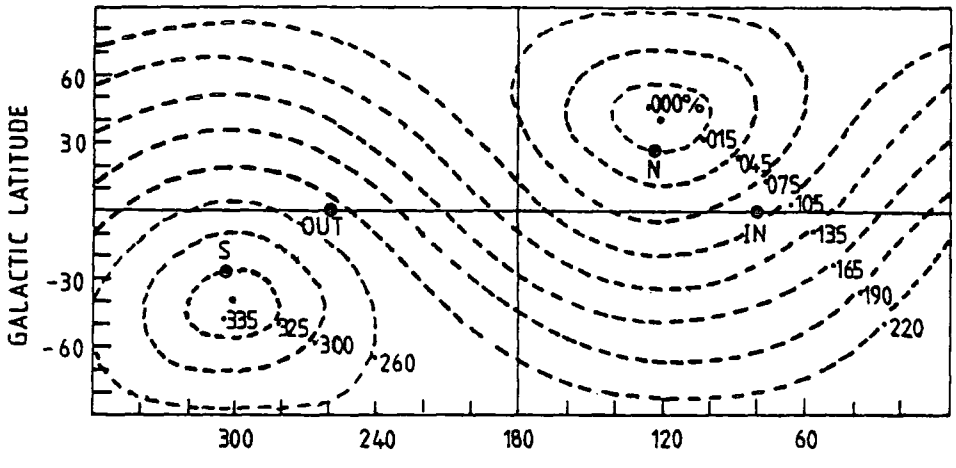

Fig 6·2

6·1 The local interstellar anisotropy at 3×10^{11} eV derived from the observed siderial variation at Holborn and Hobart, and a plausible model of the solar magnetic field, by Marsden et al. 1976. IN and OUT correspond to the direction of the local spiral arm. N is the direction of the earth's north pole. The measurements were corrected for solar motion.

6·2 As for 6·1 but combining Holborn inclined telescope and Poatina measurements.

with the polar direction. Individually the telescopes scan only part of the intensity variation. As Marsden et al. point out, the interplanetary field may be useful in offering the possibility of detecting and measuring the polar component of the anisotropy, since at higher energies this is unobservable. Their results therefore, suggested that the vector anisotropy was considerably larger than had previously been thought. This situation has, though, recently changed somewhat.

The latest measurements (Davies et al., 1978) derived from the inclined Holborn telescopes at $\bar{E}p = 5 \times 10^{11}$ eV, are shown in Figure 6.3. Obtained from 1972 - 1977 the results give a best fit direction of $\ell^{II} = 250^{o}$ $b^{II} = -60^{o}$ ($\alpha = 45^{o}$, $\delta = -42$) with amplitude 0.09% (in the local standard of rest). This new result does not suggest that there is an excessive polar component. Transformed to the solar frame, the direction changes to $\alpha = 23^{o}$, $\delta = -40^{o}$ with amplitude 0.07%, while in the gas frame these become

$\ell^{II} = 214^{o}$, $b^{II} = -64^{o}$ ($\alpha = 41^{o}$, $\delta = -25^{o}$)

It should be remembered throughout that these measurements are dependent on the adopted model of the magnetic field.

Nagashima and Mori (1976) have examined this region in some detail and drawn several conclusions. Firstly, it now appears that though the phase of the first harmonic can vary substantially in individual measurements, combined data from "conjugate pairs" of stations give phases centred around 0 - 3 hrs. This is comparable to the phases obtained at slightly higher energies (10^{12} - 10^{14} eV) where solar effects are negligible. In addition the second harmonics seem reasonably stable at about 6 hrs R.A.

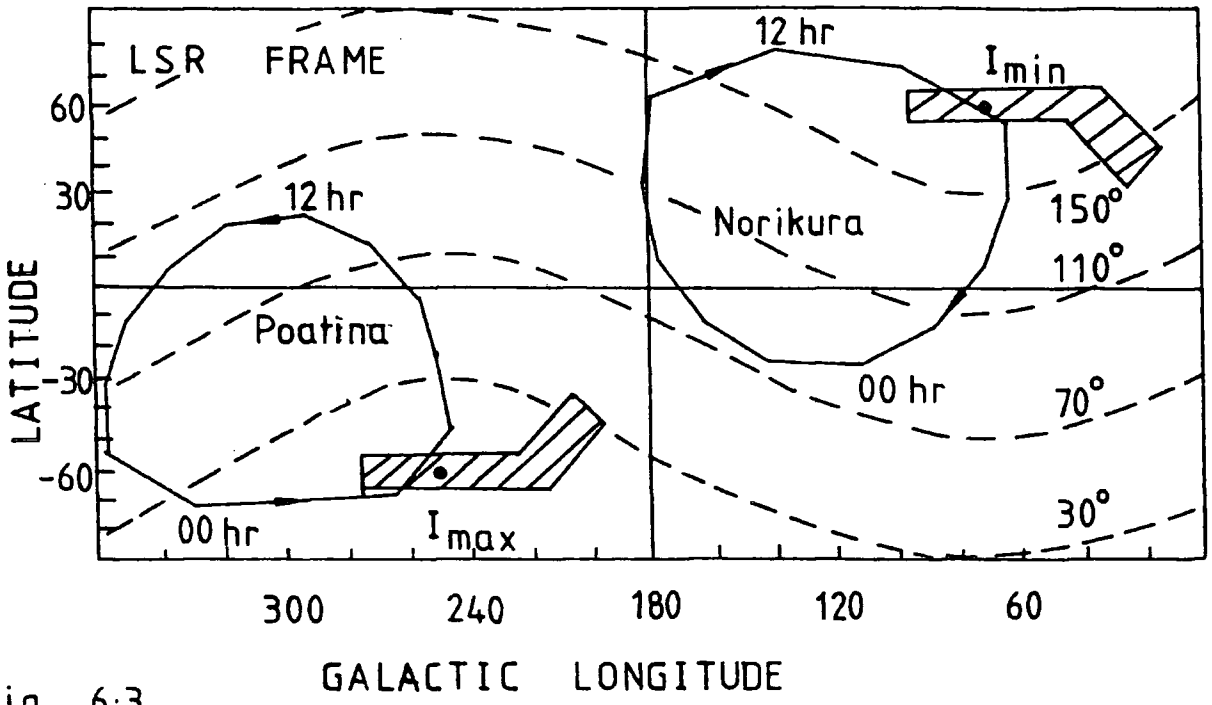

Fig 6·3

The local interstellar anisotropy at $5 \cdot 10^{11}$ eV from measurements by the inclined Holborn telescope and in the frame of the local standard of rest. The results give a best fit direction of $l^{II} = 250°$, $b^{II} = -60°$ with amplitude 0·09 %. The contours are equal angular distance from I_{max}. Also shown are the directions of look for vertically pointing detectors at Poatina and Norikura. The error boxes are the limits within which the axis of the distribution must lie to give a reasonable fit to one standard deviation.

Summarising then, measurements at these energies tend to support the existance of an anisotropy perhaps of amplitude 0.04% (measured at an individual station) while the 'true' Galactic amplitude may be an order of magnitude higher. The results are undoubtedly useful, but their real significance may not become apparent until more information is obtained about the detailed structure of the interplanetary magnetic field. Measurements in the Southern hemisphere do not appear to be affected by changes in the Solar photospheric field.

6.2 10^{12} - 10^{14} eV : Results

The most convincing evidence to date for an anisotropy has been provided by three recent measurements in this energy region : those at Poatina (Fenton et al. 1977, Fenton and Fenton, 1976) and in the Northern hemisphere at Peak Musala (Gombosi et al. 1977) and Mount Norikura (Nagashima et al. 1977)-see Table 6.1. The latter two measurements (at $\bar{E}_p$ = 6 x 10^{13} and 2 x 10^{13} eV respectively) are undoubtedly free from solar effects and furthermore both amplitudes and phases of the first and second harmonics are in close agreement. Despite the somewhat lower energy the first harmonic at Poatina is also in good agreement although the second harmonic is not statistically significant. The Musala amplitudes are rather larger than those of Poatina or Norikura, but are still compatible (the probability of larger differences is about 50%). Combining the Norikura and Musala results (they are at similar latitudes) gives values close to those of Norikura, since the count rate is considerably higher there.

Station	Median Energy (eV)	First Harmonic Amplitude (%)	First Harmonic Phase (hrs)	Second Harmonic Amplitude (%)	Second Harmonic Phase (hrs)
Poatina $42^{o}S$	10^{12}	0.050 ± 0.024	1.3 ± 1.9	Insignificant	
Norikura $36^{o}N$	2×10^{13}	0.051 ± 0.004	1.0 ± 0.3	0.026 ± 0.004	5.5 ± 0.3
Musala $42^{o}N$	6×10^{13}	0.073 ± 0.020	1.7 ± 1.1	0.055 ± 0.020	5.0 ± 0.7

Table 6.1 The measured anisotropies in the solar frame for 10^{12}eV < $\bar{E}$ < 10^{14}eV at Poatina, Norikura, and Musala. Both first and second harmonics are given.

Both the Musala and Norikura results have been analysed in detail.Sakakibara et al. (1976) have evaluated their results by considering four data sets corresponding to 3 and 4 - fold coincidences directional and local air showers. The similar sidereal harmonics thus derived give confidence that the anisotropy is genuine and is varying slowly (if at all) from (1 - 4) x 10^{13} eV. Gombosi et al., (1977) have analysed the Musala first and second harmonics at periodicities deviating from the sidereal day by up to two minutes. The results support the significance of both harmonics to better than 2σ.

It should be noted that a rather disturbing dependence on the polarity of the interplanetary magnetic field has been observed at Poatina, though this has not yet been confirmed. The Hobart results at lower energy ($\bar{E} \simeq 2 \times 10^{11}$ eV) have also given signs of a field dependence. If this is later found to be true, then not only the Poatina results but all measurements below 10^{12}eV must be regarded with suspicion until detailed knowledge of the solar field is available.

6.3 Pitch Angle Distribution and Recent Measurements

The three measurements noted above may be combined to give information on the declination dependence of the anisotropy. Propagational considerations suggest that the anisotropy is most probably explained in terms of an axially symmetric pitch angle distribution about the local direction of the Interstellar magnetic field. The anisotropy is then derived from Compton-Getting streaming resulting from solar motion with respect to the interstellar gas frame. However, phase

agreement between the first and second harmonics cannot be obtained by correcting for the interstellar wind as given in section 3.5.2. Nagashima et al. fit their measurements with a pitch angle distribution around $(\ell^{II}, b^{II}) \simeq (115^{o}, -50^{o})$ using a wind direction of $(\ell^{II}, b^{II}) \simeq (155^{o}, 0^{o})$ and a velocity of 25 kms^{-1}. However this motion is not compatible with the interstellar wind information which has now become available.

The difficulties of resolving the "true" Compton-Getting correction for solar motion with respect to the magnetic field can be avoided by using only the second harmonics and the special first harmonic, both of which are relatively unaffected by solar motion. Combining the Norikura and Poatina first harmonics gives a special first harmonic of 0.004 ± 0.012% at 20.3 hrs R.A. and an ordinary first harmonic of 0.05 ± 0.012% at 1.2 ± 0.9 hrs. The phase of the special first harmonic is obviously undefined, but if the second harmonics are axially symmetric then the small amplitude derived indicates that the symmetry axis is close to the equatorial plane. If we assume that third and higher harmonics are absent, and that the difference in energy has no effect, then the second harmonic should be the same in both the Northern and Southern hemisphere (at an equal-opposite declination). On this basis we have six parameters : the phase, amplitude, and error of the North and South second harmonics ($\underline{r}_{2N}$, r_{2S}) and the first special harmonic ($\underline{r}_{1sp}$). For a fixed (assumed) direction a best fit can be given for the magnitude of the second spherical harmonic. Defining these three parameters, and varying them, the first special

and two second harmonics may be calculated. The sum of the squares of the deviations of the observed minus calculated harmonics

$$\left(\frac{\underline{r}_{1sp} - \hat{\underline{r}}_{1sp}}{\sigma_{1sp}}\right)^2 + \left(\frac{\underline{r}_{2N} - \hat{\underline{r}}_{2N}}{\sigma_{2N}}\right)^2 + \left(\frac{\underline{r}_{2S} - \hat{\underline{r}}_{2S}}{\sigma_{2S}}\right)^2 \qquad 6.3.1$$

then follows a χ^2 distribution with 3 degrees of freedom. By continuously changing the axis direction the 5% and .1% error ellipses may be drawn about the 'best' axis direction (see figure 6.4). The region(s) centred around $\alpha = 353^o$ (172^o) correspond to a two-way minimum in the intensity distribution from the direction of the symmetry axis and higher intensities at larger pitch angles. 90^o away from these are regions of two may maxima from the axis direction. The phases of the Poatina (P), Musala (M) and Norikura (N) experiments are also shown on the diagram (transformed to the gas frame). The differences between these results and the axis direction are unfortunate but significant if the error bars shown are correct. If, however, the Holborn result is also transformed to the gas frame (shaded box) then somewhat better agreement is found. Nonetheless, the results do not justify the assumption of axial symmetry which inevitably leads to a complex situation which is not well understood.

6.4 Tensor Description of the Anisotropy

On the assumptions that only first and second harmonics are present and that the axes of the tensor anisotropy point along specific directions (the Galactic center and spiral arms for exmaple) of astrophysical interest, Somogyi(1976) notes that all components of the tensor and vector anisotropy

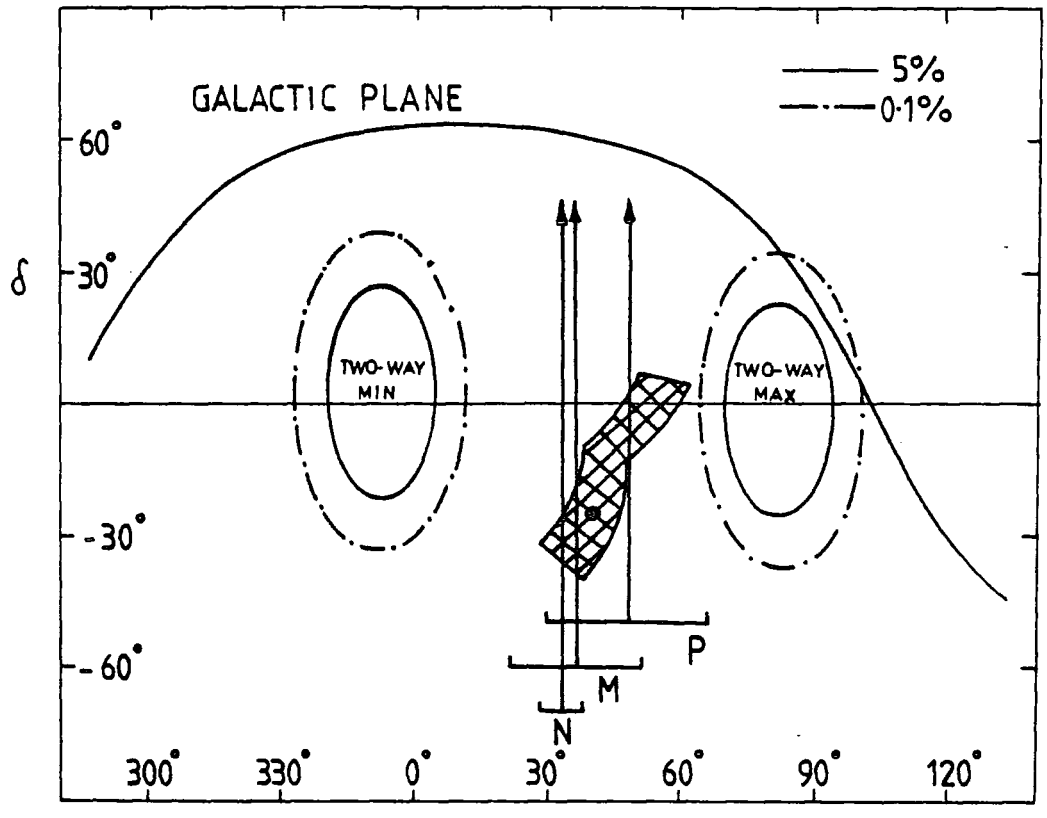

Fig 6·4

Allowed directions of the symmetry axis of the cosmic ray angular distribution (from Kiraly et al. 1979). The ellipses result from the combination of Musala, Norikura, and Poatina results in terms of propagation. The first harmonic phase for each station is also shown. The shaded box corresponds to that of figure 6·3. The measurements are shown in the frame of the local interstellar medium. That the ellipses do not correspond to the first harmonic phases indicates a more complex situation than axial symmetry.

can be derived, barring the polar vector component, from just one measurement. The Musala data, treated in this way, give a first special harmonic of .192% . This is not compatible with the small first special harmonic derived from Poatina and Norikura. The problem with an approach of this type is that adopting an arbitrary set of axes, two way maxima and minima can still appear for almost any direction one cares to adopt. In particular the data can show a streaming from the Galactic center or from either the SPIN or SPOUT directions of Figure 3.2 .

There is no experimental evidence at present concerning third or higher harmonics, nor, in view of the difficulties of detection of such harmonics, is it likely that such harmonics will be sought in the near future. Kota and Somogyi (1977) suggests that anisotropic pitch angle diffusion should produce an antisymmetric pitch angle distribution where only odd harmonics are present. Odd harmonics would then be equal in both hemispheres while even harmonics would be opposite. In addition, the axis of symmetry should point to a moderate declination since a near polar axis would give only a first harmonic while a near equatorial direction would give virtually no even harmonics. The Holborn data would also be reconciled somewhat with a moderate axis declination. Axial symmetry would still not be supported since the first and second harmonic phase discrepancy noted above would not disappear. However, such a theory is obviously beyond checking at present.

6.5 Interpretation for $E_p < 10^{14}$eV

In spite of the dissapointing absence of axial symmetry, the surprising agreement of the phase, and constant amplitude up to 10^{14}eV, is significant and provides some useful information.

Combined with the interstellar wind data, we have evidence that there is a constant propagation mechanism controlling the simple streaming over nearby distances. Propagation characteristics and sources are not dissimilar for the whole interval 10^{11} - 10^{14} eV; different sources (which would presumably produce particles of different energies and energy spectra) might be expected to introduce sudden phase reversals if some sources contributed particles parallel to the field, and others antiparallel. Consequently it is possible that we observe mainly the old and hence very diffuse component - the anisotropy is then determined by propagation along the direction of easiest escape and not by the source configuration. The long lifetime observed fits in with this possibility. In addition, the possible deficit of short path lengths for cosmic rays of 1 - 10 GeV referred to earlier also indicates that we observe old particles in the main.

Finally, the observed near constant amplitude suggests a near constant lifetime of cosmic rays over the range. Consequently the exponent β in the grammage energy dependence equation is probably smaller above 10^{11}eV than the value ~ 0.4 found below 10^{11}eV. Together with the γ-ray data, the whole provides good evidence for a Galactic origin below 10^{14}eV.

6.6 Anisotropies from 10^{14} - 10^{17} eV

Here small coincidence arrays are used to detect extensive air showers generated in the atmosphere. In theory this is an ideal region to examine the anisotropy since simple equipment is needed and the count rate is not insubstantial. In particular the change of slope of the primary energy spectrum is worth investigating. However, the anisotropy was found to be smaller than originally anticipated and the contradictory results which were obtained in the late 1950's and early 1960's have resulted in a concentration of effort at lower and higher energies.

6.7 Compilations of Data

It would appear logical to attempt to extract information about the nature of anisotropy by examining whole series of measurements, and this has indeed been done (Sakakibara, 1965). Recently, Linsley and Watson (1977) have examined all published results in the years 1951 - 1965 in the range 10^{14} - 3 x 10^{17}eV. The lower energy limit excludes just one air shower result at $\bar{E}$ = 2 x 10^{13}eV (Cachon, 1962) while the upper limit excludes the Volcano ranch data and the largest energy events from the Cornell experiment.

From the final total of 23 experiments, 50 first and 41 second harmonics were obtained together with 47 and 31 first and second harmonic phases respectively. (The smaller number of phases is a result of some phases being indeterminate when amplitudes are small, the smaller number of second harmonic amplitudes a result of omission in the original papers). For the most part the data were considered

to be statistically independent in the Linsley/Watson analysis, though this is certainly not the case. It should also be noted here that there may be a 'publication effect' in operation. Results which agree in phase with earlier measurements or which have large amplitudes or which coincide with an important direction may be more readily published than purely negative results, and this may bias results gained from series of experiments. Hopefully this effect is negligible.

In this section Linsley and Watson's main results are given and examined, followed by a reanalysis of their data.

1. It was found that in experiments where sufficient data was available to reduce statistical errors, additional fluctuations which could not be explained in terms of the Rayleigh-Poisson fluctuation were present. The actual random errors in amplitude and phases (determined empirically) when $\sigma_r < 1\%$ were greater than expected by a factor ~ 1.3 over and above the RP errors. This must be due to a systematic error or additional fluctuation, but the uncertainties prevent any definate conclusions about the nature of the anisotropy to be drawn from amplitude data alone.
2. The measured antisidereal variations were found to be less significant than had previously been thought.
3. Spurious sidereal waves (from Solar and antisidereal harmonics) were apparently non-uniform at the 6% chance level - the phases tending to cluster at 6 hrs R.A. If this were a genuine effect then a systematic error

of about 0.1 - 0.2% in amplitude would be present.

4. Additional fluctuations are likely to affect the phase distribution of sidereal waves less than the amplitudes so that information can be gained by treating the data as a set of equally weighted phases. Using the 47 first harmonic phases in this way, Linsley and Watson calculate a significance of 0.7% for the resulting amplitude with a phase of 17.4 hrs R.A. If the spurious amplitude at 6 hrs were genuine, this would strengthen the evidence for anisotropy.
5. The second harmonic phases were random with 33% chance.

Subdividing the results into four energy bins each of 1 decade, 'best estimates' of the first harmonic amplitude and phase were found using the standard error estimates (equations 5.3.18), but neglecting any extra fluctuations. These were used to infer an empirical formula for the energy dependence of $\underline{s}$, the genuine anisotropy vector:

$$\underline{s} = 0.4E^{\frac{1}{2}}\exp i(15.3 - 3.8 \log E) \qquad 6.7.1$$

or $S(\%) = 0.4^{\frac{1}{2}}$, $\alpha(\text{hrs}) = 15.3 - 3.8 \log E$ with E in units of 10^{16}eV. This equation is necessarily a kind of average since it is based on measurements obtained at many different latitudes. For equatorial viewing directions the amplitudes should be raised by a factor 1.31, the reciprocal average cosine of the set of declinations. For energies greater than 10^{17}eV the relation breaks down because of the lack of data. The formula is close to the maximum likelihood estimate which can be calculated from the same results.

Kiraly et al., (1979) have performed additional tests

to the LW measurements in view of their potential importance. The results of this analysis are here stated, much of which concerns the behaviour of the residual phases and amplitudes obtained after 'correcting' for the empirical genuine contribution. The tests supply support for a genuine anisotropy consistent with equation 6.7.1 and also for the presence of additional fluctuations.

6.8 Analysis

The extrapolation of equation 6.7.1 can be compared with recent measurements at lower and higher energies. Comparing with the lower energy Norikura and Musala experiments at 2.10^{13} and 6.10^{13}eV respectively, the extrapolated values agree well in phase (1.6 hrs and 23.7 hrs cf table 6.1) but are lower in amplitude than the measured values. At higher energies the formula is in good agreement with the recent Haverah Park results in amplitude, but the phase agreement is poor, disagreeing by about 6 hrs R.A. at 10^{17}eV. It should be noted that while the second harmonic phases are essentially random, the two lowest energy results which are significant both have phases between 5 and 6 hrs R.A., in remarkable agreement with the Norikura and Musala second harmonics. There appears, then, to be good support for the consistency of the genuine signal with the equation.

The LW data may be treated in a number of ways to evaluate the significance of the first and second harmonic phase and amplitudes. First, if no additional or genuine signal were present the $P(>r)$ distribution of the $\exp(-k_o)$ values for the measurements would be uniform, allowing for

random fluctuations. If on the other hand a genuine signal were present then the distribution should be peaked towards the more significant smaller values of exp-k_o. The deviation of the measured amplitude distribution from the random, linear, distribution expected by chance can be seen in Figure 6.5[a], where p(>r) values for the fifty first harmonics have been binned. Also shown (as on all the figures) is the χ^2 value for 9 degrees of freedom and the corresponding probability of a random set, 3.4×10^{-3}%. At first sight, this sharp peak at small chance probabilities suggests strong evidence for anisotropy. The distribution of the 47 first harmonic phases, with chance χ^2 probability 0.39% (c.f. L.W. 0.4%), also supports the presence of a genuine anisotropy. Much of this may, however, be due to additional fluctuations. In view of this the second harmonic amplitudes (Figure 6.5[d]) appear to show a too uniform distribution; the relatively low chance probability of 1.7% for amplitudes is not indicative of a clustering around low exp-k_o values. Possibly first harmonics are affected to a greater extent by fluctuations. The second harmonic phases are random with 22% chi-square probability.

The χ^2 probabilities for phases, then, are similar to those calculated by Linsley and Watson treated as equally weighted directional data. Both methods suggest strong support for a genuine first harmonic.

It should be noted that for a truly random distribution we would expect the second harmonic amplitude to be greater than the first harmonic in 50% of the cases. With the

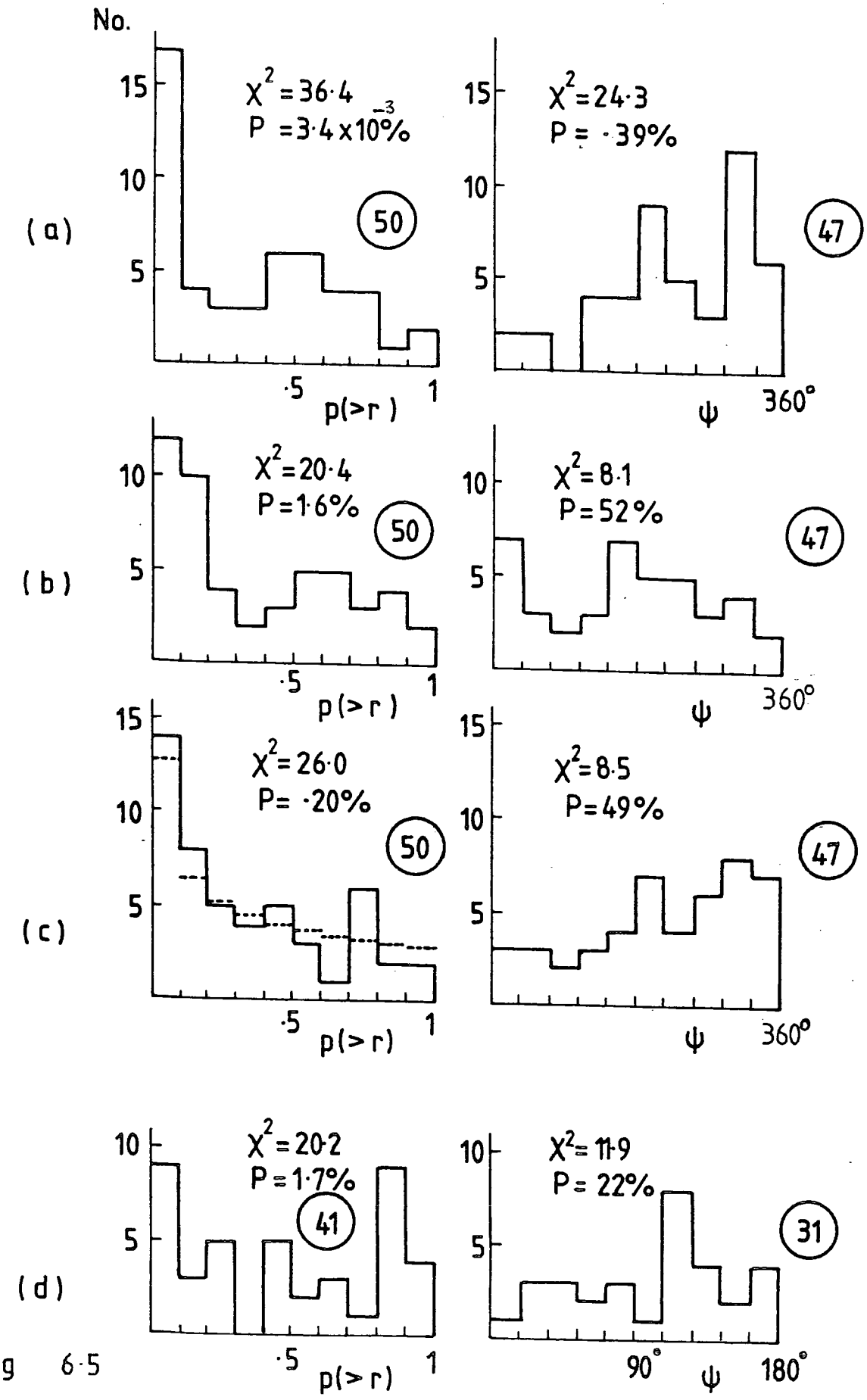

Fig 6·5

Combination of the compilation of data by Linsley and Watson. For each figure the ordinate represents the frequency, the abcissa the probability of observing an amplitude greater

than r , and the measured phase ψ . The circled numbers are the numbers of experimental results included in the figure . Also shown are the χ^2 values and the corresponding probability of each histogram resulting from chance .

a) Simple binning of the first harmonics .

b) The residual distribution of phase and amplitudes after subtraction of the "genuine " signal of equation 6·7·1 .

c) Truly independent data assuming the measurements contain integral , not differential , counts. The dashed line represents the frequency assuming fluctuations 30% greater than random errors .

d) Simple binning of the second harmonics .

Linsley and Watson data this situation occurs in 15 of the 41 measurements. The chance probability of 15 or less occurrences is 4.3%.

Figure 6.5^{b} shows the residual distribution of phase and amplitude after subtraction of the signal in equation 6.7.1. The uniformity of the resulting phase distribution (p = 52%) supports the presence of a genuine signal while enhanced fluctuations can account for the amplitude distribution (p = 1.6%).

There are two considerations to be remembered here. First, there may be spurious waves introduced into data collected at different energies in a single experiment by incomplete atmospheric or instrumental corrections. A more important consideration concerns the statistical independence of the data - can the 50 measurements be considered truly independent? In many experiments involving coincidence arrays four or five fold coincidences would also be included as 3 fold coincidences. It is better to assume that counts at lower energies include the counts at higher energies as well - in other words to consider the energy bins as containing integral rather than differential counts. Only those measurements with more than one energy bin are affected by this procedure, and moreover the data may be considered truly independent. Subtracting the higher energy phase and amplitudes from the lower energy 'cuts' the resultant histograms are shown in Figure 6.5^{c}. The modified amplitude distribution (p = 0.2%) may be explained in terms of additional fluctuations, and to this end the dashed lines of Figure 6.5^{c} represents the expected distribution if the fluctuations were

greater by a factor 1.3 over the standard $\sqrt{\frac{2}{n}}$ values.

The phase distribution of Figure 6.5^{c} is much more linear than Figure 6.5^{a} but still shows some clustering between 180^{o} and 360^{o} (χ^2 probability 49%). Using only the phases, the resultant vector amplitude has a chance probability of 4.7% as opposed to the 0.7% when treated as differential.

It should be noted that the dashed lines of Figure 6.5^{c} give a chance χ^2 probability of 78% and that they are compatible with both the amplitude histograms of figures 6.5^{b} and 6.5^{c}. However, it is hard to see why the extra fluctuations should be this large. Consequently, though the combined data does not conclusively show the presence of anisotropy in this range, it would be difficult to interpret the data as other than a genuine anisotropy, at least over part of the energy range considered. If we accept the Linsley and Watson best fit line of amplitude versus energy then there is evidence for an upturn at the or around 10^{15}eV. As seen earlier, there is known to be a change in the energy spectrum at this energy and this feature and the upturn is strongly indicative of a Galactic origin.

6.9 Interpretation : 10^{14} - 10^{17}eV

If we are prepared to accept the Linsley/Watson best-fit line of amplitude vs energy (which in actual fact is close to the maximum likelihood estimate for the data) then there is evidence for an upturn in the spectrum at an energy near 10^{15}eV. Since the energy spectrum also breaks at this energy we have good evidence for a Galactic origin.

In an earlier section the evidence for irregularities in the LISM on scales above a few pc was noted. This should lead to corresponding changes in phase. In addition, as energy increases the particles produced in the Galactic plane will follow paths that take them further away from the plane; the observed phase of these particles depend increasingly on the magnetic field in the halo. The expected asymmetry about the disc should then cause a slowly varying phase change, which is observed in the measurements.

CHAPTER 7

ANISOTROPIES ABOVE 10^{17}eV

7.1 Introduction

Data at these energies come from giant EAS arrays, largely free from instrumental instabilities. Anisotropies are expected to be much larger here, but the relatively low collection rate gives larger anisotropies on statistical grounds alone. Directional measurements are precise to a few degrees, but energy measurements are only accurate to about 30% since the determination depends on the model chosen to convert the measured parameters to the actual primary energy. The low count rate means that experiments are run for several years ensuring good separation of sidereal and solar harmonics.

An additional complication is that here particles may be of extragalactic origin, but the transition energy is difficult to locate exactly since protons of a given energy have a larmor radius some 26 times that of an Iron nucleus of the same energy per nucleon. We may, therefore, be detecting two separate components each with a different anisotropy. The particles cannot be identified from air shower experiments.

Previously, there had been several claims for large anisotropies above 10^{17}eV but later measurements had failed to confirm the results.

Recent claims for anisotropy are, however, promising; in particular the Haverah Park data at 10^{17}eV is very strong, and it appears that there is optimism for belief in a significant anisotropy at 10^{18}eV as well.

7.2 Haverah Park Data

The most exact and extensive results have come recently from the Haverah Park experiment (Edge et al. 1978). Over 70,000 events have been recorded from $6 \times 10^{16} - 10^{20}$eV and carefully measured in energy and direction. The results were

binned in energy intervals separated by factors of two, arbitrarily centered on 10^{18}eV, and the usual harmonic analysis performed. In addition an attempt was made to gain information on the declination dependence of anisotropy.

Two points are worth noting here. Firstly, although an obvious choice, harmonic analysis is not necessarily the best approach at these energies. Rather, one of the methods suggested by Kiraly and White (1975) may be better suited, particularly for the highest energies. Second, the declination information is less reliable than that gained by scanning in R.A. since the effective area of an EAS array depends in an uncertain way on the zenith angle.

Figure 7.1 shows the latest HP data for first harmonics. Also shown are the exp-k_o probabilities (Watson 1979). The most striking feature is that of an amplitude of 4.2% at 18 hrs R.A. for Ep = 10^{17}eV. This has a formal chance probability of 8×10^{-4}. The adjacent bin (exp - k_o = 1.5×10^{-2}) strengthens the evidence here, particularly since the phases of the two measurements are in such good agreement.

At higher energies the measurements are consistent with a gradual rise in r on statistical grounds alone. The phases are disparate if not indeterminate. However for 3×10^{19}eV there is a further significant result (r = 67%, $\psi \simeq$ 10 hrs, p = 0.027) which would be strengthened if the preceding bin were not nearly 180^{o} out of phase.

Taken as a whole the ten measurements have a significance of 3% according to Edge et al. It should be noted, however, that if the first two bins are neglected this significance falls drastically to nearly 50%. If it is demanded that the

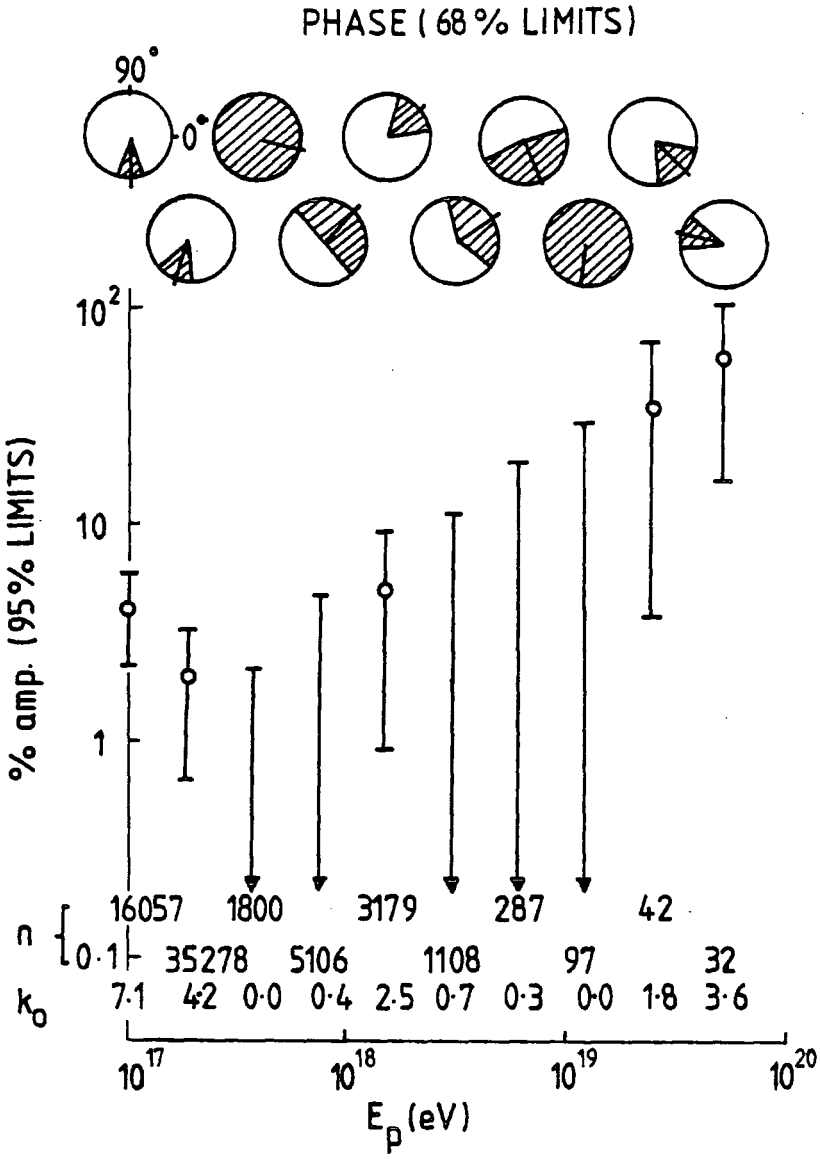

Fig 7·1

First harmonic measurements from the Haverah Park experiment. n is the number of EAS events in each energy bin. k_o is $r^2n/4$

The error bars must be regarded as underestimates — see text.

genuine anisotropy, s, varies as $s \alpha E^{\alpha}$, where α is constant from 10^{17} - 10^{20}eV, then the maximum likelihood technique may be used to determine α. The best fit value is $\alpha = -1.29$, with S = 0.04 at 10^{17}eV. This surprising result (a negative value of α) arises from the overpowering statistical weight of the lowest energy bins, combined with the low amplitude of the subsequent bin. Consequently, only the anisotropy at 10^{17}eV may be taken as really well established. The maximum likelihood fit for the upper eight results gives $\alpha = 0.86$. This is reasonably close to the $E^{0.75}$ dependence suggested by Wolfendale (1977) above 1.25×10^{17}eV.

The second harmonics derived by the HP experiment are not, in general, significant. However, attention should be drawn to the 2.77% amplitude at 3.8 hrs R.A. for $\bar{E}p = 1.5 \times 10^{17}$eV (Edge et al.). This is the most significant measurement derived by the experiment ($k_o = 6.00$) and is based on nearly half of the HP data. Such a large second harmonic is difficult to explain away and must, therefore, be considered as genuine.

One minor criticism of the Haverah Park experiment which should be mentioned concerns their evaluation of the true amplitude, s and the error bars for amplitude and phase plots. The values of s are valid only if the assumption e.g. that $0.01 < s < 0.02$ has the same probability as $0.5 < s < 0.51$ is valid (Section 5.3). In addition the error bars plotted will be too small unless the assumption is correct. However, for significant values (which we are interested in), the errors converge to those given in equation 5.3.18 and only the insignificant harmonics (of less interest) are affected.

7.3 Other Results above 10^{17}eV

No other results have approached that of Haverah Park for accuracy. Nevertheless they are useful in substantiating or disproving the HP results. Pollock et al. (1977) have examined data from $6 \times 10^{16} - 3 \times 10^{17}$eV and found good corroborative evidence for the claimed anisotropy at 15.6 hrs R.A. (with formal chance probability 5×10^{-5}).

Edge et al. have examined data close to 10^{18}eV and claimed support for an anisotropy there. Wolfendale (1977) has also summarised the earlier measurements from $(0.5\text{-}4)\times10^{18}$eV and using this data the best combination gives an amplitude of 4.1% at 1.4 hrs R.A. with formal chance probability 2.3%. However, the most recent results from Haverah Park (as examined above) have weakened the evidence here - k_o for the four energy bins closest to 10^{18}eV is now 3.6 as opposed to 4.6 previously; $< k_o > = 4$.

It is of interest to note that one of themost significant anisotropies ($k_o = 5.99$) ever recorded has been made in this range by Delvaille et al. (1962) at 1.4×10^{18}eV who found an amplitude of 38% at 23 hrs R.A. The modern data are not compatible with this measurement.

In recent years the Sydney group have claimed significant anisotropies (Bell et al., 1973). Kiraly and White (1975) have analysed the claim in detail and found no evidence for a significant grouping.

7.4 Results above 10^{19}eV

These are considered separately here in view of the established change in the slope of the energy spectrum near this energy which forms the topic of a later chapter.

The data here is very scarce in view of the very low shower rate. Watson has estimated the collection rate to be less than 10 showers per year per experiment. At these energies it becomes meaningful to examine individual shower arrival directions since it is possible that individual source regions could reveal themselves.

A useful review by Krasilnikov (1978) has summarised all the available information giving an amplitude of $\sim$ 50% for energies above 2 x 10^{19}eV. This result is compatible with the significant HP result at 10^{19}eV (Edge et al., 1978). This result appears surprising if viewed in the light of the quickly varying phase angle with energy of the HP data, however, the Krasilnikov data does include all of the HP events which form the bulk of the data.

At the highest energies > 5 x 10^{19}eV the HP group has presented evidence suggestive of the highest energy particles arriving from directions close to that of the Virgo super-cluster, nearly perpendicular to the Galactic plane.

This is somewhat at variance with the Yakutsk data > 10^{19}eV (with similar declination coverage to HP) which tends to cluster from the equatorial plane of the Galaxy (Berezinsky 1977). The favoured direction is in the direction of the Galactic anticenter. The Sydney results will be useful when reanalysis has been completed for the Southern hemisphere. Clearly further events must be awaited before the current

situation is clarified.

7.5 Interpretation for $\bar{E}_p > 10^{17}$eV

Two possibilities immediately present themselves. The simplest interpretation is in terms of a Galactic origin with the increase in r with energy a result of progressively less efficient Galactic trapping. Figure 7.2 shows a summary of the anisotropy amplitudes and phases for the whole range considered. The line marked GD corresponds to this simple Galactic drift hypothesis. There are points in favour of this interpretation.

1. There appears to be a change in slope on the amplitude vs energy plot of Figure 7.2[a] at about 10^{15}eV which is also where the energy spectrum changes shape. In terms of Galactic escape the change in spectral index from α to $\alpha+\Delta\alpha$ on the amplitude/energy plot should be equivalent to the change in the primary energy spectrum from γ to $\gamma+\Delta\gamma$. From Figure 7.2[a] the change $\Delta\alpha \simeq 0.75$ which is close to the value of $\Delta\gamma \simeq 0.6$ found in the primary spectrum.

2. The trend in phase above 10^{17}eV (Figure 7.2[b]) is in the same sense as that of the magnetic field direction referred to in section 3.2. . This suggests a simple streaming along the lines of the field. Agreement is not good, but this is to be expected as the magnetic field is poorly known and its asymmetry about the plane will undoubtedly introduce complications.

The rapidly varying phase with energy above 10^{16}eV and the change in slope of the amplitude-energy plot at $\sim 10^{15}$eV has consequences concerning the mass composition of the primaries. If we assume that the chemical composition of

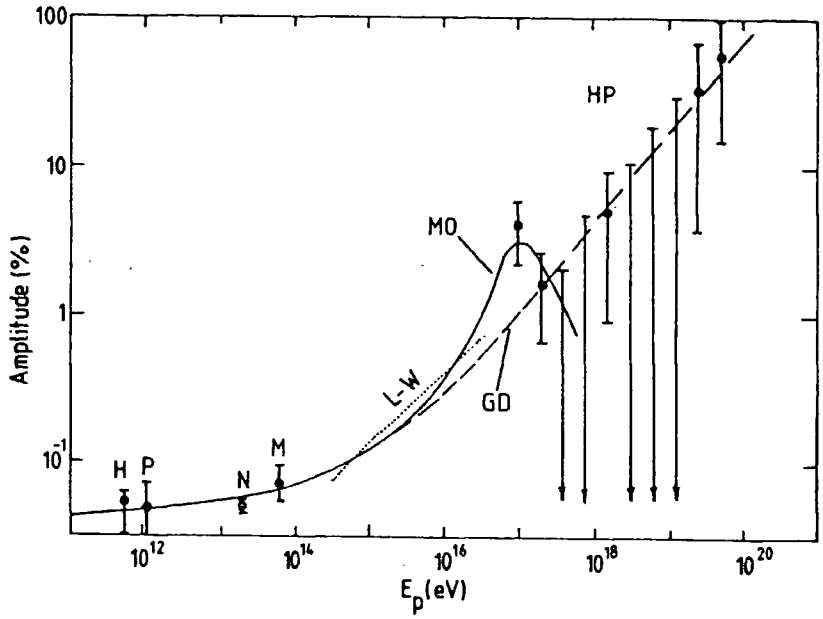

Fig 7·2 a

First harmonic data from 10^{11}eV to 10^{20}eV. H : Holborn inclined telescope P : Poatina N : Norikura M : Musala LW : Linsley and Watson summary HP : Haverah Park data GD : Smooth line drawn through the points and corresponding to "Galactic Drift" MO : Line corresponding to "Mixed Origin". The HP errors are 95% confidence limits, the others are 68 % limits.

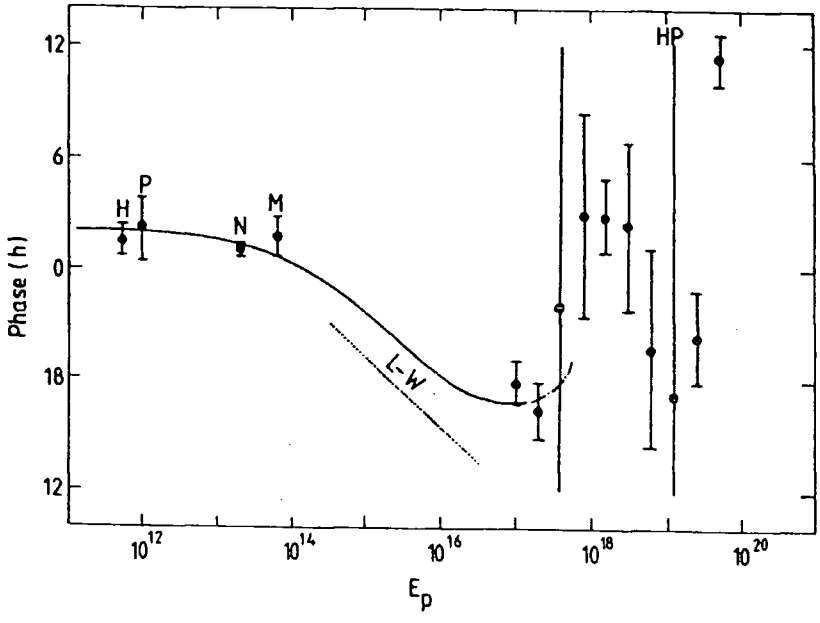

Fig 7·2 b

the primaries below the change in slope of the primary spectrum is the same as that measured at lower energies (the slow rise in amplitude with energy < 10^{15}eV supports similar sources) and that the break is due to reduced efficiency of trapping, then heavier nuclei would make up an increasing fraction of the primaries > 10^{15}. This would tend to reduce the amplitude as different mass particles at a given energy have different gyroradii and consequently different phases would be expected.

The simplest argument is that the composition consists mainly of protons so that phase changes are the result of 'anisotropy of propagation'. This is consistent with the hypothesis of Wdowczyk and Wolfendale (1976) and Stapley et al. (1977) that heavier nuclei are fragmented escaping from their sources and with the studies of Cunningham et al. (1977), Lapikens et al. (1977) and Barrett et al. (1977) on the basis of fluctuation studies.

The difficulty with this interpretation is the HP large significant anisotropy observed at 10^{17}eV; indeed the measured amplitude at that energy is larger than those measured up to 10^{18}eV. The model predicts a slow increase with energy.

7.6 Mixed Origin Model

Here we assume that the particles above 10^{17}eV are both Galactic and Extragalactic in origin. The Extragalactic component dominates as higher energies are reached so that the 10^{17}eV peak corresponds to the last region where Galactic particles make up the bulk of the radiation. A spectrum

similar to that shown of Figure 7.2[a] (denoted MO) would be expected. In this model a change in slope of the primary energy spectrum at $\sim 10^{17}$eV would not be unexpected, and it appears that this change does exist (Kempa et al. 1974). Further, the change of slope at $\sim 3 \times 10^{15}$eV for the spectrum of Galactic particles would now appear steeper, $\Delta\gamma \simeq 1$, compared with the value 0.6 for the overall spectrum (fig 7.3).

Any anisotropy observed above 10^{18}eV on this model is a result of purely Extragalactic effects. Assuming that the local supercluster provides these particles then the locally measured amplitude and phase will be a result of the internal magnetic fields of the Supercluster. Kiraly and White (1975) have examined this aspect in greater detail and attempted correlations of the observed flux with a variety of extragalactic source candidates. No significant correlation was found for particles $> 10^{19}$eV while only a marginal correlation (with Quasars) was found for energies just below 10^{19}eV. However Krasilnikov (1978) presents evidence for intensity peaks above 10^{19}eV and the HP data suggest that more particles arrive from high galactic latitudes. Consequently an extragalactic origin is suggested. In this case, above 10^{19}eV, particles are presumably travelling from only a fraction of the galaxies in the cluster.

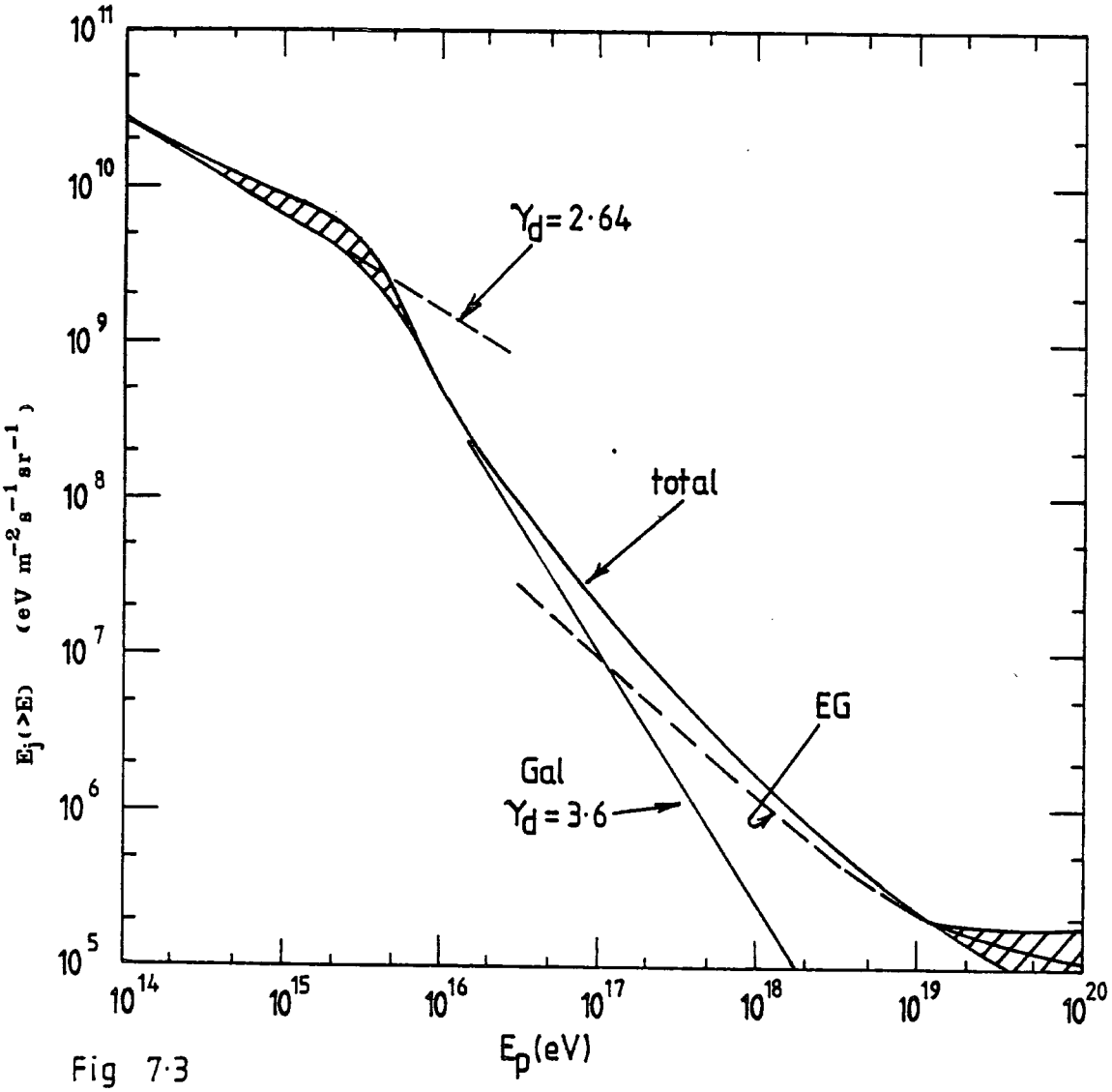

Fig 7·3

The composite spectrum of cosmic rays expected for a mixed origin (see text). Gal and EG correspond to the Galactic and extragalactic components respectively.

CHAPTER 8

THE COSMIC RAY SPECTRUM FOR ENERGIES GREATER THAN 10^{18}eV

8.1 Introduction

It now appears certain that at very high energies there is a break in the primary differential energy spectrum ($j(E) \propto E^{-\alpha}$), changing from $\alpha \simeq 3.0$ below 10^{19}eV to $\alpha \simeq 2.0$ above 10^{19}eV. In particular, there is clear evidence for particles of energy as high as 10^{20}eV and probably even higher, and at this energy there is no increased spectral steepening. This result is extremely surprising in view of the expected effects of the Universal black body radiation field, which will be considered below.

Figure 8.1 shows the measured spectra from the Haverah Park (mainly muon data) and Volcano Ranch (mainly electrons) experiments. Both are in reasonable agreement and indicate a flattening of the spectrum near 10^{19}eV. Krasilnikov et al. (1977) have given results in the same energy region for the Yakutsk EAS array, and these also indicate a change in slope at 10^{19}eV (figure 8.2).

Arguments against a Galactic origin for particles $> 10^{18}$eV have already been given in a previous section. Primarily, large anisotropies from the general direction of the Galactic plane would be expected with Galactic origin, and, in addition, a flattening of the spectrum would be unexpected since as energy increases particles are less likely to be confined. Nevertheless, a Universal origin model may be objected to on grounds of the high energy density of

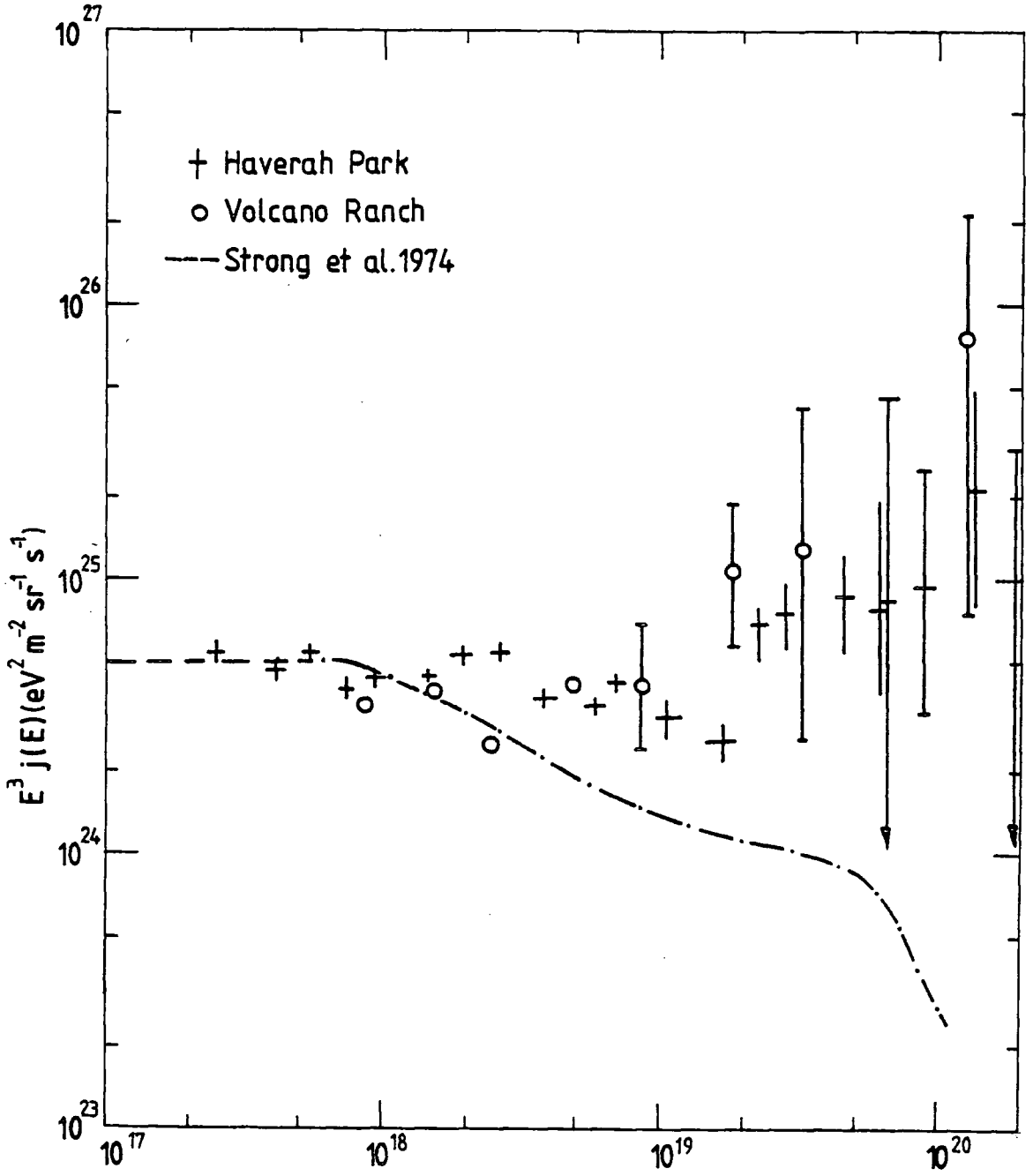

Fig 8·1

Measured differential energy spectra from the Haverah Park and Volcano Ranch experiments. The Haverah Park data are derived mainly from the detection of muons, while that of Volcano Ranch are from electrons. The dashed line shows the prediction of Strong et al. 1974

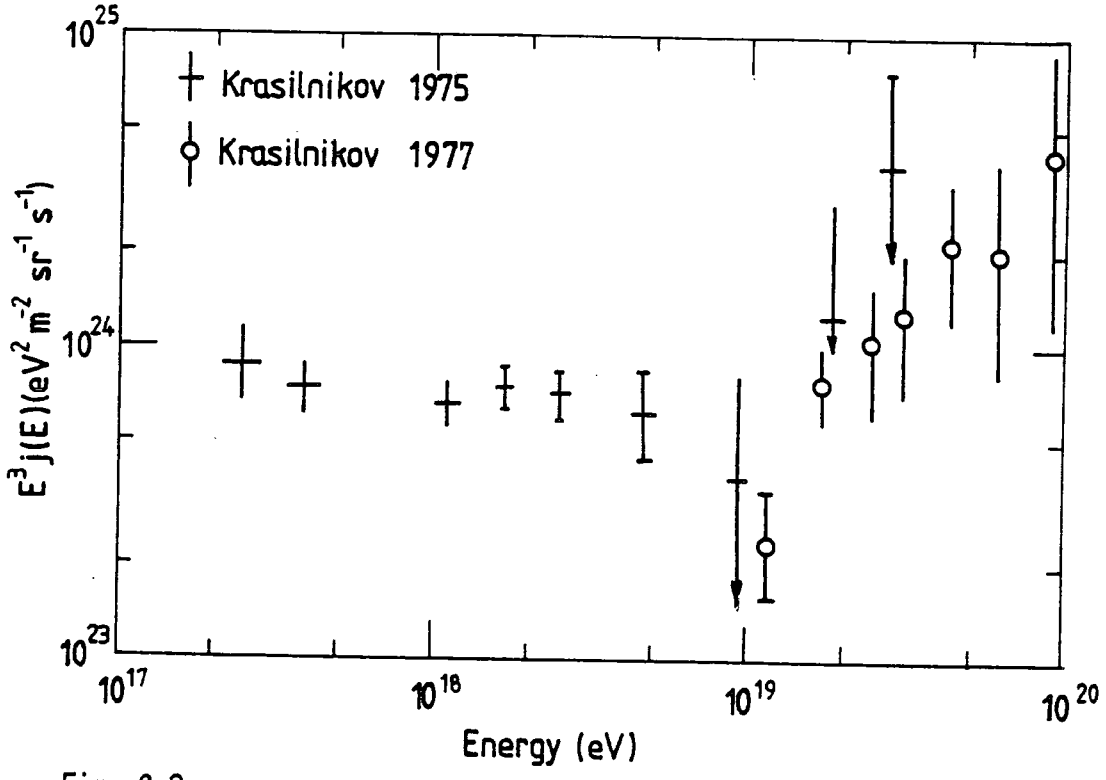

Fig 8·2

Measured differential energy spectrum from the Yakutsk EAS array. Note the similarity to figure 8·1. The essential feature is the change in slope at 10^{19} eV.

cosmic rays in the universe which would result from a uniform distribution of sources. This may be overcome by assuming that only the high energy particles are extragalactic.

An even stronger argument against a Universal origin seems to arise from the lack of a cut off in the observed cosmic ray spectrum above 6×10^{19}eV, such a cut-off being expected from the interaction of protons with black body photons. Strong et al. (1974) have derived the expected high energy spectral shape assuming Universal origin and the attenuation caused by these interactions (see figures 8.1 and 8.3). The reduction first manifests itself at 7×10^{17}eV as a result of reactions of the form $p + \gamma \rightarrow p + e^+ + e^-$. Above 6×10^{19}eV the attenuation is heightened as a result of reactions of the form $p + \gamma \rightarrow p + \pi^o$. Consequently, the observed spectrum should represent the dotted line of figure 8.1, assuming a constant production spectrum with $\alpha = 3.0$.

The first of the problems noted above may be overcome by either assuming that only the highest energy particles are extragalactic or by assuming that the majority of particles are trapped within the systems that produce them. Wolfendale (1977) notes that if the 2.7 K^o field were absent a natural explanation would be that of an extragalactic component with a smaller spectral index intervening at 10^{19}eV. Alternatively, the particles may derive from relatively nearby sources such as the local supercluster (of which the Galaxy may be a member).

It is in attempting to explain the high energy end of the cosmic ray spectrum in terms of extragalactic origin

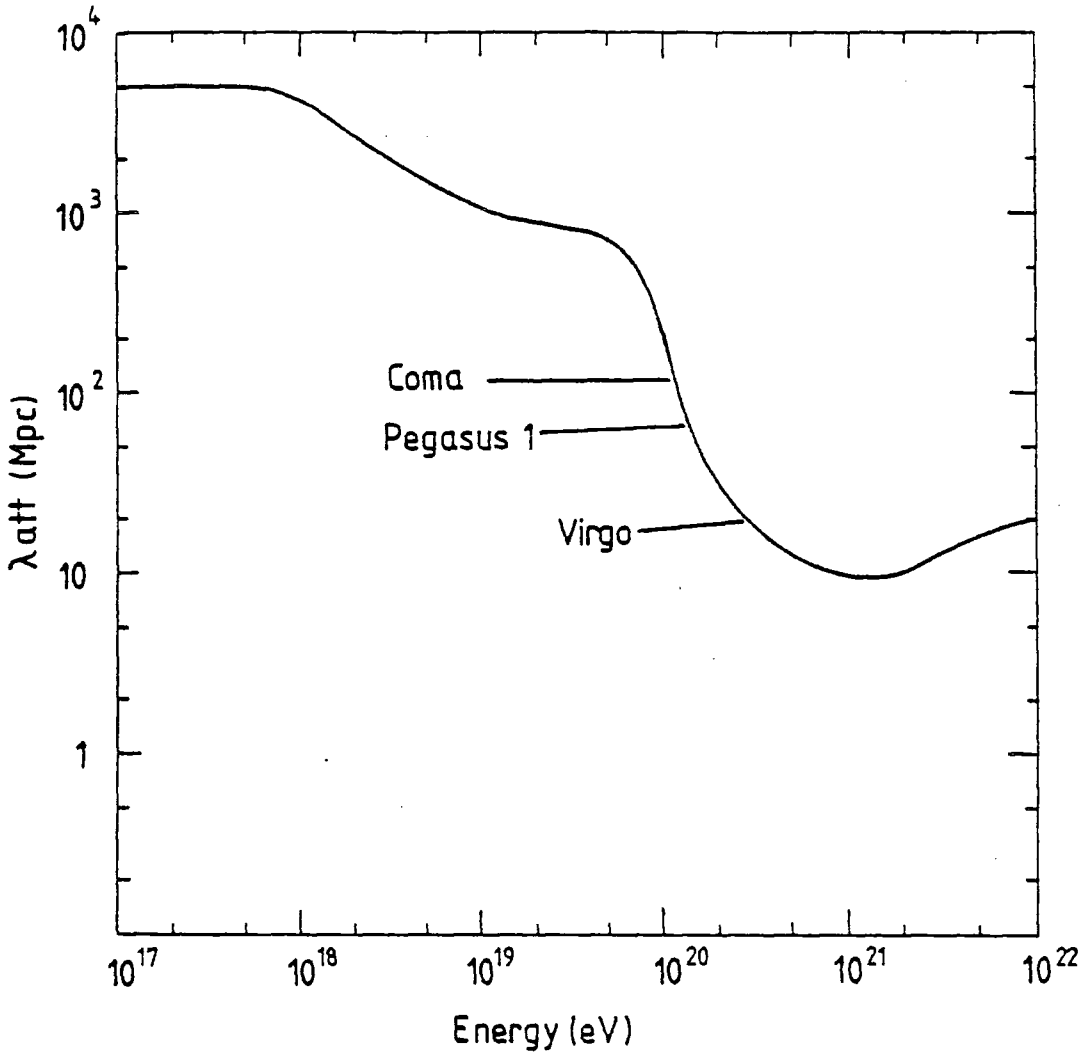

The black body attenuation curve of Strong et al.,1974. The decrease at $7 \cdot 10^{17}$eV is the result of electron pair production, that at $6 \cdot 10^{19}$eV the result of π^0 production. Also shown are the distances to some nearby clusters of galaxies.

Fig 8·3

that the ensuing sections are concerned, but first it must be noted that some doubt must remain that the energy spectra of figures 8.1 and 8.2 are in fact correct. To derive the primary energy at such high rigidities the assumption is made that nuclear reactions do not substantially change character from lower to higher energies. The change in slope could, in principle, be the result of a change in the interaction cross sections so that the derived energy is wrongly located. This possibility was considered by Wolfendale (1977) who concluded that in the absence of any positive evidence to the contrary, the measured spectrum should be sound; it is surely most unlikely that a substantial change in the character of the interaction should occur at just an energy where Galactic anisotropies are to be expected, and thereby to mask them.

8.2 Neutron cluster Model of High Energy Cosmic Rays

8.2.1 Original form of the model A number of models have been proposed to explain the apparant anomaly of the high energy spectrum. Wdowczyk and Wolfendale (1976) have considered a model in which cosmic rays are essentially trapped within clusters of galaxies following the suggestion of Brecher and Burbridge (1972). In the proposed model, an intracluster magnetic field effectively traps all but the highest energy neutrons, which are formed by fragmentation of heavier nuclei, principally iron, on the optical, infra-red and black-body fields within the cluster. Even charged particles of 10^{20}eV are assumed to be largely trapped. Only certain galaxies need provide nuclei of 10^{20}eV/nucleon which can then fragment.

Neutrons above $\sim 10^{18}$eV are increasingly able to escape the cluster before decaying into protons because of relativistic time dilation. The success of the model lies in the ability of the escaping neutrons to provide an extra source of particles in the required range 10^{19} - 10^{20}eV, leaving lower energies to be supplied by Galactic sources. An approximate treatment was given assuming sources concentrated at the center of a cluster, and for a uniform distribution of sources - which yielded a somewhat better, broader spectrum. At lower energies, between 10^{17} and 10^{18}eV, it was found desirable to assume an energy independent leakage of protons equivalent to 2% of the neutron flux to obtain the desired spectral shape. In the following, this model is extended to give a more realistic picture of the neutron hypothesis.

Extended Neutron Model : Clusters of Galaxies

8.2.2 More realistic form of the neutron model Accurate calculations demand a knowledge of both the distribution of sources within a cluster and the distribution of cluster radii. In addition, the types of cluster most likely to produce high energy particles and their proportion should be known. Unfortunately there are numerous complications in both measuring and in defining the 'radius of a cluster'; it may even be meaningless to attempt to do so since even clearly isolated galaxies may be regarded as the lower end of a spectrum of cluster sizes. The background density of isolated galaxies is also difficult to determine bearing in mind the above comments. However, Oemler (1974) has obtained some accurate data for a limited sample of clusters

and types of cluster in terms of the gravitational radius R_G defined by $E_{grav} = \frac{-GM^2}{R_G}$. In addition he has obtained the three-dimensional mass distribution of the clusters examined. In this respect clusters of the type CD are of particular interest. These clusters have been associated with "strong" radio sources (luminosity $>10^{40}$ ergs s^{-1}) suggestive of a high electron density or magnetic field (Matthews, Morgan and Schmidt, 1964, Morgan and Lesh, 1965) . Many CD clusters are also known to be X-ray sources. Optically they have the following characteristics:

(a) They consist of a giant, outstandingly bright, centrally located CD galaxy (or galaxies in the case of clusters resembling Coma). They are easily recognisable.

(b) They are regular, being rather circular in appearance, resembling globular star clusters with a well defined centre towards which the mass is concentrated.

(c) They are rich in ellipticals and are generally compact; Oemler gives the mean gravitational radius as 3.55 Mpc.

The central CD galaxies are themselves of interest. They have bright elliptical-like nuclei surrounded by extensive halos. The results of Carter (1977) and Oemler (1973) suggest that the envelope 'halo' may extend as far as 1 Mpc and may consist of a diffuse 'cloud' of stars which extends to fill the whole cluster. A typical rich cluster may have a virial mass of $10^{14} - 10^{15}$ $M_\odot$ (Abell, 1964). It is this central galaxy that is largely responsible for radio

emission when it occurs. The X-ray emission referred to earlier is expected to be caused by thermal bremsstrahlung from hot intracluster gas ($\sim 10^8$K). This gas has been detected by a reduction or 'cooling' of the black-body background radiation caused by Compton scattering of the microwave photons by the hot intergalactic gas. The measurements have established that proton densities of some 5 - 12 cm^{-3} over the clusters are present (Lake and Partridge 1977, Birkenshaw et al. 1978).

In view of the particularly favourable characteristics of CD clusters as candidates for high energy sources of cosmic rays noted above, it is hereafter assumed that only CD and related B type clusters of galaxies are responsible for production of particles at the highest energies.

8.2.3. The predicted Cosmic ray Spectrum For our own Galaxy the primary spectrum of Iron nuclei has been measured by Juliusson (1975) and others, and is consistent with the form $E^{-2.5}$. However, it is not unreasonable to expect a different spectral index for production within clusters (and indeed within our own Galaxy because the value 2.5 may result from a production exponent of, say 2.0 coupled with an energy-dependent lifetime of the form $\langle T \rangle \propto E^{-0.5}$). Furthermore our own Galaxy is unlikely to produce particles much above 10^{17}eV, yet clearly some extragalactic sources are able to produce particles of 10^{20}eV, possibly by acceleration in dense massive objects. Consequently, a variety of production spectra have been assumed for purposes of calculation, but only three are represented here for comparison, $\alpha = 2.0$,

2.25, 2.5. In addition the production of cosmic rays within a CD cluster will be assumed proportional to the density of matter as obtained from the mass distribution profile of Oemler.

The probability of a neutron of energy E_{20} (E in units of 10^{20}eV) traversing a distance ℓ Mpc before decay is simply

$$F(E) \simeq \exp -(R\ell/E_{20}) = \exp -(k\mu\ell) \qquad 8.2.1$$

where $R \simeq 1$

If the cluster radius is r and a specific source is at Q, distance a from the centre, then the proportion of particles which are emitted in the interval of angle $(\sigma, \sigma + d\sigma)$ will be (Figure 8.4).

$$\frac{2\pi\ \ell^2\ \sin\sigma\ d\sigma}{4\pi\ \ell^2} = \frac{\sin\sigma}{2}\ d\sigma \qquad 8.2.2$$

The proportion which escape from the cluster with energy^{-1}, μ, from Q is simply

$$p(\mu,a) = \int_0^{\pi} \frac{\sin\ \sigma}{2}\ \exp -\mu\ \ell(\sigma)\ d\sigma$$

substituting for $\ell(\sigma)$ using the cosine rule we have

$$p(\mu,a) = \int_0^{\pi} \frac{\sin\ \sigma}{2}\ \exp -\mu\ \left(-a\ \mathrm{Cos}(\sigma) \pm \sqrt{r^2 - a^2\ \sin^2\sigma}\right)\ d\sigma \qquad 8.2.3$$

With a = o this reduces to $p(\mu, o) = \exp - \mu r$, as required for central sources. Writing a = r, representing a source at the edge of a cluster the expression reduces to

$$p(\mu,a) = \tfrac{1}{2}\left(1 + \frac{1}{2\mu\ r}\ [1 - \exp - 2\mu\ r]\right) \qquad 8.2.4$$

Equation 8.2.3 has been evaluated for different cluster radii at energies of 10^{17} - 10^{21}eV. Some specific examples are given in figure 8.5 . For increasing μ the limiting value of 0.5 is reached at a = r, as expected.

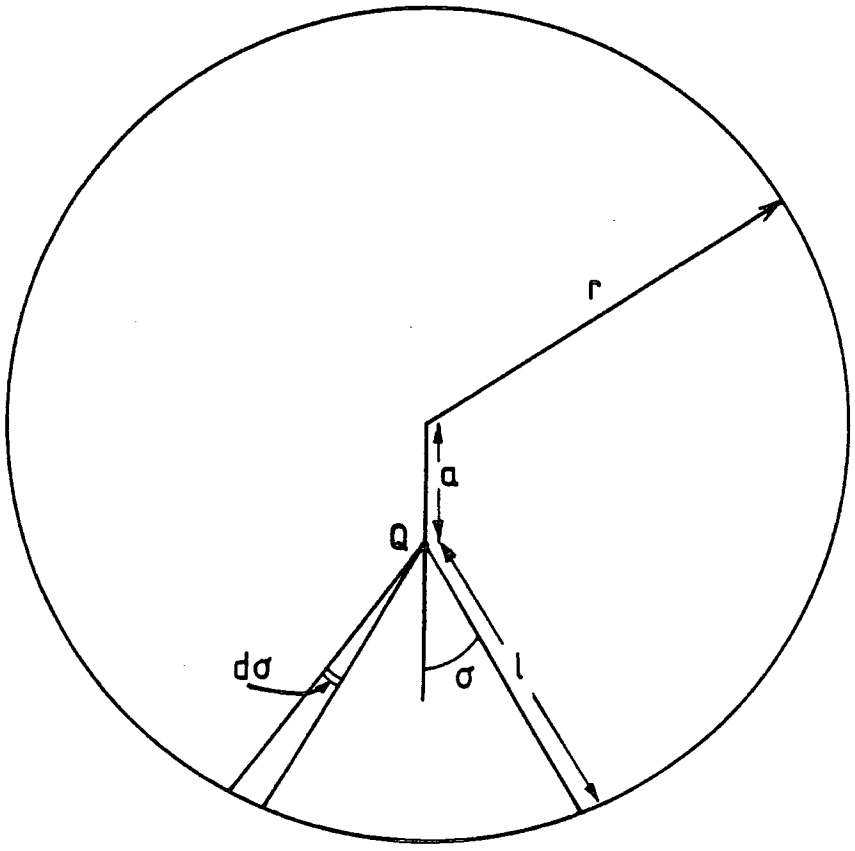

Geometry of the neutron model for a source distance a from the center of an assumed spherical cluster of radius r .

Fig 8·4

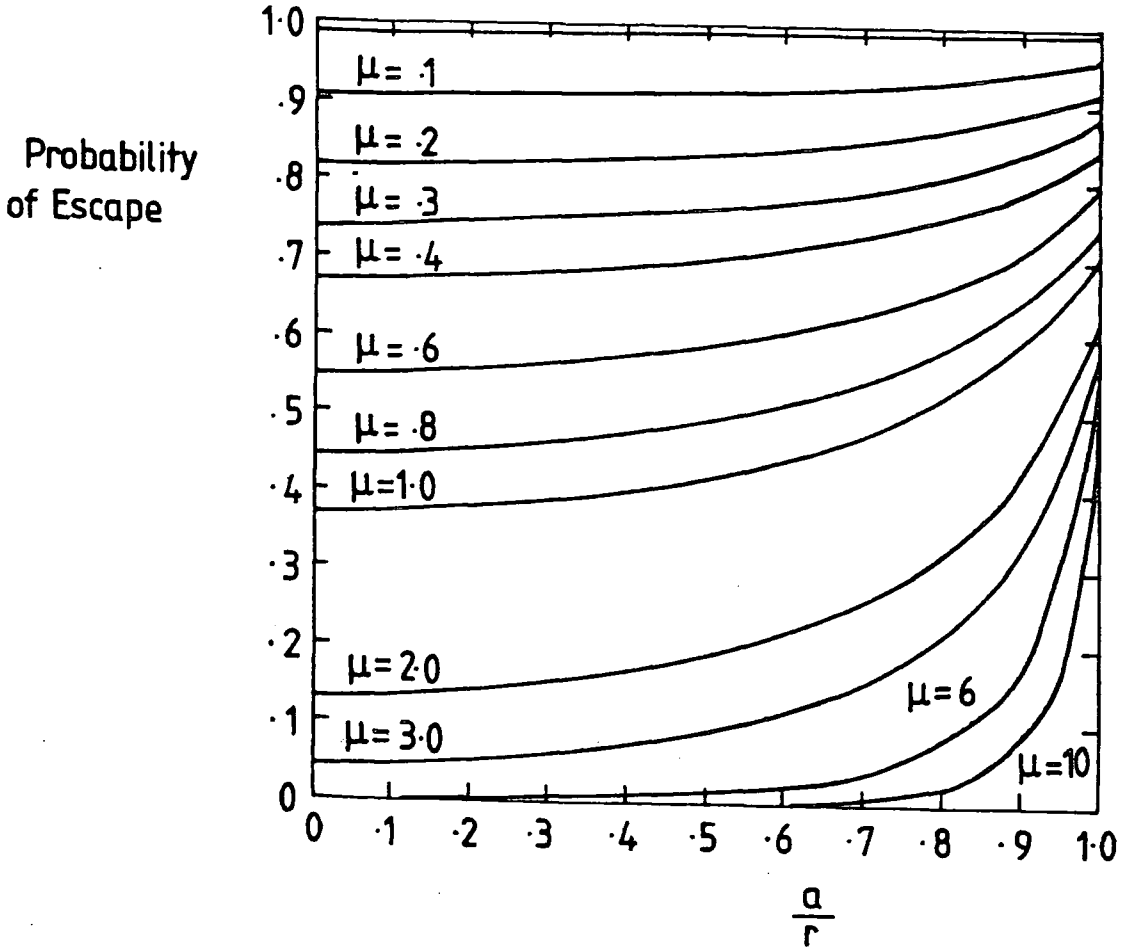

Escape probability vs. a/r for a cluster of radius 1 Mpc for varying values of $\mu = 1/E_{20}$. Note the limiting value of 0·5 at $a = r$ as μ increases. E_{20} is the energy in units of 10^{20} eV.

Fig 8·5a

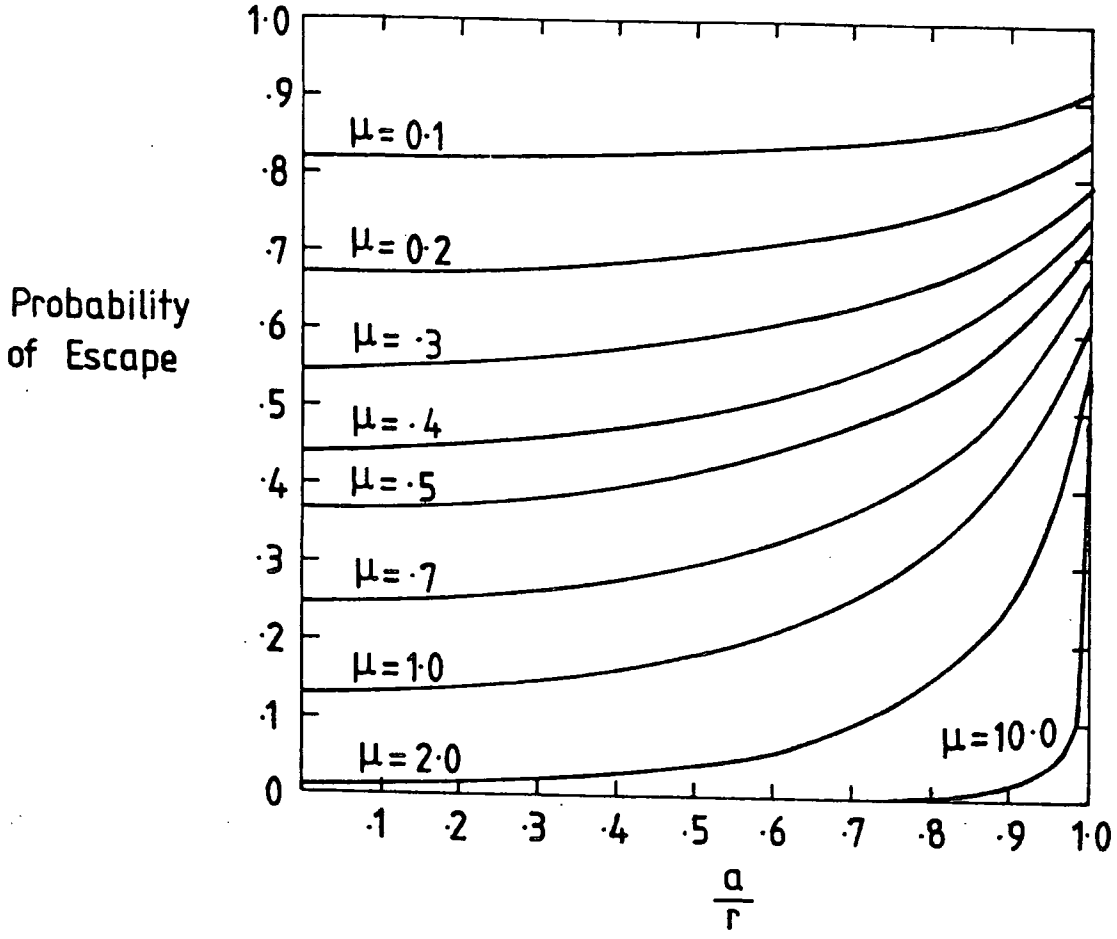

As for figure 8·5a but for a cluster of radius 2 Mpc

Fig 8·5 b

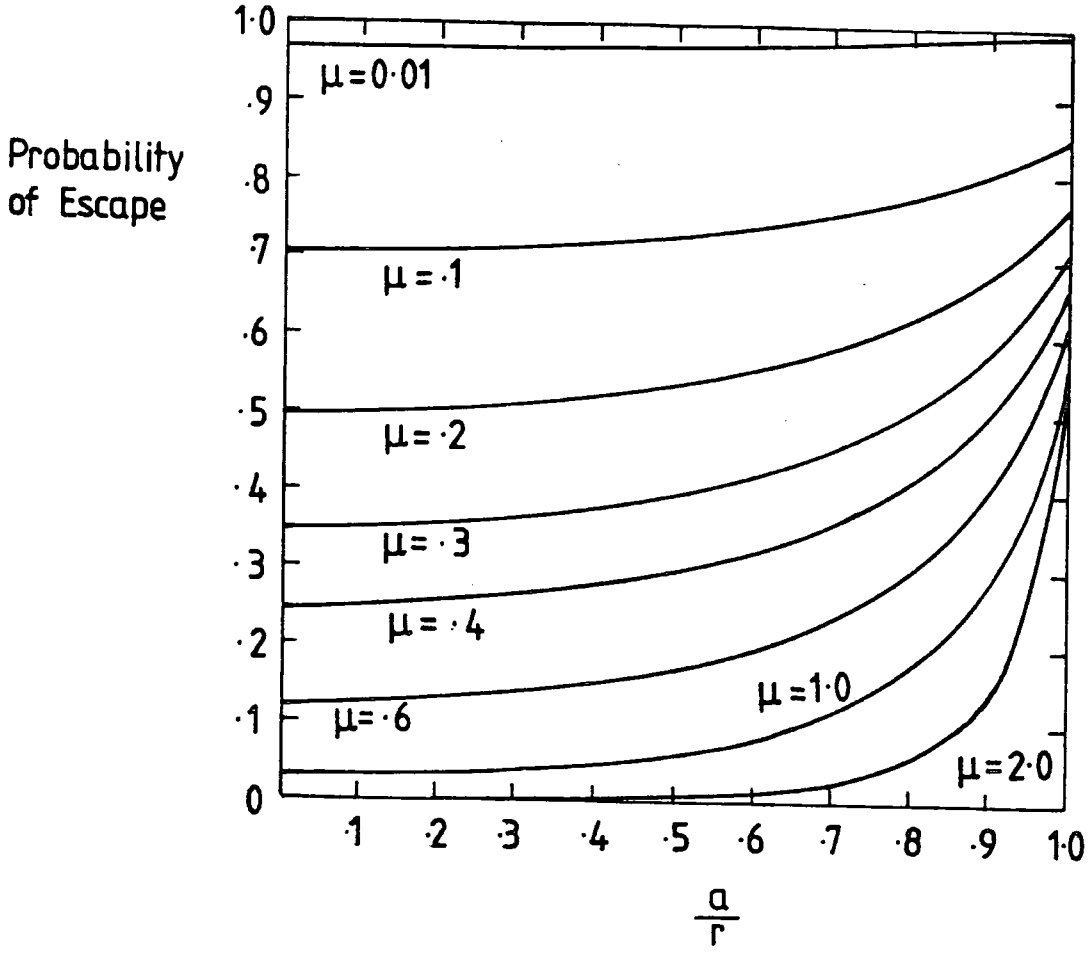

As for figure 8·5 a but with cluster radius 3·55 Mpc corresponding to Oemler's mean gravitational radius .

Fig 8·5 c

The proportion of neutrons of given energy which escape from the whole cluster is simply given by

$$P(E) = \int_0^r 4\pi\, a^2\, \rho(a)\, P(a,\mu)\, da \;/\; \int_0^r 4\pi\, a^2\, \rho(a)\, da \qquad 8.2.5$$

where $\rho(a)$ is the mass density. The product $P(E)$ with an assumed spectrum $j(E) \propto E^{-2.25}$ and the black body attenuation curve $B(E)$ yields the high energy local cosmic ray spectrum. $P(E)$ has been evaluated for a mean radius $\bar{R}_G = 3.55$ Mpc as observed by Oemler. Figure 8.6 shows the results; the calculated spectrum is denoted $Sp(E)$. The dotted line represents an assumed 0.6% leakage protons inserted in rather arbitrary fashion to smooth the transition to Galactic particles at lower energies. Also shown is the expected spectrum assuming only central sources ($S_c(E)$) while the dashed lines represent the limits of the measured spectrum. As can be seen, the prediction peaks somewhat near 6×10^{19}eV before tailing off. The fit is seen to be close to the observed spectrum. Figure 8.7 shows the corresponding results if production spectra of the form $E^{-2.0}$ and $E^{-2.5}$ are assumed. With $\alpha^{\dagger} = 2.5$ the spectra is reasonably flat from 10^{18} - 10^{19}eV and no cluster leakage protons are needed to fit the observed spectrum. With a spectrum $\propto E^{-2.0}$ the prediction is not so accurate, with a sharp peak near 6×10^{19}eV. Some 0.7% of cluster leakage protons are required on this model. On this basis alone the best fit is obtained with $\alpha^{\dagger} \simeq 2.5$.

8.2.4. The Energy Density and gamma-ray Flux The neutron hypothesis can lead to unreasonably large production rates and energy densities within a cluster. The analysis of Abell's Catalogue (Abell 1958) by Rood and Sastry (1971) enables a rough estimate of the number of contributing clusters

† α is the exponent of the production spectrum

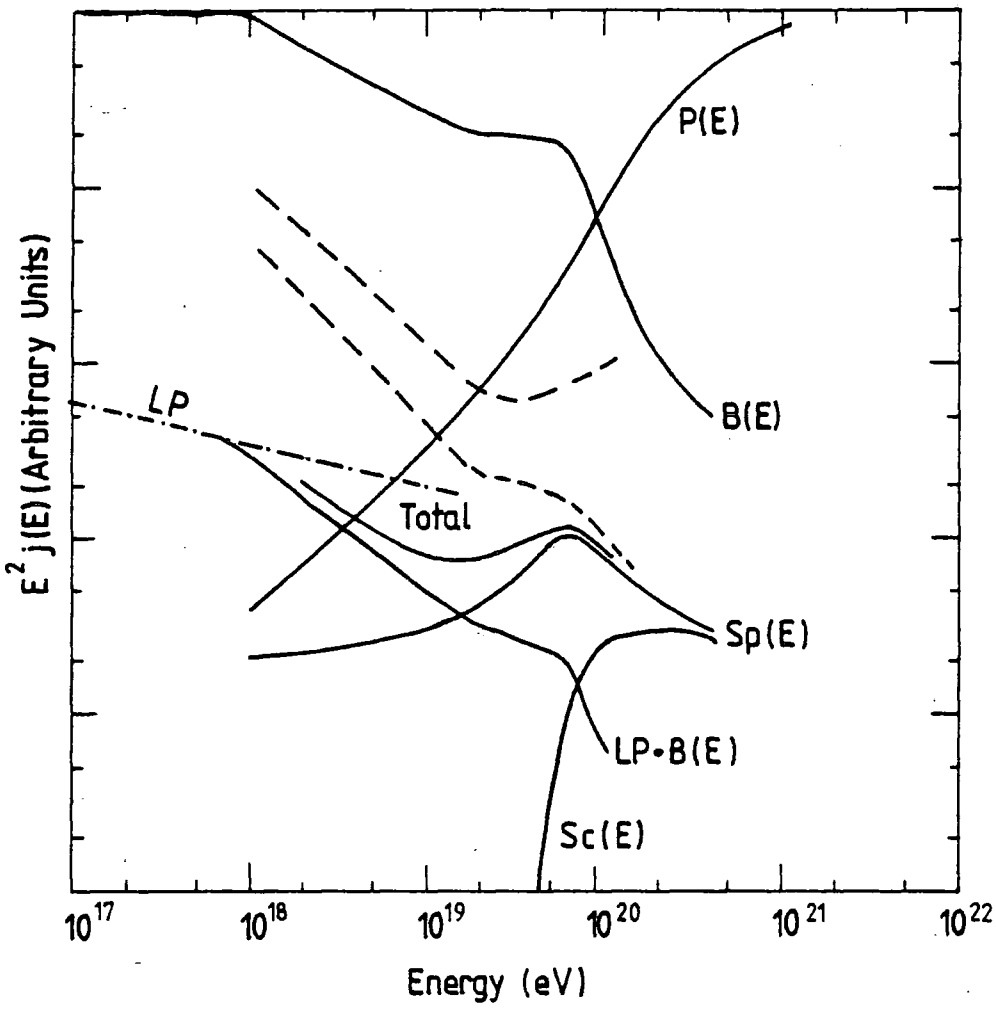

Prediction of the neutron model for an assumed production spectrum of the form $E^{-2\cdot25}$. B(E) is the black body attenuation curve, P(E) the escape probability, Sc(E) the prediction with only central sources, Sp(E) the prediction for a distribution of sources and LP is an assumed 0·6 % leakage protons. Also shown are the limits of the observed spectrum.

Fig 8·6

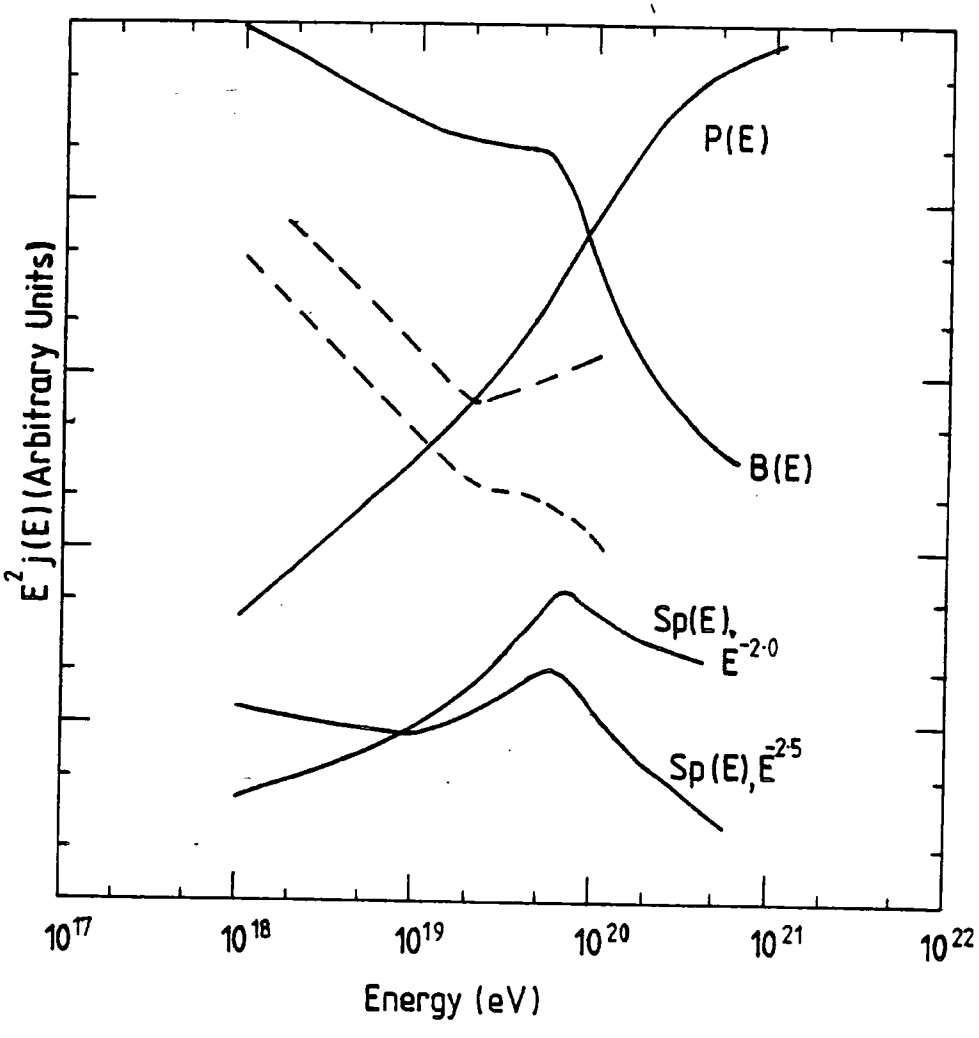

Predictions of the neutron model for assumed production spectra of the form $E^{-2\cdot0}$ and $E^{-2\cdot5}$, denoted Sp(E). P(E) is the escape probability, and B(E) the black body attenuation curve.

Fig 8·7

to be made. 33 CD and related B type clusters are found within Abell distance group 3 (about 377 Mpc with Ho = 60). Allowing for obscuration, unobserved clusters and the fact that the survey covers only half the sky, the density of contributing clusters is estimated as $N = 5.9 \times 10^{-7}$ Mpc^{-3}, or some 2×10^5 within the Universe. Assuming $\alpha = 2.25$ for the range 10^{10} - 10^{20}eV and allowing for the so far neglected proton component and the reduction in intensity from the black body component, the cluster production spectrum may be estimated as

$$j(E) = 5.0 \times 10^{12} E^{-2.25} \text{ m}^{-2} \text{ s}^{-1} \text{ sr}^{-1} \text{ eV}^{-1} \qquad 8.2.6$$

Without trapping, the particle density that would occupy the universe is then

$$N(> 10^{10}\text{eV}) = \frac{4\pi}{c} \int_{10^{10}}^{\infty} j(E)\, dE \simeq 5.3 \times 10^{-8} \text{ m}^{-3} \qquad 8.2.7$$

If V is the "volume" of the Universe and assuming clusters produce at a rate R particles s^{-1} for a Hubble time of $\tau_H = 13 \times 10^9$ years, then we can equate

$$\frac{R\tau_H}{V} = \frac{N(>10^{10})}{2 \times 10^5} \qquad 8.2.8$$

which gives $R \simeq 5 \times 10^{48}$ s^{-1}.

The energy density of the particles with no trapping is obtained using

$$W_{CR}\ (>10^{10}) = \frac{4\pi}{c} \int_{10^{10}}^{\infty} (E - mc^2)\, j(E)\, dE \simeq 2.6 \times 10^{-3} \text{ eV cm}^{-3} \qquad 8.2.9$$

Consequently, within a cluster we must scale by V/V_{cl} where V_{cl} is the volume occupied by the clusters. The energy density within a cluster will then be some 20 eV cm^{-3}.

The expected gamma ray production rate (> 100 MeV) from a cluster may be calculated using the results of Stecker (1975) who gives for local (1 eV cm^{-3}) conditions

$$q = 1.3 \times 10^{-25} n_H \text{ cm}^{-3} \text{ s}^{-1}$$

Assuming $n_H \simeq 10^{-4}$ cm^{-3} throughout a typical 3.55 Mpc cluster, the gamma ray emission will be about 1.3×10^{48} γ s^{-1}. The Coma cluster at a distance of $\sim$ 113 Mpc (Allen 1973) would, therefore, be expected to give a flux of some 9×10^{-7} γ $cm^{-2}s^{-1}$. The background flux from a uniform distribution of clusters is given by

$$j = \frac{1}{4\pi} \int_0^{r_H} \varepsilon \, dr \, d\Omega \qquad 8.2.10$$

where ε is the emissivity. Consequently $j \simeq 2.7 \times 10^{-5}$ γcm^{-2} s^{-1} st^{-1}.

The gamma ray flux and background has been measured by the SAS II Satellite. There are no data for the Coma cluster, but SAS II data for M87 puts an upper limit of 10^{-6} γ cm^{-2} Sec^{-1} (>100 MeV), and it is unlikely that the Coma flux is higher than this. Thus, the predicted flux is probably just allowed by the observations. The background flux has been measured as $0.9 \pm 0.2 \times 10^{-5}$ cm^{-2} s^{-1} st^{-1} (Fichtel et al., 1978) and is thus a little lower than predicted. However, the discrepancy is not too serious.

Calculations similar to those above for $\alpha = 2.0$ give $W_{CR} = 0.5$ eV cm^{-3}, $j = 6 \times 10^{-7}$ γ cm^{-2} s^{-1} st^{-1}; for $\alpha = 2.5$ the corresponding values are $W_{CR} = 3.7 \times 10^3$ eV cm^{-3}, $j = 3.8 \times 10^{-3}$ γ cm^{-2} s^{-1} st^{-1}. The last mentioned situation is clearly not allowed.

8.2.5. Discussions of the Neutron Model. The results obtained are strongly dependent on the exact production spectrum adopted for Iron. While $\alpha = 2.5$ gives the best fit to the observed spectrum the energy density within a cluster would need to be unrealistically high and the gamma ray background predicted is nearly two orders of magnitude too high. With $\alpha = 2.0$ the background predicted is about two orders of magnitude lower than observation (and thus allowed, but local proton spectrum is not as satisfactory as with the other models). On balance the overall best fit comes from assuming $j(E) \propto E^{-2.25}$ which gives reasonable values for both the background flux and the local spectrum, although the energy density ($\sim$ 20 eV cm^{-3}) may still be considered rather high.

As noted by Wdowczyk and Wolfendale a potential problem with models of this type is the need for mean cluster fields of the order of 1 μG in order to ensure adequate trapping (a 10^{20} eV particle has a Larmor radius of $\sim$ 0.1 Mpc in such a field). Observations of the radio synchrotron emission from the Perseus and Coma clusters of galaxies (Willson 1970) have given indirect measurements of the field - Willson quotes an uncertain value of 10^{-6} gauss for the extended radio sources.

Field (1974), in a review of intergalactic gas, notes that if thermal bremsstrahlung is indeed responsible for the X-ray emission from rich clusters of galaxies then a mass of gas equal to a few percent of the virial mass with $T \simeq 10^{8}$K

may be present. In the case of the Coma cluster the best fit is provided by assuming central gas densities of $\sim 4 \times 10^{-3}$ cm^{-3} with T = 10^8K, and other clusters yield similar results. In the case of Coma there also appears to be a diffuse optical emission between (4-5) x 10^3 Å which may be due to a cooler component of the intra-cluster gas (Welch and Sastry 1972). These measurements are in accord with the derived densities of Lake and Partridge and Birkenshaw et al. from microwave background cooling experiments.

Field gives the one dimensional rms velocity of a particle in a fully ionised gas with He/H = 0.1 as 1100 km s^{-1}. If we assume equipartition of energy such that

$$W_{CR} = \frac{B^2}{8\pi} = \tfrac{1}{2} \rho v^2 \qquad 8.2.11$$

then with gas densities of 10^{-29} g cm^{-3} throughout the whole cluster, fields of about 1 μG would be expected. With central gas densities of $\sim 10^{-3}$ cm^{-3} fields an order of magnitude greater could in theory be sustained. It is of course, difficult to envisage mechanisms by which fields even of 1 μG could be generated and maintained over such an extended range. Turbulence of intergalactic gas may provide some amplification of the magnetic field between galaxies but not to the extent suggested by the above calculations. Brecher and Burbridge (1972) conclude that fields as high as 1 μG could conceivably be present but the evidence is at best scanty. However, it is quite possible that the magnetic fields in individual galaxies within a cluster are much greater than the 3 μG measured in our own Galaxy so that substantial trapping could occur within the galaxies themselves.

Lastly, we note the argument of Biermann and Davis (1960) that it is unlikely that cosmic rays can be confined if their energy density exceeds that of the magnetic energy density, at least if not much matter is present. An energy density in cosmic rays of 20 eV cm^{-3} would,therefore, require a field of 2.8×10^{-5} gauss to confine the cosmic rays. Again, the fields in individual galaxies could alleviate this problem to some extent, although for the whole cluster we have little reason to expect fields much greater than 10^{-8} gauss. Further data on intergalactic magnetic fields would greatly clarify the situation.

8.3 General remarks

Despite what has just been stated, the neutron hypothesis does lead to a feasible explanation of the high energy cosmic ray spectrum. Two points are worth noting. Firstly, if large numbers of clusters with radii smaller than $\sim$ 3 Mpc were sources of high energy particles, then these would dominate and a somewhat more peaked spectrum would result. The required energy density within a cluster would decrease while the amount of cluster leakage protons necessary to explain the observed spectral shape would increase. Finally, if the Galaxy were itself a member of the local supercluster then a similar model may still be used if slow diffusion of protons with consequent energy loss is the case (Wdowczyk and Wolfendale 1976).

In the next section a diffusion model with extragalactic origin will be considered as an alternative to the neutron model.

8.4 Diffusion Model of Ultra High Energy Cosmic Rays

8.4.1 Principle of the model. With the neutron hypothesis the increasing escape probability with energy ensured that the generated spectrum was sufficiently flat to derive the observed spectrum even allowing for black body attenuation. In this section the possibility of diffusion, rather than rectilinear motion, as the means of propagation of high energy particles will be considered. With diffusion, the experimental spectrum can be modelled rather easily if the bulk of the high energy particles propagate from the centre of the local supercluster.

The black body attenuation curve of figure 8.3 shows that particles of energy $>10^{20}$eV can only be effectively provided by sources within a distance of some 200 Mpc, if they are extragalactic in origin. Above 3×10^{20}eV the attenuation length for protons is less than 20 Mpc so that only the nearest rich cluster (Virgo) is readily accessible to provide particles. The next large cluster, Pegasus I, is about 65 Mpc (Allen 1973) distant with a corresponding energy of $\sim 1.3 \times 10^{20}$eV. Clearly, if scattering or deflections result in any non-linear propagation whatsoever, and if the main sources of cosmic rays are situated at the cluster centres, particles of energy $> 10^{20}$eV will only arrive from Virgo.

For diffusion, a critical parameter is the length over which the magnetic field may be considered as regular; perhaps the distance over which the field doubles or halves

its strength or changes direction considerably. For clusters, a not unreasonable estimate of this "cell size" may be a few tenths of a Mpc, say 0.1 Mpc (a few Galactic diameters). In a cluster field of 10^{-8} gauss, this dimension is equal to the Larmor radius of a proton of 10^{18}eV. Thus, for energies below this value diffusion may be considered important for particles from all extragalactic sources. For particles below 10^{20}eV ($r_L \simeq 10$ Mpc) diffusion will be important for particles originating within a few tens of Mpc's.

A consequence of diffusion is that the intensity of low energy particles tends to be suppressed while high energy particles are able to travel relatively rapidly, and even for long distances arrive within their lifetime. In this respect the diffusion model leads naturally to the required spectral shape and is not critically dependent on the diffusion coefficient adopted.

8.4.2 Characteristic of Diffusion We are concerned with the three-dimensional diffusion equation

$$\nabla^2 f(x,t) = \frac{1}{D} \frac{\partial f(x,t)}{\partial t} \qquad 8.4.1$$

where D is the diffusion coefficient. For a continuously emitting source a distance x away, and if we neglect the losses inherent in propagation (not the black body losses), the solution is

$$f(x,t) = \frac{q}{(4\pi tD)^{3/2}} \exp - \frac{x^2}{4Dt} \qquad 8.4.2$$

where q is the output of the source per unit time.

The flux of cosmic rays arriving at distance x is consequently given by

$$n(x) = \frac{c}{4\pi} \frac{q}{(4\pi D)^{3/2}} \int_0^T \frac{\exp -\frac{x^2}{4Dt}}{t^{3/2}} \, dt \qquad 8.4.3$$

where T is the effective lifetime of the particles as derived from figure 8.3.

The above equation is more readily calculated by making the substitution $y^2 = x^2/2Dt$ to give

$$n(x) = \frac{cq}{8\pi^2 Dx} I\left(\sqrt{\frac{x^2}{2DT}}\right) \qquad 8.4.4$$

where $I(z) = \frac{1}{\sqrt{2\pi}} \int_z^\infty \exp - y^2/2 \, dy$

or, putting $w = x^2/4DT$,

$$n(x) = \frac{cqTw}{2\pi^2 x^3} I(\sqrt{2w}) \qquad 8.4.5$$

The anisotropy can be calculated from

$$\beta = \frac{3D}{c} \frac{1}{n(x)} \frac{dn(x)}{dx}$$

Noting that $\frac{dn(x)}{dx} = -\exp(-w)/\sqrt{4\pi DT}$ we have

$$\beta = \frac{3D}{cX} \left[1 + \left(\frac{w}{\pi}\right)^{\frac{1}{2}} \frac{\exp(-w)}{I\sqrt{2w}}\right] \qquad 8.4.6$$

There is little or no information available about the energy dependence of D. For cosmic rays in our own Galaxy the break in energy spectrum near 10^{15}eV can be interpreted in terms of a change in the functional dependence of D(E) from D(E) ≈ constant below 10^{15}eV to D(E) $\propto E^{\frac{1}{2}}$ above 10^{15}eV, but there is no reason why this form should hold in clusters at the energies we are dealing with. Equation 8.4.5 has consequently been evaluated for a range of different choices of δ and constants of proportionality.‡ The values of D chosen are such that the mean free path between scatterings, ℓ_s at 10^{19}eV, varies from ∿ 100 Kpc to 10^3 Kpc ($D = \frac{1}{3} \ell_s c$)

‡ assuming $D(E) = A E_{19}^{\delta}$ cm^2/ s ; E_{19} in units of 10^{19}eV

(as indicated earlier). The form of D is assumed to hold for the whole range 10^{17} - > 10^{20}eV.

Figures 8.8 - 8.11 show the shape of the expected energy spectrum independent of the form of the production spectrum (in other words multiplied by E^{γ} where γ is the index of the production spectrum). In general a slower variation of D(E) gives a better effect whereas with higher values of δ the spectrum exhibits a peaking with a quite sharp lower energy cut off. With the small values of δ the calculated results reproduce the spectrum well above 10^{18}eV. Below 10^{18}eV, unless a high value of diffusion coefficient is used, there is an increasing discrepancy with the experimental results and a fit cannot be achieved at 10^{17}eV. However, it is likely that Galactic particles dominate at lower energies and there is thus no insurmountable problem here.

Above 10^{20}eV all the calculated spectra show a fairly rapid trailing off. The ultra high energy end of the spectrum will, however, be extended when allowance is made for the fact that at energies near and above 10^{21}eV particles are effectively pursuing rectilinear paths, i.e. that diffusion is unimportant because the Larmor radii are so large. Above 10^{20}eV diffusion becomes progressively less important so that between 10^{20} - 10^{21}eV an intermediate situation may be taken.

8.4.3 Virgo Production Spectrum The experimentally observed flux allows an estimate of the total output in cosmic rays from Virgo to be made. Near 10^{19}eV the estimate is not critically dependent on the exact values or form of the

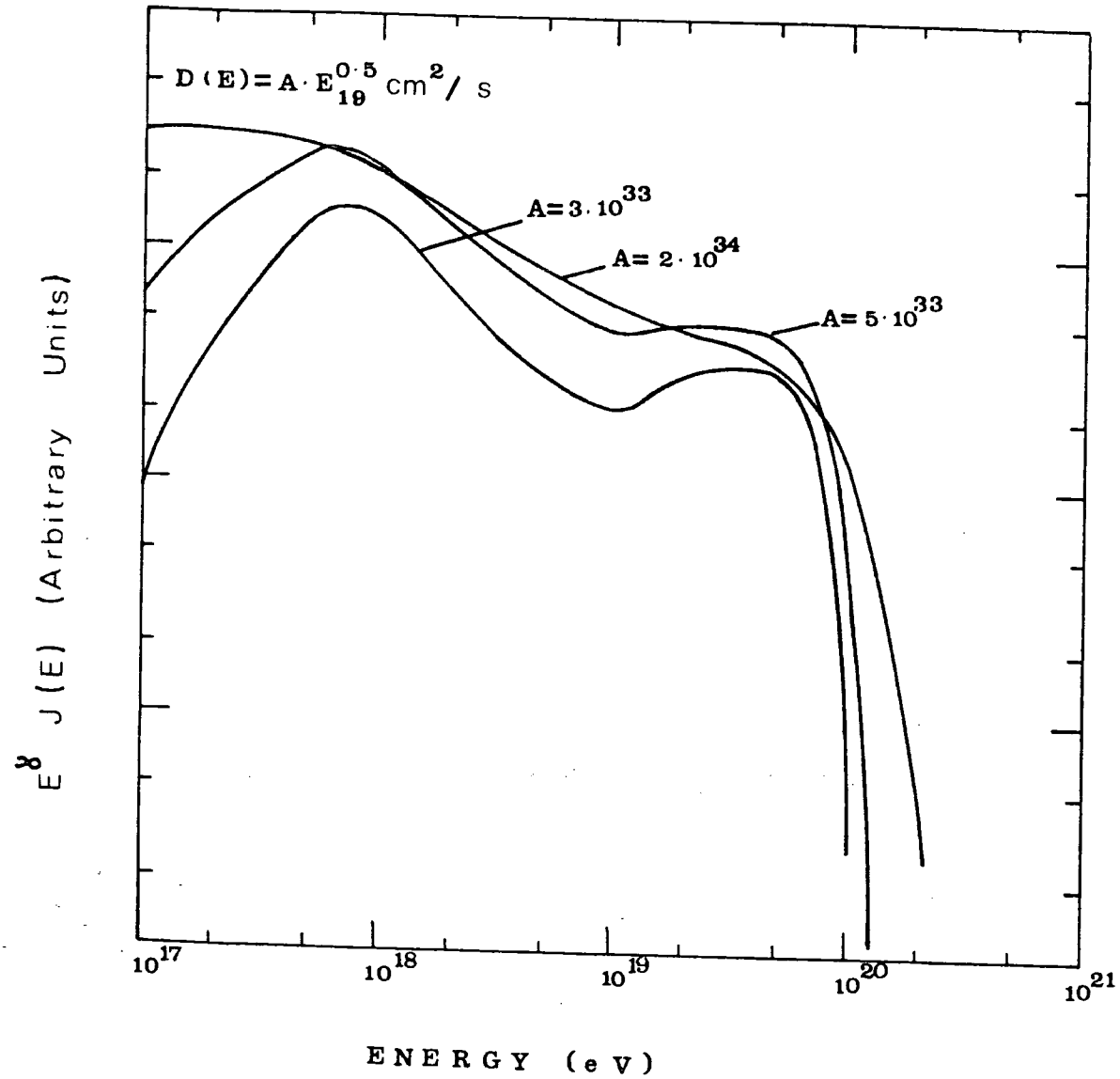

Diffusion model prediction for the high energy cosmic ray spectrum, with diffusion coefficients as shown, E_{19} in units of 10^{19}eV.

Fig 8·8

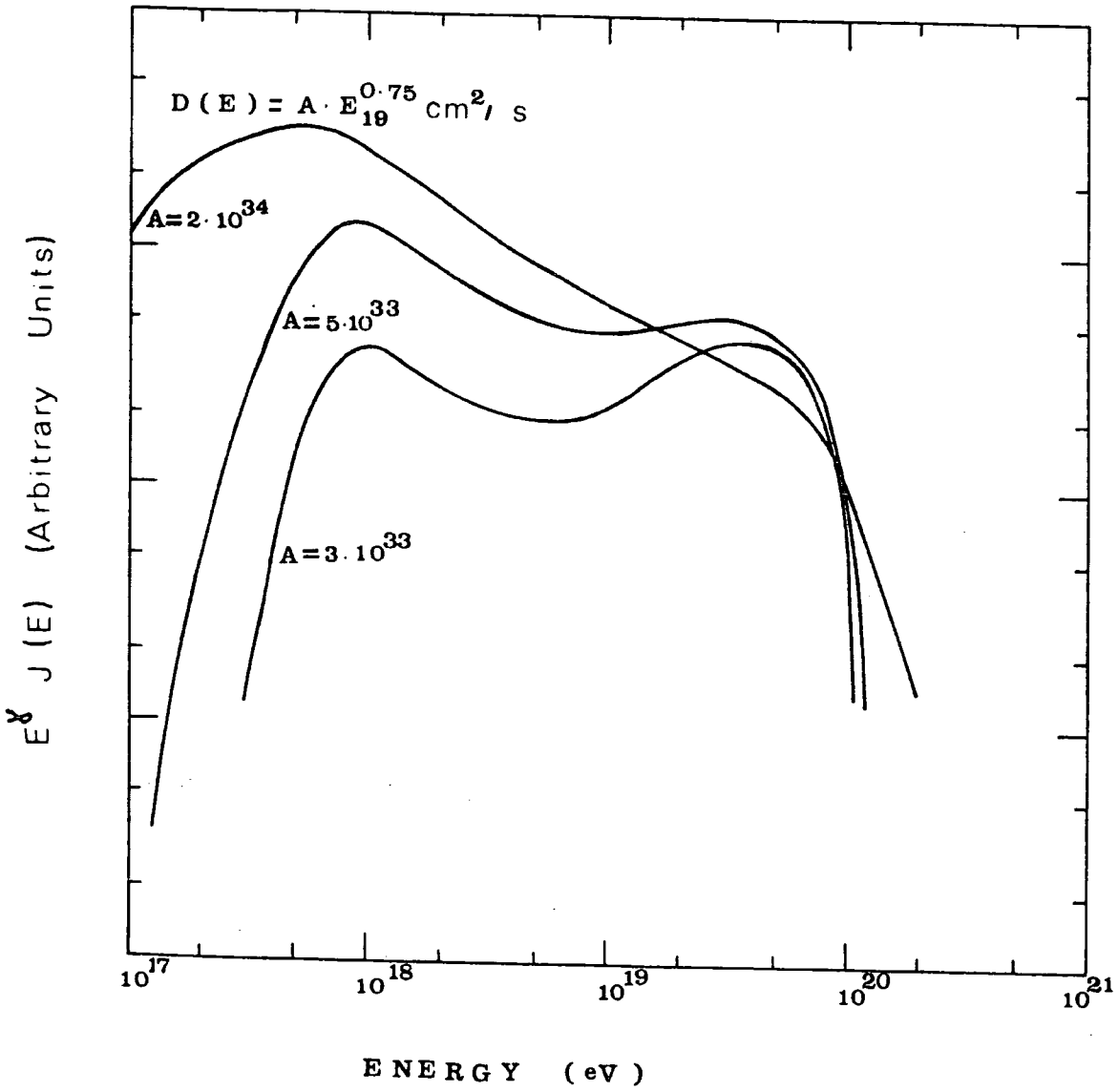

Diffusion model prediction for the high energy cosmic ray spectrum, with diffusion coefficients as shown, E_{19} in units of 10^{19} eV.

Fig 8·9

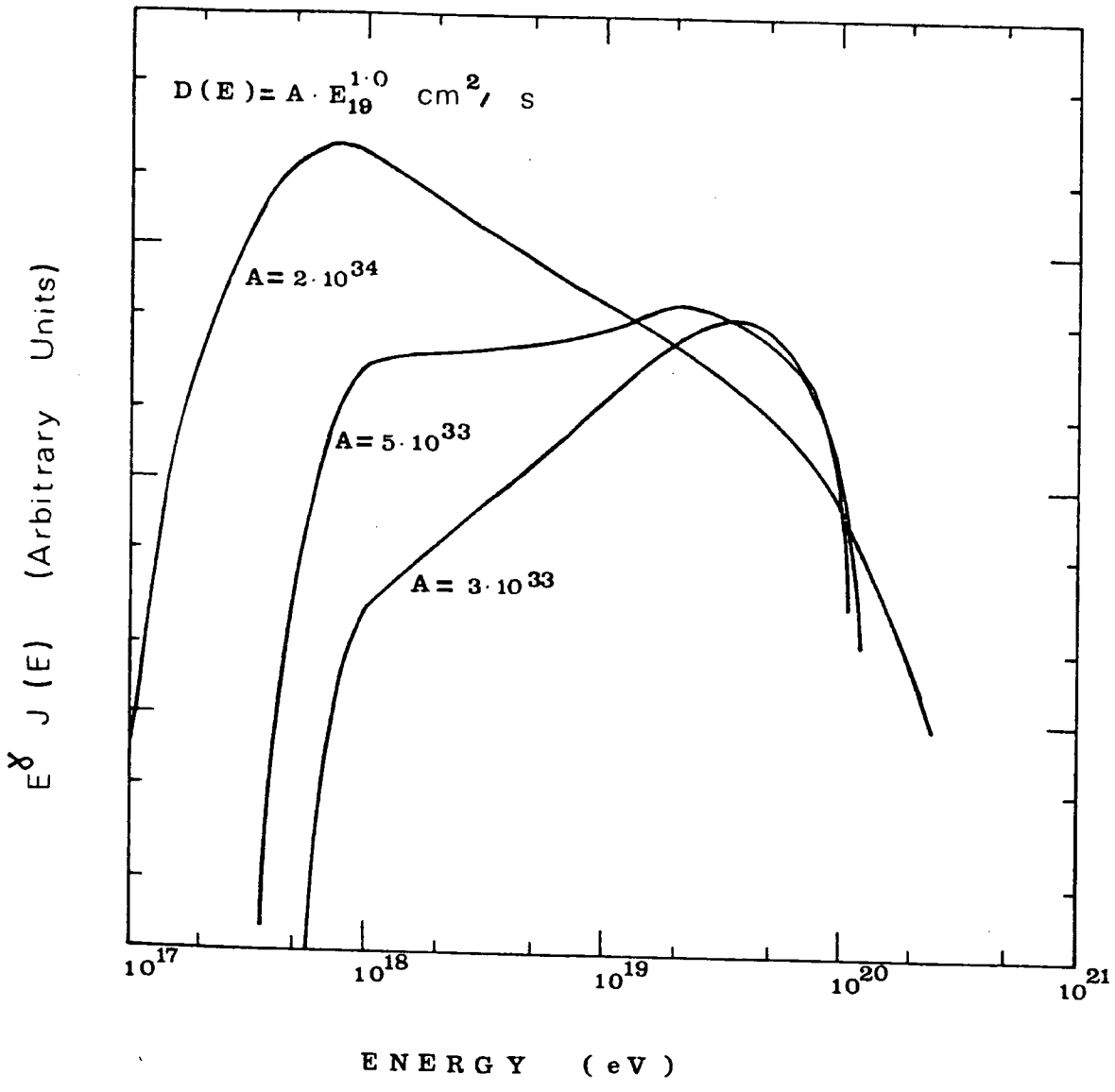

Diffusion model prediction for the high energy cosmic ray spectrum, with diffusion coefficients as shown, E_{19} in units of 10^{19} eV.

Fig 8·10

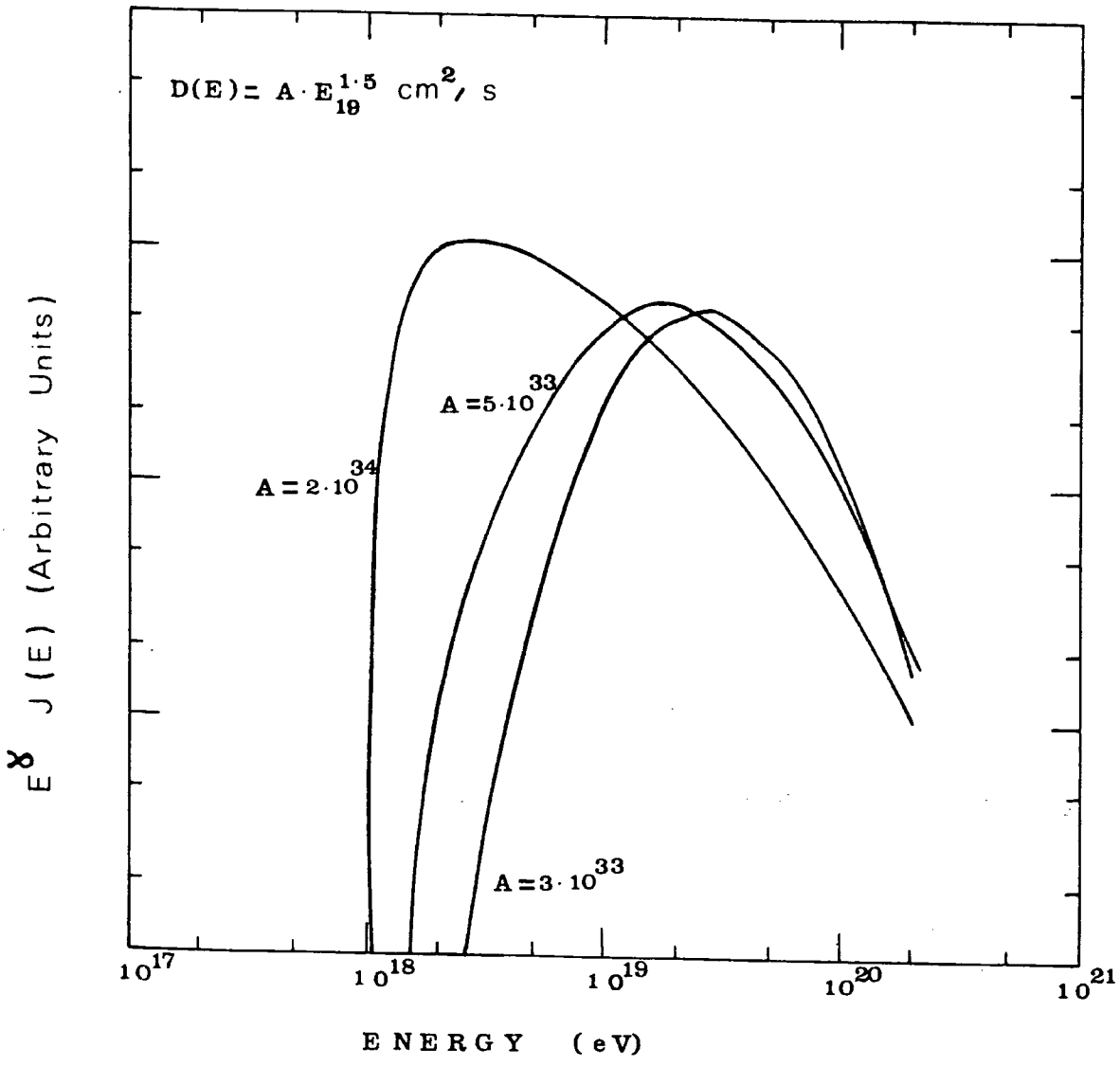

Diffusion model prediction for the high energy cosmic ray spectrum, with diffusion coefficients as shown, E_{19} in units of 10^{19} eV.

Fig 8·11

diffusion coefficient. From figure 8.1 the measured intensity at 10^{19}eV is $\sim 3 \times 10^{-33} eV^{-1} m^{-2} s^{-1} sr^{-1}$. Adopting a diffusion coefficient of $5 \times 10^{33} \left(\frac{E(GeV)}{10^{10}}\right)^{\frac{1}{2}}$ cm $^2 s^{-1}$ (the preferred choice, figure 8.8) the production intensity at 10^{19}eV will be 7.4×10^{24} $s^{-1} GeV^{-1}$.

The production spectrum which gives a reasonable fit to the actual spectrum is then

$$q(E) = 7.4 \times 10^{24} \left(\frac{E(GeV)}{10^{10}}\right)^{-2.44} s^{-1} GeV^{-1} \qquad 8.4.7$$

again assuming the preferred diffusion coefficient.

Although there is no information on the actual energy dependence of q(E), the electron spectrum of radiogalaxies is often somewhat flatter than that of the Galactic proton component ($\simeq E^{-2.6}$), so the choice is not unreasonable.

If this production spectrum holds back to 1 GeV, the total energy output of the cluster will be

$$\int_1^\infty E\, q(E)\, dE = 7 \times 10^{46} \text{ ergs } s^{-1}$$

Osborne et al., (1977) give the total for our Galaxy as about 6×10^{40} ergs s^{-1} so Virgo would need to be about 10^6 times as active. Considering that Virgo is some 10^4 times as massive this is not an inhibiting requirement.

The cluster output near 10^{19}eV can also be compared with the equivalent Galactic output that would be required to maintain the experimental intensity, provided a suitable propagation model is adopted. If we assume the disc residence time for 10^{19}eV particles to be of the order of 5×10^2 - 5×10^3 yrs then for a disc thickness of $\sim$ 200 pc

(corresponding to a disc volume of $\sim 4 \times 10^{60} m^3$) the required Galactic output is some $3 \times (10^{18} - 10^{19})$ $GeV^{-1}s^{-1}$. This is again a factor of some $10^5 - 10^6$ down on the Virgo requirement.

We may further compare the Galaxy and Virgo in terms of the diffuse X-ray emission. Wdowczyk (1979) has estimated the diffuse luminosity of the Galaxy in X-rays as about 10^{38} ergs s^{-1}. At the Galactic center this will presumably be at least an order of magnitude greater. Forman et al., (1978) give the Virgo luminosity as $\simeq 3.1 \times 10^{43}$ ergs s^{-1} of which they estimate half should be the diffuse component. This gives a factor of 10^5 for the Virgo/Galaxy ratio. It should be noted that this, and the above, calculations are sensitive to the precise production spectrum of Virgo adopted. If a slightly flatter form for q(E) is chosen, the energy requirement for Virgo is eased considerably.

8.4.4 The Predicted High Energy Spectrum The predicted high energy spectrum is obtained by the product of equations 8.4.5 and 8.4.7. The fit with $D(E) = 5 \times 10^{33} \sqrt{E_{19}}$ cm^2/s is shown in figure 8.12 against the volcano ranch/Haverah Park data, though other values of D can be made to fit almost as well. The dashed line in the figure represents the situation if diffusion is assumed negligible at 10^{21}eV, with a transition between 10^{20} and 10^{21}eV. Below 3×10^{17}eV the fit is not good, but in this region Galactic particles are assumed to give the required shape.

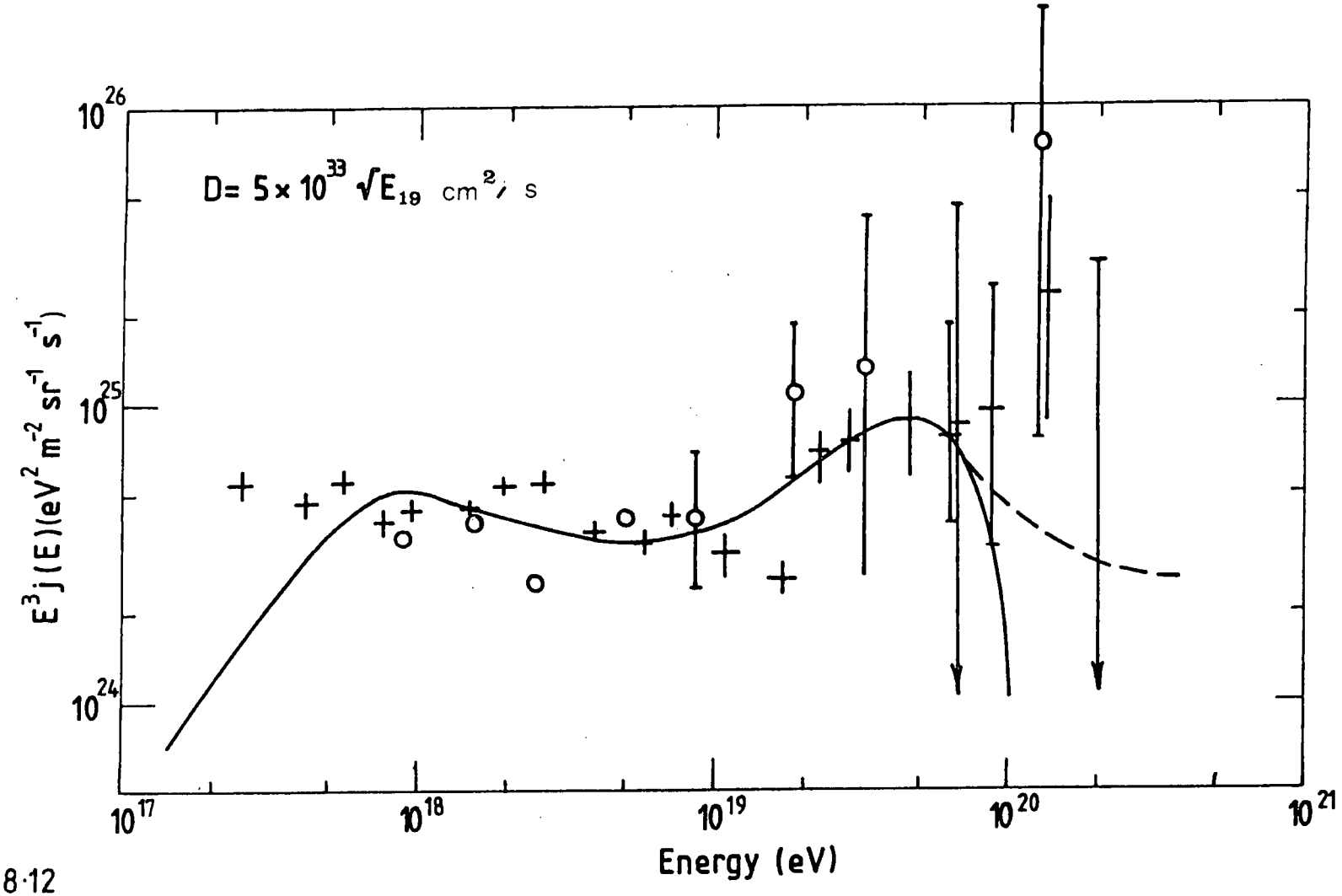

Fig 8·12

The diffusion model prediction compared against the Haverah Park and Volcano Ranch data, with $D = 5 \times 10^{33} \sqrt{E_{19}}\ cm^2/s$. The dashed line assumes a transition to rectilinear propagation. E_{19} is in units of 10^{19} eV.

8.4.5 The predicted anisotropy Figure 8.13 shows the predicted values for anisotropy calculated from equation 8.4.6 with the preferred value of D(E). As with the intensity measurements the anisotropy fit is not particularly sensitive to choice of diffusion coefficient. The critical parameters are the distance to Virgo and (indirectly) the black body attenuation. For comparison figures 8.14 and 8.15 show the spectral shape and anisotropy curve for $D(E)=5\times10^{33}E^{0.75}\ cm^2/s$ and $D(E) = 2 \times 10^{34}E^{1.0}\ cm^2/s$.

As noted previously the anisotropy phases at the high energy end ($E > 10^{18}$eV) are not in good agreement with the Virgo direction. However, the Galactic magnetic field and irregularities in the extragalactic field make it unlikely that the phases should correspond to the Virgo direction until at least 3×10^{19}eV and indeed it is above this energy that the Haverah Park group claim an excess of particles from high Galactic latitudes. The data available are, of course, limited, and further information must be awaited before the hypothesis is confirmed.

8.5 Radio Galaxy Spectral Model

8.5.1 Philosophy of the Model A third alternative for the high energy cosmic ray spectrum arises from consideration of the distribution of spectral indices of radio galaxies. From the radio frequency spectrum of a typical galaxy, the source electron spectrum may be easily obtained, making the usual assumption that synchrotron losses are responsible for the observed emission. If the cosmic ray spectrum can be obtained from the electron spectrum by assuming that the

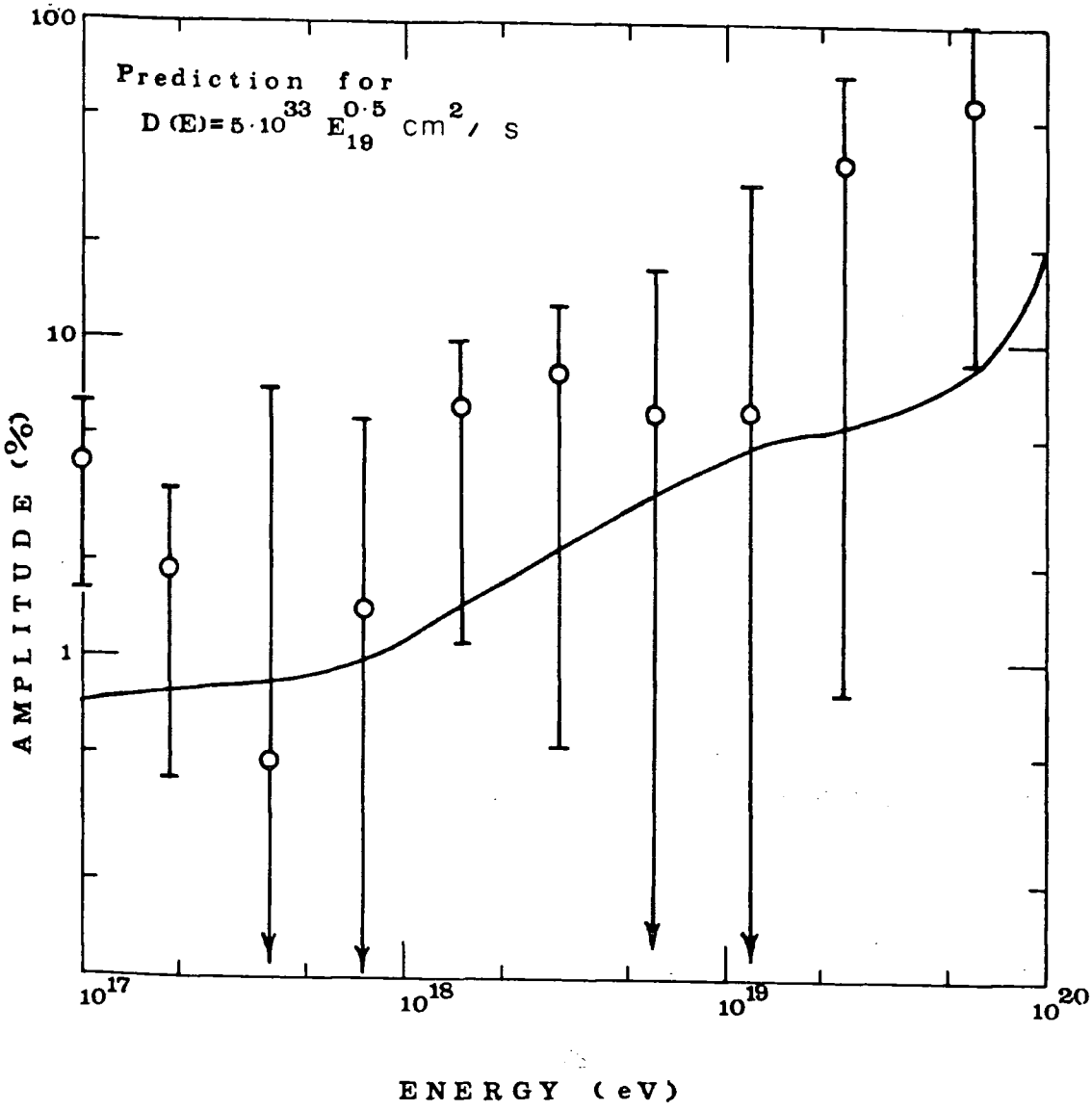

The diffusion model anisotropy prediction for a diffusion coefficient $D(E) = 5\times10^{33}\sqrt{E_{19}}\ cm^2/s$. The measurements are those of Haverah Park. E_{19} is in units of 10^{19} eV.

Fig 8·13

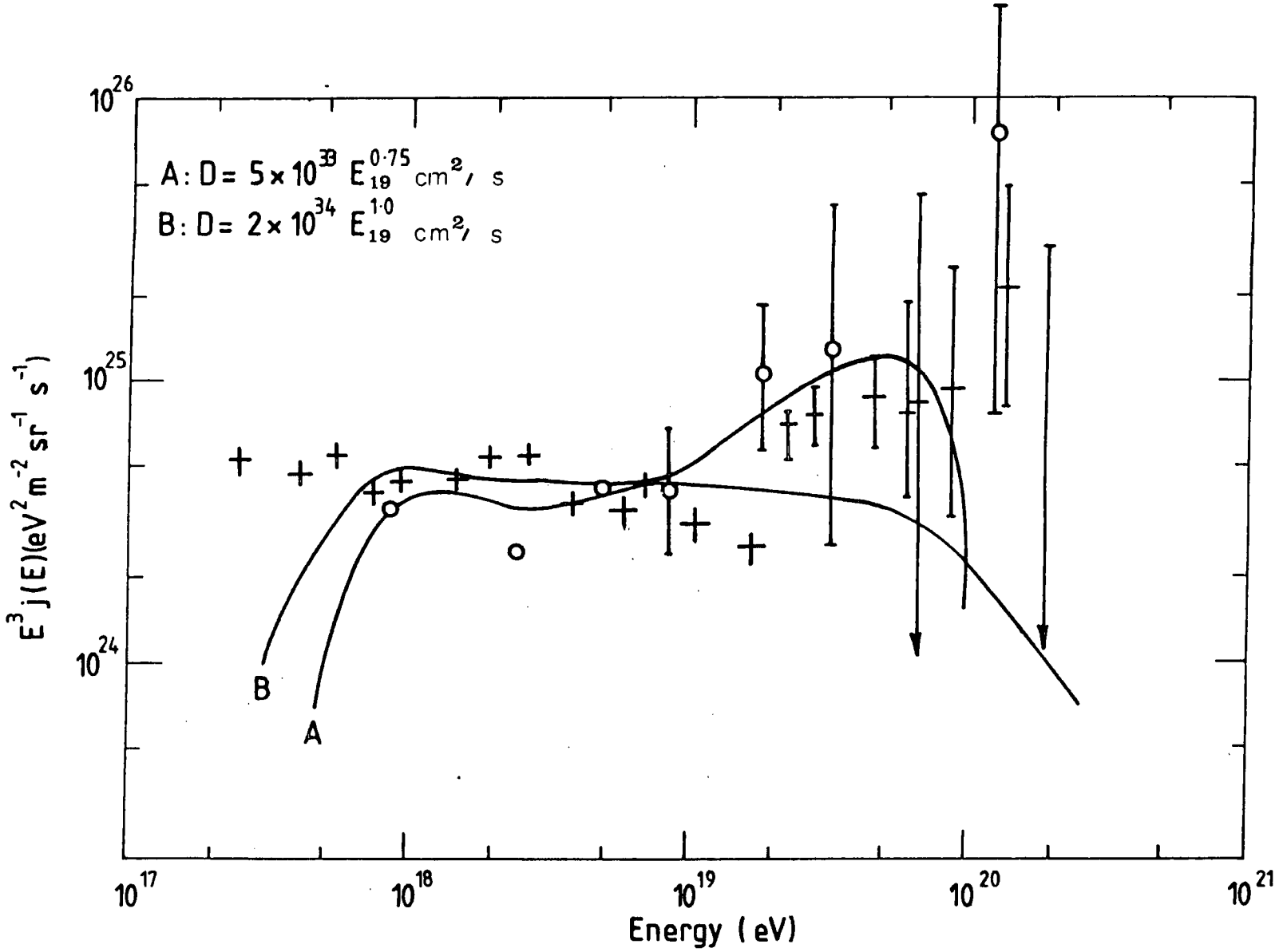

Fig 8·14

The diffusion model prediction for the high energy spectrum with diffusion coefficients as shown. The measurements are from Haverah Park and Volcano Ranch. E_{19} is in units of 10^{19} eV.

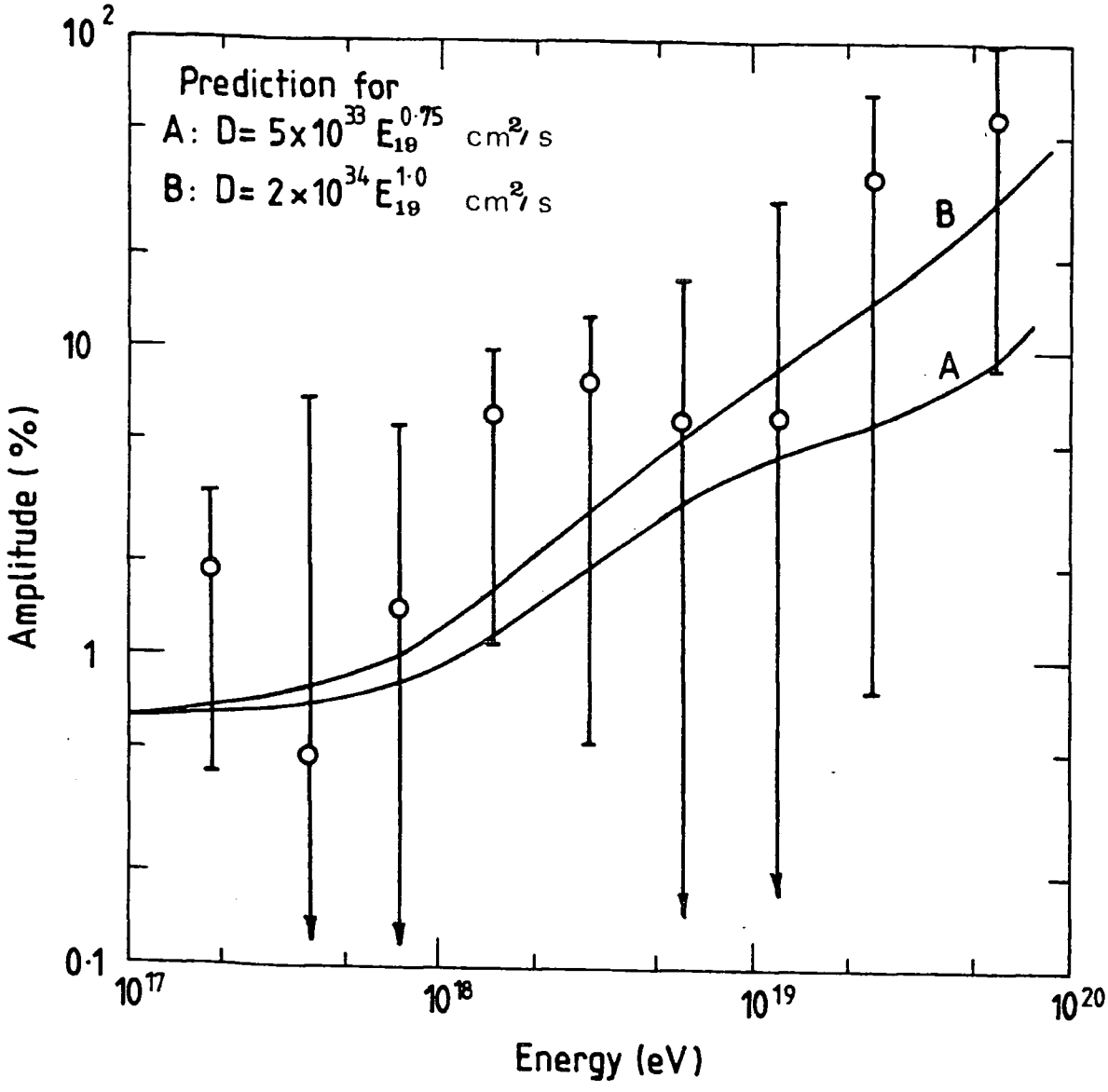

The diffusion model anisotropy prediction with diffusion coefficients as shown. The measurements are from Haverah Park. E_{19} is in units of 10^{19} eV.

Fig 8·15

spectral index is the same for both, then knowledge of the distribution of radio indices enables the high energy spectrum to be calculated assuming that the spectral indices apply at very high energies also. A similar model has been proposed by Berezinsky et al. (1973).

8.5.2 Radio Galaxy Spectra A number of problems arise with this model of which the first is the need to obtain complete samples of sources to a given flux limit, as noted by Williams and Bridle (1967) and others. The problem arises since observations at a given frequency bias the composition of samples complete to a particular flux density : observation at a different frequency to a certain flux limit would give a different sample of objects.

The most appropriate for the present analysis appears to be the catalogue of sources at 1400 MHz of Bridle, Davis, Fomalont and Lequeux (1972). The Catalogue is estimated by the authors to be 98 ± 2% complete for objects with flux densities greater than 4.0 flux units (1 f.u. = 10^{-26} W $M^{-2}Mz^{-1}$) in the region $|b| > 15^{o}$, $-5^{o} < \delta < 70^{o}$. According to the revised flux density scale of Roger, Bridle and Costain (1973), sixty-seven sources constitute a complete sample in the specified region to the given limits. Of these, 52 have been observed at five or six frequencies from 10 - 1400 MHz, while the remaining 15 have been observed at four higher frequencies (70 - 1800 MHz) only. The spectra of each of the 67 objects, and the spectral index of each source at preselected frequencies, has been given by Roger et al. and in addition, wherever possible, an optical identification

of each source has been made. For the sample in question, 10 sources have been identified as Quasars while 2 sources do not correspond to any identifiable source. These are rejected, noting that the Quasars have significantly flatter spectra than other groups of sources.

The 52 remaining galaxies are identifiable as Normal, Double, or Seyfert galaxies. Only 24 of these, however, have spectra which are well represented by power laws, at least from 600 - 1800 MHz. The rest have more complex spectra which give little indication of the high frequency end of the spectra apart from general trends.

8.5.3. The ensuing Cosmic Ray Spectrum The 24 'regular' galaxies may roughly be represented by a Gaussian distribution with mean spectral index $\alpha = .775$ and $\sigma_\alpha = .12$. This agrees well with the results of Kellerman et al. (1969) who find, for an incomplete sample of galaxies at (40 - 750) MHz, a distribution with $\alpha = .753$ and $\sigma_\alpha = .15$, and with the conclusions of Berezinsky et al. who give $\alpha = 0.8$, $\sigma_\alpha = 0.2$. The assumption of a Gaussian distribution is, however, only approximate, since it is known that the distribution of spectral indices exhibits some skewness to higher (more negative) values of α at lower frequencies < 100 MHz, while at higher frequencies the distribution appears skewed with a low index tail.

Adopting the usual relationship between the electron spectrum and radio frequency spectrum, $\gamma = 2\ \alpha + 1$, the distribution of γ may consequently be represented by a Gaussian with $\bar{\gamma} = 2.55$, $\sigma_\alpha = .24$. Note that at 1400 MHz there should

be little interference in the measurements from black body effects, while the frequency is not so low that the observations may be at a region of turn-over in the electron spectrum (the energy of an electron emitting at 1400 MHz is $\sim$ 10 GeV).

Two assumptions are now made. Firstly, it is assumed for simplicity that each source has about the same cosmic ray strength and secondly that the cosmic ray spectrum follows the electron spectrum. For our own Galaxy this second assumption is not quite valid, since the electron spectrum has $\alpha \simeq 2.8$ while the cosmic ray spectrum has $\alpha \simeq 2.6$ above 10^{15}eV (although there may be good reasons for the difference in terms of energy-dependent lifetime effects and energy losses for electrons). The expected cosmic ray spectrum (assuming a uniform distribution of radio galaxies and no diffusion) is then found by extrapolating the electron spectra to the highest energies and weighting according to the Gaussian distribution. The resultant spectrum is shown in figure 8.16, with due allowance for black body cut-off.

As expected, the shallower spectra contribute more at the high energy end, but the greater number of sources with spectral index near the mean value offsets this to some extent. Although from the Gaussian distribution a proportion of sources have positive slope spectra (i.e. the cosmic ray intensity increases with energy) these make less than a 0.1% contribution to the cosmic ray intensity at 10^{21}eV since the

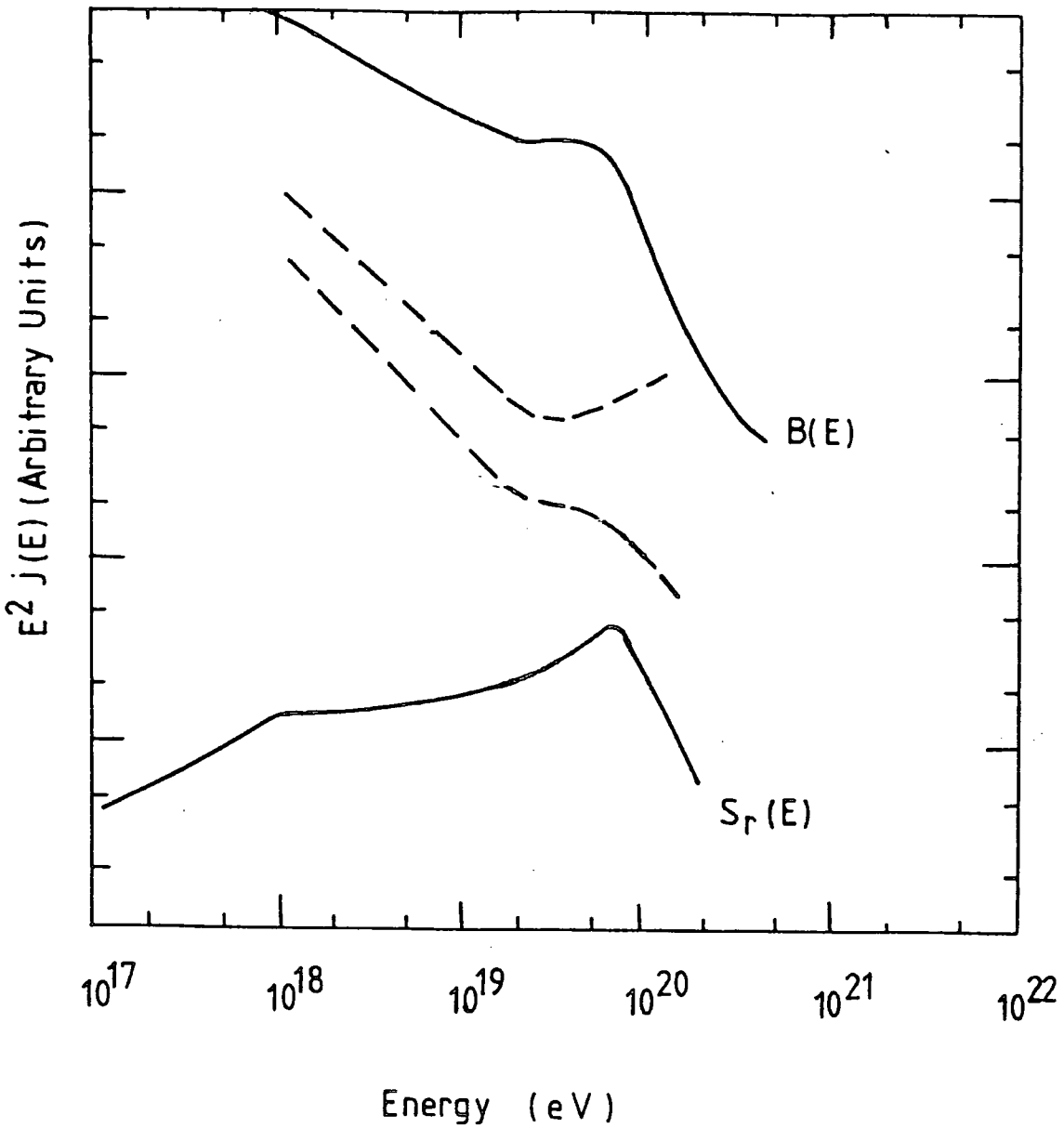

Radio galaxy model high energy spectrum prediction, denoted S_r (E). The dashed lines are the limits of the observed spectrum while B (E) is the black body attenuation curve.

Fig 8·16

proportion of such sources is so small. Some 50% of the cosmic ray intensity at 10^{21}eV is contributed by sources with $\gamma < 1.0$; less than 1% is contributed by sources with $\gamma > \bar{\gamma}$.

8.5.4 Discussion of the model The model has obvious inherent disadvantages, not least of which is the overriding contribution made by sources with small γ. Nor is the predicted spectrum as satisfactory as with the other models considered earlier - galactic sources would need to provide particles up to 10^{19}eV for the model to work properly. In addition, the lack of data on complete samples of galaxies and the difficulties in assigning and evaluating the measured spectra do not give great confidence; furthermore, the need to extrapolate the spectra over many orders of magnitude causes worry. Nevertheless it remains a possibility for explaining the high energy end of the cosmic ray spectrum.

CHAPTER 9

CONCLUSIONS

Despite the many difficulties of obtaining precise measurements of anisotropies which have been mentioned, the concensus of experimental results in recent years does indicate that genuine anisotropies are present in some, if not all, decades of energy. Below 10^{12}eV results must be treated with care, and allowance made for the interplanetary field. However, experiments are worthwhile at these energies since they can allow measurement of the polar component of the anisotropy, although if the latest Holborn result is correct this is not excessive. In this light, the agreement in phase of the Holborn experiment with those of Norikura, Poatina and Pk. Musala, and the conclusions of Nagashima and Mori (1976) is seen as firm evidence for anisotropy.

At the energies of these latter three experiments, interplanetary field effects are negligible and it is here that the reliability of the detectors and the high count rates involved combine to give the most reliable measurements. The agreement in amplitude and phase of about 0.05% at (1 - 2) hrs R.A. must be regarded as a genuine anisotropy effect, and evidence that in the range 10^{12} - 10^{14}eV there is only a slow change of anisotropy with energy. There is also firm evidence of a second harmonic with phase near 5.5 hrs R.A. Hopefully, these and future measurements can produce some much needed conclusion on the three dimensional aspect of anisotropy, particularly since at present there does not appear to be a well defined axis of symmetry even when allowance has been made for, and results transformed to,

the frame of the local interstellar medium and hence the frame of the local magnetic field. The consistency of the measurements of the parameters of the interstellar wind is of obvious importance to the propagation and anisotropy of cosmic rays.

While the constancy of phase below 10^{14}eV becomes harder to explain in the absence of axial symmetry, the constancy of amplitude points to a constant lifetime of cosmic rays and hence against an extragalactic origin. In addition, the anisotropy measurements together with the measurements of the interstellar medium point to smooth propagation independent of local sources. The particles can hence be considered as somewhat "old", with propagation and sources of the particles nearly identical over the energy band.

The region 10^{14}eV - 10^{17}eV is more confused. The break in the cosmic ray spectrum near 10^{15}eV is indicative of a region of transition which should be apparent in the anisotropy measurements. In the regrettable absence of reliable recent measurements, the analysis of computations of data, as performed here, offers the best prospects at present. When treated as truly independent data, the analysis of the Linsley-Watson data does not lead to particularly promising results, and the sceptic would be justified in disinclining to believe the evidence. While supporting a change in phase of the form $\alpha = (15.3 - 3.8 \log E_{16})$hrs, the data also shows signs of fluctuations additional to the Rayleigh-Poisson. Indeed, the independent amplitude data can be well fitted by assuming 30% additional fluctuations. Overall the evidence in this energy regime is not conclusive though a reasonable

case for steadily increasing amplitudes and steadily altering phase can be made. It would be surprising if cosmic rays were truly isotropic in this range.

At and above 10^{17}eV the evidence is more convincing. The existence of a maximum anisotropy amplitude at 10^{17}eV (of some 4%) must be considered established in view of the Haverah Park results. However, this measurement brings problems in that the reason for so large an amplitude is difficult to explain, particularly when the amplitudes near 10^{18}eV are considered. Further measurements in this regime and particularly for 10^{16} - 10^{17}eV would be of great value.

Near 5 x 10^{19}eV there is again good evidence for a significant anisotropy, but the apparent rapidly varying phase angle with energy would lead one to suspect low amplitudes over a wide energy range.

Consequently, the results from 10^{17} - 10^{20}eV favour a mixed origin model in which the peak in amplitude at 10^{17}eV is seen as the tail of the predominance of Galactic particles. Above 10^{18}eV, extragalactic effects are observed with anisotropies above 10^{19}eV the result of particles arriving from particular extragalactic sources, which would explain the rapidly changing phase and the predominance of high energy particles from high Galactic latitudes in the direction of Virgo observed by the Haverah Park experiment.

The 'ankle' in the cosmic ray spectrum above 10^{19}eV is also then more readily interpreted as an effect of extra-galactic origin with several possible explanations.

The first of those considered here - the neutron model - allows a simple explanation in terms of neutrons escaping from clusters of galaxies before decaying into protons.

The need for high trapping fields within the cluster is the most serious drawback with this model, as has been noted. To be effective, the model requires that individual cluster members are capable of a much higher degree of trapping than our own Galaxy or alternatively that there is sufficient intracluster material to maintain the high magnetic field necessary.

The spectral shape derived with the neutron model does, however, provide a good fit to the experimental observations of the Yakutsk and Haverah Park arrays, provided a small percentage of cluster leakage protons are acceptable. On balance the best fit is provided assuming a spectral shape of $j(E) \propto E^{-2.25}$ for the source particles.

The second model adopted assumes diffusion rather than rectilinear motion as a means of propagation. Allowing for black body attenuation, diffusion limits the source of high energy particles to within some 200 Mpc. Only the Virgo supercluster is seen as effectively providing particles of $\sim 10^{20}$eV. A variety of diffusion coefficients based on a mean free path of 10^2 - 10^3Kpc at 10^{19}eV are able to give a satisfactory high energy spectrum. A choice of $D(E) = 5 \times 10^{33} \sqrt{E_{19}}$ $cm^2 s^{-1}$ gives a reasonable spectral shape as well as satisfactorily predicting the anisotropy amplitudes.

Undoubtedly the diffusion model offers both a more realistic model and a better overall fit to the experimental data than the Neutron model. In addition the model has some support in the claim by Haverah Park that high energy particles tend to arrive from high Galactic latitudes, and approximately from the direction of Virgo.

In contrast to the diffusion model, the radio galaxy model must be considered as the weakest of the models considered. Its weakness lies in the lack of data, the need to extrapolate the measured spectra, and above all the critical effect of sources with shallow spectra. The predicted cosmic ray spectrum is also not as satisfactory as the predictions of the neutron and diffusion models. On balance, the radio galaxy model should be discounted as a serious contender to explain the high energy end of the cosmic ray spectrum.

In conclusion, however, if one accepts that the highest energy cosmic rays are indeed extragalactic (for which the evidence is considerable) then models of the type considered above must contain at least part of the answer to the question of the origin of cosmic rays.

APPENDIX 1

From equation 5.3.14 we have

$$P_{ko}\, dk_o = e^{-(k + k_o)} I_o(2\sqrt{kk_o})\, dk_o$$

The expectation value of k_o is thus:

$$\langle k_o \rangle = \int_o^\infty e^{-(k + k_o)} k_o I_o(2\sqrt{kk_o})\, dk_o$$

Now

$$I_o(z) = \sum_{n=o}^{\infty} \frac{(z/2)^{2n}}{(n!)^2}$$

So we have

$$\langle k_o \rangle = e^{-k} \int_o^\infty e^{-k_o} k_o \left[1 + kk_o + \left(\frac{k\,k_o}{2!}\right)^2 + \ldots + \left(\frac{k\,k_o}{n!}\right)^n\right] dk_o$$

$$= e^{-k}\left\{\int_o^\infty e^{-k_o} k_o\, dk_o + \int_o^\infty k_o^2\, ke^{-k_o} dk_o + \ldots + \int_o^\infty \left(\frac{k}{n!}\right)^n k_o^{n+1} e^{-k_o} dk_o\right\}$$

Now $\int_o^\infty k_o^n\, e^{-k_o} dk_o = \left[-e^{-k_o}(k_o^n + nk_o^{n-1} + (n-1)nk_o^{n-2} + \ldots + n!k_o + n!\right]_o^\infty = n!$

Hence

$$\langle k_o \rangle = e^{-k}\left\{1 + k2! + \frac{k^2 3!}{(2!)^2} + \ldots + \frac{n!k^{n-1}}{[(n-1)!]^2}\right\}$$

$$= e^{-k}\left\{1 + 2k + \frac{3k^2}{2!} + \ldots + \frac{(n+1)k^n}{n!}\right\}$$

$$= e^{-k} \sum_{n=o}^{\infty} \frac{(n+1)k^n}{n!}$$

$$= e^{-k} \sum_{n=o}^{\infty} \frac{nk^n}{n!} + e^{-k} \sum_{n=o}^{\infty} \frac{k^n}{n!}$$

$$= e^{-k}\{ke^k + e^k\} \text{ since } e^x = \sum_{m=o}^{\infty} \frac{x^m}{m!}$$

So that

$$\langle k \rangle = k + 1 \text{ as required.}$$

ACKNOWLEDGEMENTS

The Science Research Council is thanked for the provision of a Research Studentship during the period of the work.

I wish to thank Professor Wolfendale F.R.S. for making available the facilities of the Department of Physics at the University of Durham and for his supervision and encouragement during and after the period of research.

I would like to thank Dr. J.L. Osborne for much help and guidance and Mr. P. Kiraly of the Hungarian Academy of Science for many hours of discussion and encouragement.

I would also like to thank Professor Wdowczyk, Dr. J. Kota, Dr. A.W. Strong and Dr. D. Worrall for many useful discussions on various aspects of the work.

Finally, the facilities provided by the Durham University computer unit are gratefully acknowledged.

REFERENCES AND BIBLIOGRAPHY

Abell, G,O., 1964, IAU Symp. 63, P79.

Abell, G.O., 1958, Ap.J.Suppl. 3, 211 (No. 31)

Adams, T.F., and Frisch, P.C., 1977, Astrophys. J., 121, 300.

Allen, C.W., 1973, Astrophysical Quantities, The Athlone Press, 292.

Anderson, R.C., and Weiler, R.J., 1978, Astrophys. J., 224, 143.

Arjello, J.M., 1978, Astrophys. J., 222, 1068.

Axon, D.J., and Ellis, R.S., 1976, M.N.R.A.S., 177, 499.

Barrett, M.L., Walker, R., Watson, A.A., and Wild, P., 1977, Proc. 15th Int. Cos. Ray Conf., 8, 172.

Bell, C.J., et al., 1973, Proc. 13th Int. Cos. Ray. Conf., 4, 2525, Denver.

Bell, M.C., Kota, J., Wolfendale, A.W., 1974, J. Phys. A, 7, 420.

Berezinsky, V.S., Grigoreva, S.I., and Zatsepin, G.T., Proc. 13th Cos. Ray. Conf., 1, 603, Denver, 1973.

Berezinsky, V.S., 1977, Proc. 15th Int. Cos. Ray. Conf., 10, 84.

Berkhuijson, E.M., 1971, Astron. and Astrophys., 14, 359.

Biermann, L., and Davies, L., 1960, z.s.f. Ap., 51, 19.

Bertaux, J.L., Blamont, J.E., Taberie, N., Kurt, W.G., Bourgin, M.C., Sminov, A.S., and Dermenteva, N.N., 1976, Astron. Astrophys., 46, 19.

Birkenshaw, M., Gull, S.F., and Northover, K.J.E., Nature, 275, 40, 1978.

Brecher, K., and Blumenthal, G.R., 1970, Astrophys. J. Letts., 6, 169.

Brecher, K., and Burbidge, G.R., 1972, Ap. J, 174, 253.

Bridle, A.H., Davis, M.M., Fomalont, E.B., and Lequeux, J., 1972, Ap. J., 77, 405.

Brindle, C., French, D.K., and Osborne, J.L., Proc, 15th Int. Cos. Ray Conf., 1, 386, 1977.

Cachon, A., 1962, Proc. 5th Interamerican Seminar on Cosmic Rays, 2, XXXIX.

Caldwell, J.H., and Meyer, P., 1977, Proc. 15th Int. Cos. Ray Conf., 1, 243.

Carter, D., 1977, M.N.R.A.S., 178, No. 1.

Chevalier, R.A., 1977, Astrophys. J., 213, 52-57.

Cini-Castagnoli, G., Marocchi, D., Elliot, H., Marsden, R.G., and Thambyapillai, T., Proc. 14th Int. Cos. Ray Conf., 4, 1453, 1975.

Clark, D.H., and Caswell, J.L., 1976, M.N.R.A.S., 174, 267.

Cunningham, G., Pollock, A.M.T., Reid, R.J.O., and Watson, A.A., Proc. 15th Int. Cos. Ray Conf., 1977, 2, 303.

Daniel, R.R., 1977, Proc. 15th Int. Cos. Ray Conf., 10, 217.

Daudin, A., and Daudin, J., 1952, C.R. Acad. Sci., 234, 1551.

Davis, L., and Greenstein, J.L., 1951, Astrophys. J., 114, 206.

Davies, S.T., Elliot, H., Marsden, R.G., Thambyahpillai, T., and Dutt, J.C., 1978, Preprint, Imperial College, London.

Davies, S.T., Elliot, H., and Thambyahpillai, T., 1977, Proc. 15th Int. Cos. Ray Conf., 4, 105.

Delvaille, J., Greisen, K., Kendziorski, F., and Simoppoulos, E., 1962, Proc. 5th Interamerican Seminar on Cosmic Rays, 2, No. 40.

Dodds, D., Strong, A.W., and Wolfendale, A.W., M.N.R.A.S. 171, 569, 1975.

Dupree, A.K., Baliunas, S.L., and Shipman, H.L., 1977, Astrophys. J., 218, 261-369.

Duperier, A., 1946, Nature, 158, 196 (London).

Earl, J.A., 1975, Proc. 14th Int. Cos. Ray Conf., 5, 1733.

Edge, D.M., Pollock, A.T.M., Reid, R.J.O., Watson, A.A., Wilson, J.G., J. Phys. G., 4, 113, 1978.

Ellis, R.S., and Axon, D.J., 1978, Astrophys. and Space Sci., 54, 425.

Fahr, H.J., 1974, Space Sci. Rev., 15, 683.

Farley, F.J.M., and Storey, J.R., 1954, Proc. Phys. Soc. A., 67, 976.

Fenton, A.G., Fenton, K.B., and Humble, J.E., Proc. 15th Int. Cos. Ray Conf., 11, Late Papers, 1977.

Fenton, A,G., and Fenton, K.B., 1976, Proc. Int. Cos. Ray Symp., Tokyo, 313.

Fenton, A.G., 1976, Proc. Int. Cos. Ray Symp., Tokyo, 308.

Fenton, K.B., 1975, Proc. 14th Cos. Ray Conf., 11, 3907.

Field, G.B., 1974, IAU Symp., 63, 13.

Fichtel, C.E., Simpson, G.A., and Thompson, D.J., 1978, Goddard Space Flight Center X-662-77-271.

Fontes, P., Meyer, J.P., and Perron, C., 1977, Proc. 15th Int. Cos. Ray Conf., 2, 234.

Forman, W., Jones, C., Murray, S., and Giacconi, R., 1978, Ap.J., 225, L1-4.

Freeman, J., Paresce, F., Bowyer, S., and Lampton, M., 1976, Astrophys. J., 208, 747.

Garcia -Munoz, M., Mason, G.M., and Simpson, J.A., Proc. 15th Int. Cos. Ray Conf., 1977, 1, 307.

Garcia-Munoz, M., Mason, G.M., and Simpson, J.A., Proc. 15th Int. Cos. Ray Conf., 1977, 1, 224.

Gardner, F.F., and Whiteoak, J.B., 1963, Nature, 197, 1162.

Gardner, F.F., Morris, D., and Whiteoak, J.B., 1969, Aust. J. Phys., 22, 813.

Ginzburg, V.L., and Syrovatskii , S.I., 1964, The Origin of Cosmic Rays, Pergamon Press, P272.

Ginzberg, V.L., and Ptushin, V.S., 1976, Rev. Mod. Phys., 48, 161.

Gombosi, T., Kota, J., Somogyi, A.J., Varga, A., Betev, B., Katsarsky, L., Kavlakov, S., Khirov, I., 1975, Nature, 225, 687.

Gombosi, T., Kota, J., Somogyi, A.J., Varga, A., Betev, B., Katsarsky, L., Kavlakov, S., Khirov, I., 1977, Proc. 15th Int. Cos. Ray Conf., 11, 109 (Late Papers) (also KFKI preprint ISBN 963 371 327-7).

Hall, J.S., 1949, Science, 109, 166.

Heiles, C., 1976, Ann. Rev. Astron. Astrophys., 14, 1.

Hiltner, W.A., 1949, Astrophys. J., 109, 471.

Hodson, A.L., 1951, Proc. Phys. Soc. A., 64, 1061.

Hogg, A.R., 1950, J. Astrovs. Terr. Phys., 1, 56.

Howard, T., 1974, Sol. Phys., 38, 283.

Humble, J.E., and Fenton, A.G., 1977, Proc. 15th Int. Cos. Ray Conf., 2, 245.

Ichinose, M., and Murakanii, K., Proc. Int. Cos. Ray Symp., Tokyo, 1976, 291.

Juliusson, E., Astrophys. J., 1974, 191, 331.

Juliusson, E., 1975, Proc. 14th Int. Cos. Ray Conf., 8, 2689.

Kecskemeti, K., 1978, Private Communication.

Kellerman, K.I., Pauliny-Toth, I.I.K., and Williams, P.J.S., 1969, Ap. J., 157, 1.

Kempa, J., Wdowczyk, J., and Wolfendale, A.W., J. Phys. A., 7, 1213, 1974.

Kiraly, P., Kota, J., Osborne, J.L., White, M., and Wolfendale, A.W., 1975, J. Phys. A., 8, 2018.

Kiraly, P., and White, M., 1975, J. Phys. A., 8, 1336.

Kiraly, P., Kota, J., Osborne, J.L., Stapley, N.R., and Wolfendale, A.W., Riv. del Nuovo Cim., 2, No. 7, 1979.

Kiraly, P., Kota, J., Osborne, J.L., Stapley, N.R., and Wolfendale, A.W., 1979, Proc. 16th Int. Cosmic Ray Conf., MG7, 221.

Kluyver, J.C., 1906, Nederlanda Akademi Wetenskk, Proc., A8, 341.

Kota, J., and Somogyi, A.J., 1977, Proc. 15th Int. Cosmic Ray Conf., 11, 102.

Krasilnikov, D.D., 1978, VI European C.R. Symp., Kiel, Preprint.

Krasilnikov, D.D., Dyakonov, M.N., Egorov, T.A., Kerschenholz, I.M., Kolosov, V.A., Kuznin, A.I., Orlov, V.A., Steptsov, I.Ye., 1977, Proc. 15th Int. Cos. Ray Conf., 8, 159.

Kronburg, P.P., 1977, Astron. Astrophys., 61, 771.

Lake, G., and Partridge, 1977, Nature, 270, 502.

Lapikens, J., Norwood, H.M., Reid, R.J.O., Ridgway, S., and Watson, A.A., 1977, Proc. 15th Int. Cos. Ray Conf., 8, 166.

Lezniak, J.A., Webber, W.R., Kish, J.C., and Simpson, G.A., 1977, Proc. 15th Int. Cos. Ray Conf., 1, 237.

Linsley, J., 1975(a), Phy. Rev. Letts., 34, 1530.

Linsley, J., 1975(b), Proc. 14th Int. Cos. Ray Conf., 2, 592.

Linsley, J., and Watson, A.A., 1977, Proc. 15th Int. Cos. Ray Conf., 12, 203.

Manchester, R.N., 1972, Astrophys. J., 172, 43.

Manchester, R.N., and Taylor, T.H., 1977, Pulsars, W.H. Freeman.

Matthews, T.A., Morgan, W.W., and Schmitt, M., 1964, Ap. J., 140, 35.

Mathewson, D.S., 1968, Astrophys. J. Letts., 153, L47.

Mathewson, D.S., Broten, N.W., and Cole, D.J., 1966, Aust. J. Phys., 19, 93.

Marsden, R.G., Elliot, H., Hynds, R.J., and Thambyallai, T., 1976, Nature, 260, 491.

McClintock, W., Henry, R.C., Linsley, J.L., Moos, H.W., 1978, Astrophys. J., 225, 465.

McIvor, I., Proc. 14th Int. Cos. Ray Conf., 2, 627, (Plovdiv), 1975.

Mitton, S., 1972, M.N.R.A.S., 155, 373.

Moos, H.W., Linsky , J.L., Henry, R.C., and McClintock, W., 1974, Astrophys. J., 183, L93.

Morgan, W.W., and Lesh , J.T., 1965, Ap. J., 142, 1364.

Nagashima, K., and Mori, S., 1976, Proc. Int. Cos. Ray Symp., Tokyo, P326.

Nagashima, K., Sakakibara, S., Fujimoto, K., Fujii, Z., Ueno, H., and Kondo, I., Proc. 15th Int. Cos. Ray Conf., 2, 1977, 154.

Nagashima, K., Fujimoto, K., Fujii, Z., Ueno, H., and Kondo, I., 1972, Rep. Ion. Space Res. Japan., 26, 31.

Obayashi, The Physics of Solar Cosmic Rays, 1970.

Oemler, A., 1973, Ap.J., 180, 11.

Oemler, A., 1974, Astrophys. J., 194, 1-19.

Osborne, J.L., French, D.K., 1977, Proc. 15th Int. Cos. Ray Conf., 1, 386.

Pacholczyk, A.G., 1970, Radio Astrophysics, P63 f.f.

Parker, E.N., 1976, Proc. Int. Symp. NASA Goddard Space Flight Center.

Parker, E.N., 1955, Astrophysics J., 122, 293.

Piddington, J.H., 1969, Cosmic Electrodynamics, 23.

Pollock, A.M.T., Reid, R.3O, and Watson, A.A., Proc. 15th Int. Cos. Ray Conf., 1977, 2, 292.

Rassmussen, I.L., 1975, Origin of Cosmic Rays, 97-133 (D. Reidel).

Rassmussen, I.L., and Peters, B., 1975, Nature, 258, 412.

Rayleigh, 1880, Phil. Mag., 10, 73.

Roger, R.S., Bridle, A.H., and Costain, C.H., Astron J., 1973, 78, 1030.

Rood, H.J., and Sastry, G.N., P.A.S.P., 83, 313, 1971.

Rubin, V.G., Ford, W.K., Thonnard, N., Roberts, M.S., and Gordon, J.A., 1976, Astron. J., 81, 687.

Sakakibara, S., 1965, J. Geomag. Geoelectr., (Japan), 17, 99-112.

Sakakibara, S., Fujimoto, K., Fujii, Z., Ueno, H., Kondo, I., and Nagashima, K., 1976, Proc. Int. Cos. Ray Symp., Tokyo, 316.

Sakurai, S., 1974, The Physics of Solar Cosmic Rays, Tokyo Press.

Sekido, Y., 1971, Proc. 12th Int. Cos. Ray Conf., 1 302.

Shapiro, M.M., and Silverberg, R., Proc. 12th Int. Cos. Ray Conf., 1, 64, 1971.

Simard-Normandin, M., and Kronberg, P.P., 1979, Nature 279, 155.

Skilling, J., Proc. 14th Int. Cos. Ray Conf., 2, 624, 1975.

Smoot, G.F., Gorenstein, M.V., and Muller, R.A., 1977, Phys. Rev. Letts., 39, 898.

Somogyi, A.J., 1976, Proc. Int. Cos. Ray Symp., Tokyo, 142.

Stecker, F.W., 1978, Ap. J., 223, 1032.

Stecker, F.W., 1975, The Origin of Cosmic Rays, D. Reidel, Ed. A.W. Wolfendale.

Stapley, N.R., Wdowczyk, J., and Wolfendale, A.W., 1977, Proc. 15th Int. Cos. Ray Conf., 2, 316.

Strong, A.W., Wolfendale, A.W., Bennet, K., and Wills, R.D., 1978, M.N.R.A.S., 181, 751.

Strong, A.W., Wdowczyk, J., and Wolfendale, A.W., 1974, J. Phys. A., 7, 1767.

Strong, A.W., Wolfendale, A.W., Bennet, K., Wills, R.D., Proc. XII ESLAB Symp., Frascati, 1977, 167.

Spoelstra, T.A.T., 1972, Astron. and Astrophys., 21, 61.

Swinson, D.B., 1976, J. Geophys. Res., 81, 2075.

Tamman, G.A., 1977, Eigth Texas Symp. on Rel. Astroph., Ann., N.Y., Acad. Sci., 302, 61.

Vallee, J.P., and Kronburg, P.P., 1975, Astron. and Astrophys., 43, 233.

Vershuur, G.L., 1972, IAU Colloquim 23, Review Paper.

Watson, A.A., 1979, Private Communication.

Watson, A.A., and Wilson, J.G., 1974, J. Phys. A., 7, 1199.

Wdowczyk, J., 1979, Private Communication.

Wdowczyk, J., and Wolfendale, A.W., 1976, J. Phys. A., 9, L197.

Wdowczyk, J., and Wolfendale, A.W., 1979, Nature 281, 356.

Webber, W.R., and Kish, J.C., 1979, Proc. 16th Int. Cos. Ray Conf., 1, 389.

Webber, W.R., Lezniak, J.A., Kish, J.C., and Simpson, G.A., 1977, Astrophys. Letts., 18, 125.

Welch, G.A., and Sastry, G.N., Ap. J., 171, L81, 1972.

Weller, C.S., and Meier, R.R., 1974, Astrophs. J., 193 471.

Weller, C.S., and Meier, R.R., 1979, Preprint.

White, M.P., Ph.D. Thesis, Univ. of Durham, 1977.

Whiteoak, J.B., 1974, IAU Symposium 60, Galactic Radio Astronomy, 137.

Wilkenson, A., and Smith, F.G., 1974, M.N.R.A.S., 167, 593.

Williams, P.J.S., and Bridle, A.H., 1967, Observatory, 87, 280.

Willson, M.A.G., 1970, M.N.R.A.S., 151, 1.

Wilson, J.G., 1978, J. Phys. G., 4, 113.

Wolfendale, A.W., 1977, Proc. 15th Int. Cos. Ray Conf., 10, 235.

Wolfendale, A.W., 1975, The Origin of Cosmic Rays, D. Reidel.